TRANSMOTOR-FLYWHEEL POWERTRAIN ASSISTED BY AN ULTRACAPACITOR FOR VEHICLE APPLICATIONS

A Dissertation

by

RAMIN TAFAZZOLI MEHRJARDI

Submitted to the Graduate and Professional School of
Texas A&M University
in partial fulfillment of the requirements for the degree of

DOCTOR OF PHILOSOPHY

Chair of Committee,	Mehrdad Ehsani
Committee Members,	Shankar Bhattacharyya
	Reza Langari
	Karen Butler-Purry
Head of Department,	Miroslav Begovic

May 2023

Major Subject: Electrical Engineering

ABSTRACT

Battery Electric Vehicles (BEVs) can recuperate the kinetic energy of the moving vehicle by the process of regenerative braking. However, this feature is limited by the battery recharge power rating which often is significantly less than the BEV propulsion power rating. Moreover, the Li-ion battery technology that is commonly used in commercial BEVs, are limited by thermal constraints for safety reason. Furthermore, the Li-ion battery's State of Health (SOH) could be noticeably affected by utilizing regenerative braking in harsh braking scenarios. This article is an attempt to alleviate some of the summarized battery technology shortcomings.

In this research, various transmotor-based powertrains are explained, and their advantages and possible limitations are explained. Next, based on previously published articles, the transmotor-flywheel powertrain assisted with the ultracapacitor is proposed. This powertrain is capable of improving regenerative braking significantly by utilizing a lightweight flywheel and a small ultracapacitor pack as dual power buffers. In order to connect the flywheel and ultracapacitor to the drive shaft effectively and more efficiently, a two-shaft electric motor called the transmotor is utilized. Further, the proposed powertrain, transmotor-flywheel assisted by an ultracapacitor, enables us to reduce the power rating of the battery pack to the extent that it only be used for low power demand loads such as cruising and providing vehicle’s range.

Various braking scenarios, from harsh to mild vehicle braking, in regenerative mode, are simulated and presented to show possible regenerative braking enhancement. Finally, an experimental setup is developed to verify the powertrain’s power flow and control algorithm.

DEDICATION

To my devoted parents,

ACKNOWLEDGEMENTS

I would like to thank my committee chair, Dr. M. Ehsani, and my committee members, Dr. Bhattacharyya, Dr. Langari, and Dr. Butler-Purry, for their guidance and support throughout the course of this research.

Thanks also go to my friends and colleagues and the department faculty and staff for making my time at Texas A&M University a great experience. Further, I would like to express my gratitude to my colleague, Dr. Ershad, who help me during this research project.

Finally, thanks to my parents for their encouragement and support.

CONTRIBUTORS AND FUNDING SOURCES

This work was supervised by a dissertation committee consisting of Professor M. Ehsani, advisor, and Professor S. Bhattacharyya and Professor K. Butler-Purry of the Electrical Engineering Department, and Professor R. Langari of the Mechanical Engineering Department.

All other work conducted for the thesis (or) dissertation was completed by the student independently.

Graduate study was supported by a teaching assistantship from Texas A&M University. Further, it is supported by various scholarships, including Thomas Powel'62 Fellowship (2019-2022) and Chevron Scholarship (2018).

NOMENCLATURE

BEV	Battery Electric Vehicle
HEV	Hybrid Electric Vehicle
ICEV	Internal Combustion Engines Vehicle
HESS	Hybrid Energy Storage System
SOH	State of Health
FC	Fuel Cell
PEM	Polymer Electrolyte Membrane
SOFC	Solid Oxide Fuel Cells
M_f	Flywheel's Mass
r_1,r_2,r_3,r_4,b_1,b_2	Flywheel's Geometry
J_f	Flywheel's Inertia
K_f	Inertial Constant
E_f	Flywheel's maximum Energy
C_{total}	Total Ultracapacitor Capacitance
V_{total}	Total Ultracapacitor Voltage
E_{max}	Ultracapacitor's Maximum Energy
SCDMP	Squirrel Cage Dual Mechanical Port
PMSM	Permanent Magnet Synchronous Machine
T	Torque
ω	Angular Velocity
P	Power
R	Resistance

λ	Magnetic Flux
v	Voltage
i	Current
B	Viscous Friction
λ	Magnetic Flux

Subscript

m	Mechanical
e	Electrical
q, d	q, and d Axis
ir	Inner Rotor
or	Outer Rotor
FW	Flywheel
W	Wheel
TRM	Transmotor
Cap	Ultracapacitor
max	Maximum
min	Minimum

TABLE OF CONTENTS

Page

LIST OF FIGURES

LIST OF TABLES

1. INTRODUCTION*

Electrification of the vehicle powertrain is becoming a major trend in the auto industry [1, 2]. Battery Electric Vehicles (BEVs), a fully electrified powertrain, offer zero local emission and superior performance compared to conventional vehicles [3]. However, there are many challenges that need to be addressed before electric vehicles become commercially dominant. First, the electric vehicle range is still limited, and the battery charging time is considerably long [7]. For example, the Chevrolet Bolt's range is 240 miles, and the charging rate is 4 miles/h when connected to a 110 V AC outlet [9]. As a result, the BEV is not even close to dominating the auto industry, yet [4].

Furthermore, the electric machines used in electric vehicles are usually dependent on rare earth magnets. This dependency causes uncertainty in the vehicle supply chain since it comes from limited sources. Thus, there is a trend in the automotive industry to reduce this dependency to have a more stable supply chain and a more successful product for mainstream consumers.

However, the main challenge that BEVs are facing is a proper energy storage system that makes possible a competitive range and can be manufactured at a competitive cost [5, 6]. The BEV needs a high-power density and high-energy density energy storage system to let the BEV have acceptable performance and range. The best-known candidate that can satisfy these requirements is the Li-based battery technology and virtually all present commercially available BEVs are utilizing them in their powertrain [7]. However, Li-based batteries are heavy, bulky, and expensive. This is due to the fact that the battery used in transportation needs to have both high-power and high-energy density. For instance, the Chevrolet Bolt, a commercially available BEV, has a Li-ion battery pack that weighs 437 kg (27% of the vehicle's total mass). Moreover, the battery pack is estimated to cost around 8700$ [8, 9, 28].

To address the above challenges, many solutions have been proposed. The first approach is hybridizing the propulsion system (also known as Hybrid Electric Vehicle (HEV)), which means using electric machines in combination with a conventional combustion engine. This approach addresses many of the mentioned shortcomings, such as, increasing the range and decreasing the cost [30]. Several propulsion systems are suggested for HEV to improve its performance and efficiency. However, the car is still dependent on gasoline to operate, and it is no longer an emission-free vehicle. Moreover, the HEVs propulsion system often needs a more complicated control approach in comparison to Battery Electric Vehicles (BEVs) or Internal Combustion Engines Vehicles (ICEVs) since they need to couple the engine and the electric motor to each other and to the wheels.

Another approach is to hybridize the energy storage system, also known as Hybrid Energy Storage System (HESS) [12, 13, and 29]. In other words, instead of hybridizing the propulsion system, different types of energy storage systems are utilized to overcome the aforementioned challenges. Many research projects have been conducted to utilize high-power density energy storage as a power buffer, such as ultra-capacitors or flywheels, alongside the high-energy density storage battery [15, 19, 31, and 32]. Therefore, high-power demands, such as acceleration are managed entirely or partially by the high-power density energy storage, and the rest, such as cruising, is supplied by the battery pack. In this way, the battery life is prolonged, the overall efficiency is increased, and the driving range is extended. A common approach to extend the BEV range is to utilize regenerative braking during vehicle deceleration. Regenerative braking lets the batteries recuperate the kinetic energy of the moving vehicle. Thus, theoretically, a significant amount of vehicle energy kinetic energy that is usually dissipated as heat during the braking can be recovered.

However, battery degradation could accelerate when the power demand increases rapidly and frequently [6]. In other words, when the BEV has a sudden acceleration or regenerative braking, the battery current profile needs to change from discharging to charging mode and vice versa which could significantly reduce the state of health (SOH) of the battery [10, 11]. Further, battery thermal management can be challenging in the BEV, especially when the power demand is high. A precise cooling solution that potentially can increase the battery pack cost is required to cool down or heat up the battery, especially during high-power demands, such as regenerative braking events [12].

In order to protect the battery pack, a common design practice in the BEV is to limit the battery's regenerative braking power. For example, Chevrolet Bolts' electrical power rating is designed to be 160 kW, but the regenerative braking maximum power is limited to 65-70 kW. This method of protecting the battery pack could significantly reduce the regenerative braking capability, and consequently, be less effective in increasing the BEV range [25, 27].

One approach to remedy the above challenges is to hybridize the energy storage system [13-18]. Other energy storage media, such as ultracapacitors and flywheels, tend to have high-power densities and low energy densities. These energy storage media can be combined with the battery pack to reduce the maximum power demand from the battery pack. Thus, it is even possible to utilize the battery technology with a lower power rating for the BEV powertrain [5, 19]. For instance, Li-air batteries have a very high energy density, which, in theory, could be as much as gasoline energy density [4, 7]. However, since their power density is low, they are not favored for transportation applications.

The alternative energy storage media that is recently got more attention in various studies for BEVs is Fuel Cell (FC). There are many FC technology available that can be utilized as energy storage media. Polymer Electrolyte Membrane (PEM) fuel cells technology is the most considered

fuel cell technology in transportation applications. It has high power density and offers the advantages of low weight and volume compared with other fuel cells [35]. Furthermore, compared to Li-based battery technology, it can offer up to 3 times the energy density. However, unlike battery technology, it cannot be charged during regenerative braking and has noticeably lower efficiency. The PEM can offer about 40% efficiency, while the li-based battery can offer around 80% efficiency.

The proposed transmotor-flywheel powertrain assisted by an ultracapacitor can be utilized with Li-based or Fuel Cell technology as its main energy storage media. Chapter IV compares possible regenerative braking improvement by utilizing the transmotor-flywheel powertrain assisted by an ultracapacitor in conjunction with each of the energy storage technologies in a simulation environment. Then, the required consideration for each technology is explained.

In this research, the transmotor-flywheel technology [20], enhanced by an ultracapacitor [36], is proposed to increase the vehicle's regenerative braking power and reduce the power rating of the battery. In order to compare the proposed powertrain with a conventional BEV, the commercially available Chevrolet bolt is chosen, and its parameters are considered in the proposed design. It is shown here that the proposed powertrain increases the regenerative braking power limit to more than even the propulsion system electrical rating while reducing the battery power rating by 80%.

Alternatively, if the main energy storage is chosen to be FC, the regenerative braking could be superior to the commercially available BEVs. Furthermore, since the ultracapacitor and flywheel manage the sudden power demand, the energy storage media, FC here, does not need to have a quick power response which is often a challenge with FC technology.

This research proposes the transmotor-flywheel powertrain assisted with the ultracapacitor to address some of these challenges. This powertrain consists of a lightweight flywheel, rotating at sub-critical speed and a small ultracapacitor pack as power buffers, and an energy storage media, such as a battery pack. The transmotor is utilized as a means of coupling the flywheel to the vehicle's driveshaft. This study's main contributions can be summarized as follows:

1. The vehicle equipped with the transmotor-flywheel powertrain assisted with the ultracapacitor can have access to the maximum torque at higher speed, and field weakening may not be required.

2. The regenerative braking feature of the BEVs equipped with the transmotor-flywheel powertrain assisted with the ultracapacitor can be significantly improved.

3. The power rating of the main storage media such as battery pack or FC technology could be significantly reduced. Furthermore, no fast dynamic power response is required.

4. In the case of utilizing battery technology as the main energy storage media, the battery SOH (State of Health) could be noticeably improved, without any vehicle's performance degradation.

5. The battery cooling system can be simplified, and the battery pack cooling system can be significantly reduced.

The article is organized as follows: Chapter II briefly reviews the energy storage media technology in terms of energy and power density. Next, Chapter III reviews the transmotor and various transmotor-flywheel-based powertrains and compares them to the proposed powertrain. In Chapter IV, a comparison between the conventional BEV and proposed powertrain regenerative braking performance is presented in various simulated braking scenarios. Finally, in Chapter V,

an experimental emulation is presented, and the transmotor-flywheel electrical system behavior is discussed.

2. ENERGY STORAGE MEDIA TECHNOLOGY

This chapter reviews some of the available energy storage media for transportation applications with an emphasis on 4-passenger vehicles (1200-1600 kg). The energy storage media technologies reviewed in this chapter are battery technology, Fuel Cell (FC) technology, flywheel technology, and ultracapacitor technology. Next, based on the reviewed materials, a proper energy storage media system for the transmotor-flywheel powertrain assisted by an ultracapacitor is designed for a 1600 kg vehicle. These parameters are utilized in the braking scenario simulation provided in Chapter 4.

2.1. Battery Technology

A battery can be described as an energy storage media that keeps the energy in chemical form and is capable to release the energy in an electrical form [37]. The battery can be categorized into two groups rechargeable types and non-rechargeable types. The rechargeable battery types are the most common battery technology used in devices such as cell phones, laptops, BEVs, etc. The Li-ion battery is a rechargeable battery type with the highest energy and power density available. Therefore, it is commonly used in devices that need researchable batteries.

A battery cell is made of a positive electrode, a negative electrode, and an electrolyte. The positive electrode accepts electrons, while the negative electrode release electrons. The electrolyte's role is to conduct ions and isolates the electrodes [37]. A battery pack forms when some numbers of the battery cell are connected in series or parallel [38].

The Energy Capacity (EC) is a way of presenting the battery's total energy capacity in Wh (kWh). The EC can be defined as the electrical energy that can be supplied by the battery pack before the battery voltage drops to a specified cut-off voltage. Alternatively, the battery capacity

can be presented in Coulometric (C). The C can be defined as the electrical charge that can be demanded from the battery pack before the battery voltage drops to a specified cut-off voltage. C is presented in Ah, and thus, it does not show the battery energy capacity as the voltage of the battery pack is not known.

The following terms are important battery characteristics in transportation (mobile) applications:

- Energy Density: The energy density of a battery pack in BEV refers to the available energy capacity per unit of volume. Energy density in transportation applications is usually present in Wh/L.
- Power Density: The power density of a battery pack in BEV refers to the maximum available power per unit of volume. Power density in transportation applications is usually present in kW/L.
- Specific Energy: The specific energy of a battery pack in BEV refers to the available energy capacity per unit of mass. Specific energy in transportation applications is usually present in Wh/kg.
- Specific Power: The specific power of a battery pack in BEV refers to the maximum available power per unit of mass. Energy density in transportation applications is usually present in kW/kg.

Terms such as energy/power density are more crucial in the BEV design as the space is limited under the hood. The utilized battery in BEVs needs to have a high energy density and a high power density. The battery needs to have a high energy density as the energy density defines the vehicle's maximum range, and the battery needs to have a high power density as it correlates with the performance of the vehicle. The proposed transmotor-flywheel powertrain assisted with an

ultracapacitor, however, only needs a battery pack with high energy density as the high-power loads can be managed with the power buffers.

2.2. Fuel Cell Technology

Similar to batteries, Fuel Cells (FC) are electrochemical energy storage media that supply electrical energy to various electrical loads. The FC working principle is that the fuel oxidizes at the anode and the oxygen supply at the cathode. The byproducts of this reaction are water and heat [39].

Various fuels are adaptable to fuel cell use. The most preferred fuel is hydrogen which has H_2O and heat as the reaction byproduct. Hydrogen is a common fuel for various FC technology such as Proton Exchange Membranes (PEMs) and Solid Oxide Fuel Cells (SOFCs) [39].

The general efficiency of the FC technologies, such as PEM, used for transportation applications is relatively low in comparison to the battery technology. Furthermore, charging the FC onboard for recovering the kinetic energy during the regenerative braking is challenging to implement. Therefore, utilizing the regenerative braking feature could not be available in FC-based vehicles, unlike most BEVs. Finally, FC technology often has a hard time tracking dynamic loads such as vehicle acceleration that need to be assisted with other energy storage media.

2.3. Flywheel Technology

Flywheel is an energy storage media that stores energy in a mechanical form. If the flywheel is connected to an electric motor, the kinetic energy stored in the flywheel can be converted to electrical form and vice versa. Flywheel technology can be used in various applications, such as in power utility or in transportation applications.

There are two ways to utilize the flywheel in transportation applications. The first approach is to utilize it as a flywheel battery also referred to as a mechanical battery. In this topology, the

flywheel is connected to a high-speed electric motor and the electrical energy is stored in the flywheel similar to a battery but in a mechanical form. Flywheel has various advantages over other energy storage media, such as high energy density and no environmental dependency, especially temperature.

However, in order to store a high amount of energy, the flywheel needs to rotate at high angular velocity. Furthermore, the flywheel needs to be constructed into specific shapes and has a certain amount of mass. Therefore, the flywheel and other peripherals such as the bearing need to be constructed out of expensive materials. Moreover, the flywheel needs to be in a special vacuum housing to reduce mechanical losses such as aerodynamic drag.

These requirements are difficult to meet in mobile applications, such as in 4-passenger vehicles, and hence, utilizing a flywheel rotating at high angular velocity is not desirable. Therefore, utilizing the flywheel as the main energy source in the vehicle is not recommended. If the flywheel is utilized as a power buffer and not a main energy source, it can be a lightweight mass rotating at a subcritical speed. Thus, no special requirements such as vacuum casing are needed, and the total cost of utilization can be significantly reduced.

Alternatively, the flywheel can be utilized with the new technology called transmotor. The transmotor technology will be presented in chapter III, and the unique power flow of this device will be explained. By utilizing the transmotor, it is possible to connect the flywheel to one shaft and connect the second shaft to the drive shaft and transfer the power between them magneto-mechanically with little energy conversion as is shown in Fig 1. As a result, energy transfer has a higher efficiency in comparison to mechanical or chemical battery technology.

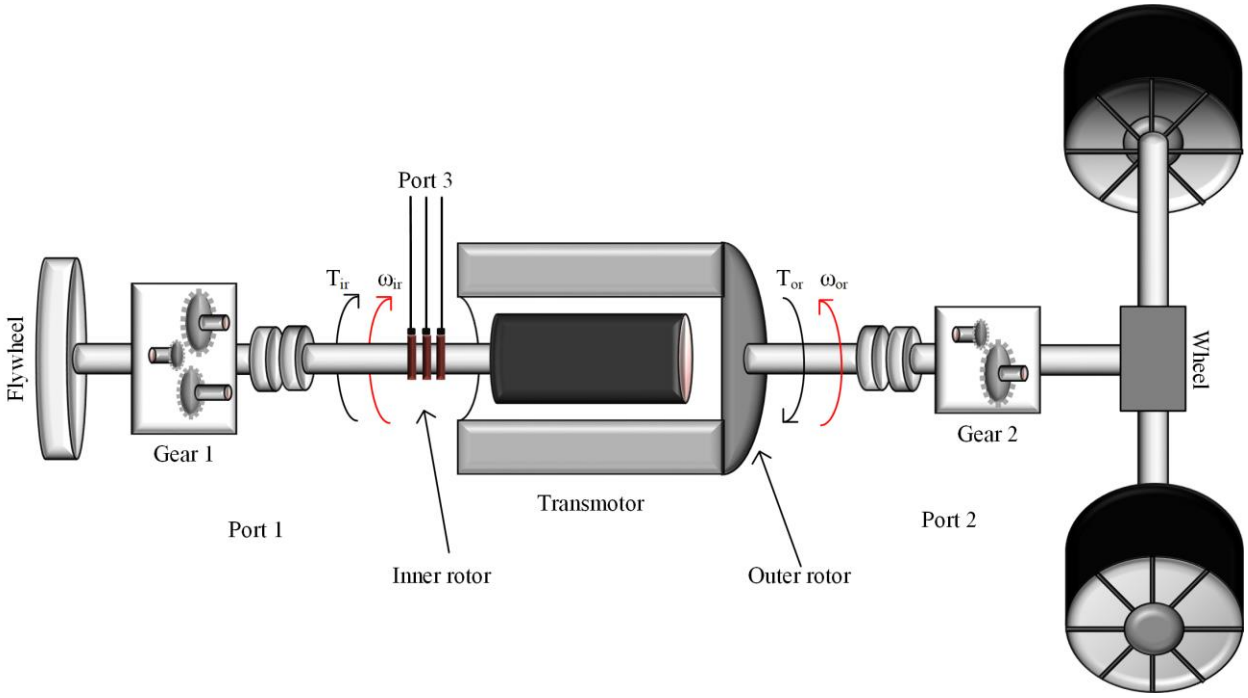

Fig.1. Transmotor-Flywheel-Based Powertrain

The energy stored in a flywheel can be expressed as equation 1. where J_f and ω_f are the moments of inertia of the flywheel in kgm^2 and the angular velocity of the flywheel in rad/s, respectively.

$$J_f = M_f\left(\frac{b_1\left(r_1^4 - r_2^4\right) + b_2\left(r_2^4 - r_3^4\right)}{b_1\left(r_1^2 - r_2^2\right) + b_2\left(r_2^2 - r_3^2\right)}\right) \quad (1)$$

The moment of inertia of a flywheel per mass unit mainly depends on the flywheel geometric design and can be calculated as follow: Where M_f is the flywheel mass, and r_1, r_2, r_3, r_4, b_1, and b_2 are related to the flywheel geometry and shape as is shown in Fig. 2.

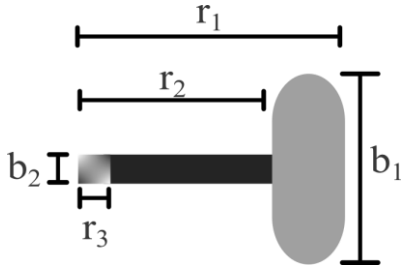

Fig. 2. Flywheel Geometry to Calculate the Total Inertia

2.4. Ultracapacitor Technology

The ultracapacitor, also known as the supercapacitor, technology is a form of energy storage media that could have significantly higher specific power than battery technology. Furthermore, ultracapacitor technology has higher efficiency, excellent temperature adaptability, and much longer service life in comparison to batteries. However, they have a lower specific energy than battery technology. Thus, while they are not suitable to be utilized as stand-alone energy storage media in-vehicle applications, they are a suitable candidate to be utilized as a power buffer.

Two data can often be found in the ultracapacitor datasheet regarding the specific power rating: Specific power at 95% efficiency, and specific power at matched impedance (50% efficiency). The specific power at 95% efficiency is lower than the specific power at the matched impedance noticeably. Based on these two specific powers for ultracapacitors, two statements are common in the literature. Some believe that lithium batteries and ultracapacitor has the same power capability, and other believe that ultracapacitors have a significantly higher power capability than lithium-based battery technology. However, in order to make any general statement the application that the ultracapacitor is utilized need to be considered [40]. Furthermore, ultracapacitors can be designed to have higher energy capacity at the cost of lower power capability and vice versa.

The ultracapacitor technology in vehicle applications has high power capability on average. However, the specific energy of the ultracapacitor is significantly lower, and the stored energy is dependent on its voltage. Despite various efforts, such as SupperBattery from Skeleton, to adopt them as the main energy source, they are still utilized as a power buffer alongside the main energy source such as a battery. Therefore, the most common approach to utilize the ultracapacitor technology is to hybridize it with energy-dense energy storage devices, such as batteries or flywheels.

Table I presents the ultracapacitor's individual cell characteristics, from various Maxwell and Skeleton. For a 1600kg vehicle equipped with the transmotor-flywheel powertrain assisted with an ultracapacitor, the 325F ultracapacitor technology from Maxwell is suitable. A costume design for a 1600kg vehicle is presented in section 2.5. Alternatively, the 300F ultracapacitor from Skeleton would suffice for a 1600 kg vehicle equipped with the transmotor-flywheel powertrain assisted with an ultracapacitor.

Table I: Ultracapacitor Technology Per Cell [40]

Device	V rated	C (F)	R (mΩ)	RC s	Wh/kg	kW/kg (95%)	kW/kg match. imped.	Mass (kg)	Vol. lit.
Maxwell [41]	3	180	4	0.66	6.5	5.7	11.9	0.029	0.00125
Maxwell [42]	3	100	8	0.8	6	6.4	13.4	0.021	0.0223
Maxwell [43]	2.7	325	1.6	0.52	5.4	8.4	17.5	0.065	0.068
Skeleton [44]	2.85	300	1.6	0.48	5.3	NA	20	0.064	0.053
Skeleton [45]	2.85	500	0.6	0.3	5.1	8.8	80	0.111	0.079
Skeleton [45]	2.85	1200	0.24	0.288	5.4	18.5	73	0.253	0.178
Yunasko [40]	2.75	1275	0.11	0.13	4.55	8.8	78.13	0.22	0.15

2.5. Energy Storage Media in The Proposed Powertrain

The transmotor-flywheel assisted by an ultracapacitor has one main energy storage media and two power buffers. The main energy storage media could be based on battery technology or based on Fuel Cell (FC) technology. The main storage media is required to provide the range for the electric vehicle, so it should have a high energy density. On the other hand, the power buffers have high power density, to manage the high-power demands such as acceleration or regenerative braking. The utilized power buffers are flywheel and ultracapacitor. This section calculates the utilized energy storage media and power buffers for a 1600 kg (based on Chevrolet Bolt) that is simulated in Chapter 4.

2.5.1. Flywheel Sizing

For a 1200-1600 kg vehicle, a 12-16 kg flywheel is recommended which is roughly 1% of the total vehicle mass. The flywheel is utilized for high-power demand loads, such as vehicle acceleration or deceleration. The inertia of the flywheel can be estimated by the following equation (equation 2):

$$J_f = K_f \times M_f \times \frac{b_2}{2} \tag{2}$$

Where J_f, K, M_f, and b_2 are the flywheel inertia, inertial constant, flywheel mass, and flywheel diameter, respectively. It is assumed that K=0.5, which is valid for a solid disk of uniform thickness.

For a 12kg and 0.3m radius flywheel we have:

$$\rightarrow J_f = 0.5 \times 12 \times 0.3^2 = 0.54 kgm^2$$

For a 16 kg and 0.35m radius flywheel, we have:

$$\rightarrow J_f = 0.5 \times 16 \times 0.35^2 = 0.98 kgm^2$$

The maximum flywheel angular velocity needs to be around 20 krpm, which is in the sub-critical range. Thus, the flywheel's maximum energy can be estimated as follow (equation 3):

$$E_f = \frac{1}{2} \times J_f \times {\omega_f}^2 \tag{3}$$

For a 0.54 kg.m^2 flywheel and 20 krpm angular velocity we have:

$$\rightarrow E_f = \frac{1}{2} \times 0.54 \times 2094^2 = 1184 kJ = 0.33 kWh$$

For a 0.98 kg.m^2 flywheel and 20 krpm angular velocity we have:

$$\rightarrow E_f = \frac{1}{2} \times 0.98 \times 2094^2 = 2148 kJ = 0.6 kWh$$

Finally, it is possible to estimate the energy/weight ratio of the required flywheel for the transmotor-flywheel powertrain:

- ✓ Specific Energy for a 12 kg flywheel = 0.0275 kWh/kg
- ✓ Specific Energy for a 16 kg flywheel = 0.0375 kWh/kg

Thus, the specific energy should be around 0.0275 to 0.0375 kWh/kg. It is worth mentioning that the flywheel act as a power buffer in the transmotor-flywheel powertrain. In other words, the flywheel should have enough energy to accelerate the vehicle and subsequently recuperate the vehicle's kinetic energy during the regenerative braking. That is why only a lightweight flywheel rotating at the subcritical speed is required in the proposed powertrain.

2.5.2. Ultracapacitor Sizing

For a 1600 kg vehicle, a 16-20 kg ultracapacitor is recommended, depending on the main energy storage media technology, which is about 1% of the total vehicle mass. The ultracapacitor is utilized to mitigate the high-power transfer between the flywheel and the vehicle's loads, such as acceleration and regenerative braking. "BCAP0325 P270 S19" with 345F capacitance and rated voltage of 2.7V is chosen to design the required ultracapacitor pack as shown in Table II [43].

Table II: Maxwell BCAP0325 P270 S19 (Per Cell)

Symbol	Parameter	Value	Unit
V_R	Rated Voltage	2.7	V
C_R	Rated Capacitance	345	F
R_s	Equivalent Series Resistance (ESR_{DC})	1.6	mΩ
n_{CYCLE}	Projected Cycle Life	1,000,000	cycles
t_{25C}	Projected Lifetime	10	years
P_{max}	Impedance Match Specific Power	17.5	kW/kg
E_{max}	Stored Energy	0.35	Wh
P_d	Usable Specific Power	8.4	kW/kg
E_d	Gravimetric Specific Energy	0.35	Wh/kg
M	Mass	65	g

For a 1600 kg vehicle, 220 cells of the ultracapacitor with the parameters presented in Table II is recommended in the case of the transmotor-flywheel powertrain assisted with an ultracapacitor.

The capacitor needs to be arranged as shown in Fig. 3 to have a high voltage and enough power input/output for this design. The total mass of the ultracapacitor without the packaging is estimated to be around 14.8 kg, and with proper packaging and cooling is estimated to be around 16 kg. The ultracapacitor pack parameters can be estimated as follow:

$$\rightarrow C_{total} = \frac{C}{Number\ of\ Cells} \times Number\ of\ branches = \frac{345}{110} \times 2 = 6.27F$$

$$\rightarrow V_{total} = V_{cell} \times Number\ of\ Cells\ in\ Each\ Branches = 2.7 \times 110 = 297V$$

$$\rightarrow E_{max} = \frac{1}{2}CV^2 = \frac{1}{2} \times 6.27 \times 297^2 = 277kJ = 0.077\ kWh$$

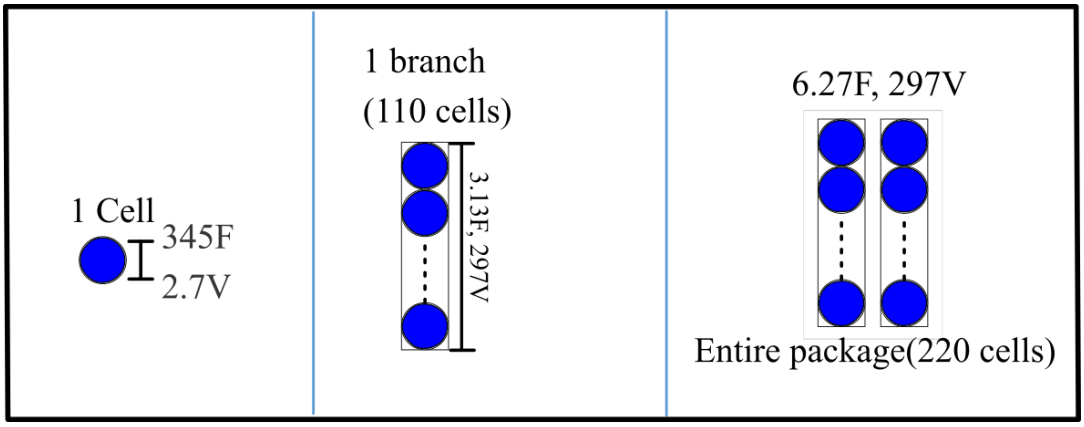

Fig. 3. Ultracapacitor Cells Arrangement

In the case of utilizing a non-rechargeable main energy storage media, such as FC, a relatively larger ultracapacitor is required (25% larger). The total number of cells needs to be 500, and the total capacitance is estimated to be around 7.5 F with the same voltage rating ("BCAP0150 P300 S17" is used instead of "BCAP0150 P300 S17")

$$\rightarrow C_{total} = \frac{C}{Number\ of\ Cells} \times Number\ of\ branches = \frac{150}{100} \times 5 = 7.5F$$

$$\rightarrow E_{max} = \frac{1}{2}CV^2 = \frac{1}{2} \times 7.5 \times 300^2 = 337.5kJ = 0.093\ kWh$$

2.5.3. Battery Sizing

The battery characteristic of the Chevrolet bolt that is used as a commercially available BEV is summarized in Table III [7]. Table IV presents the battery characteristics of the proposed powertrain that is designed based on the Chevrolet Bolt battery technology. The battery package of the proposed powertrain is similar to the Chevrolet Bolt, but the battery arrangement is modified. Chevrolet Bolt has 3 branches of 96 cells that are connected in a series manner. However, since the ultracapacitor is utilized between the battery and ultracapacitor, the battery arrangement is modified to be 6 branches of 48 cells that are connected in a series manner. The described battery cell arrangement is presented in Fig. 4.

Table III: Chevrolet Bolt Battery Characteristics	
Battery Package	
Total cell number	288
Total energy capacity	60 kWh
Total mass	436 kg
DC buss voltage	320 V
Individual Cell	
Energy capacity per cell	208 Wh
Voltage per cell	3.3 V
Number of branches	3
Number of cells in each branch	96

Table IV: Proposed Powertrain Battery Characteristics	
Battery Package	
Total cell number	288
Total energy capacity	60 kWh
Total mass	436 kg
DC buss voltage	160 V
Individual Cell	
Energy capacity	208 Wh
Voltage per cell	3.3 V
Number of branches	6
Number of cells in each branch	48

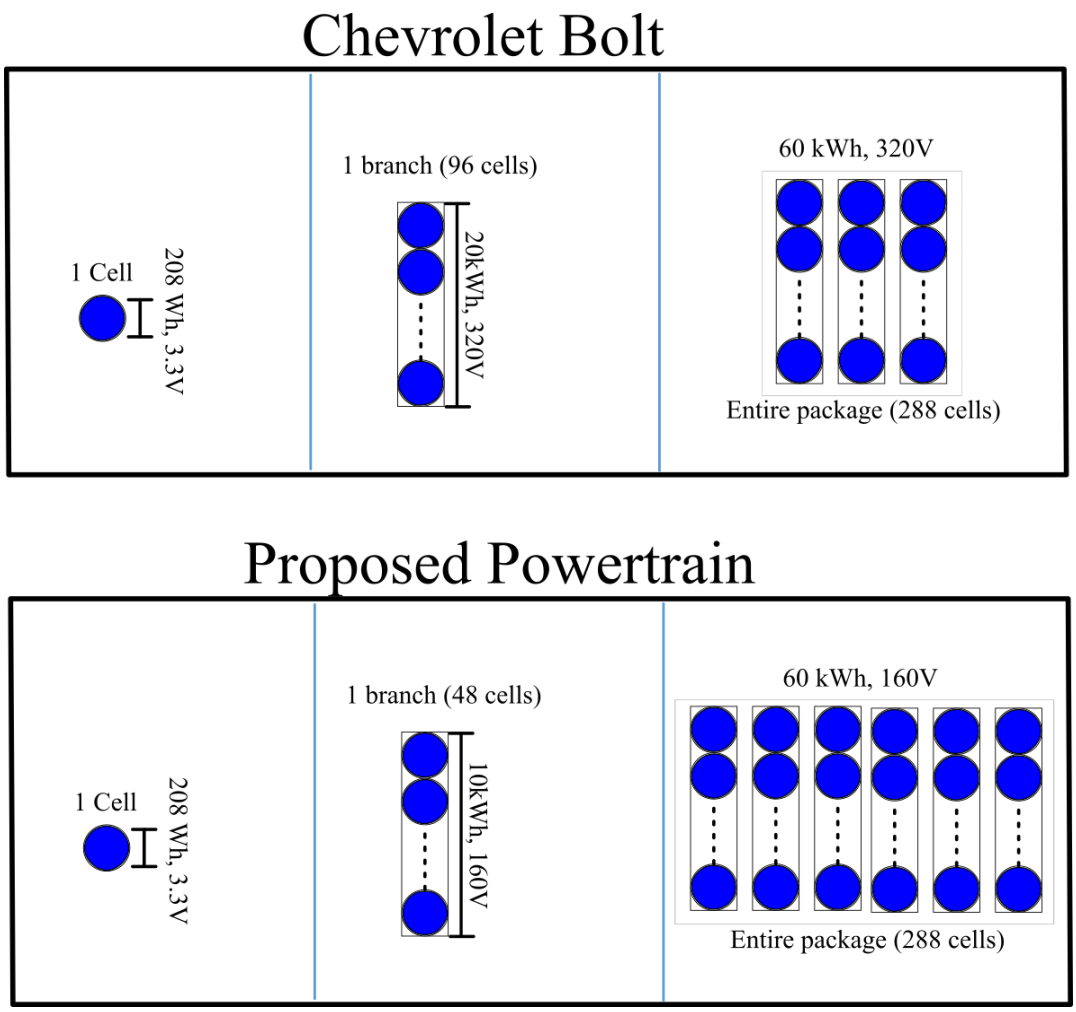

Fig. 4. Battery Cells Arrangement

3. TRANSMOTOR-FLYWHEEL TECHNOLOGY*

In this chapter, the transmotor and transmotor-flywheel powertrain are explained, and the transmotor-flywheel powertrain modes of operations are reviewed. Then, the advantages and possible disadvantages of the transmotor-flywheel-based powertrain are briefly discussed. Next, the 4WD transmotor-flywheel-based powertrain is reviewed to remedy some of the shortcomings of the transmotor-flywheel powertrain. While this topology solves some of these disadvantages, it also introduces limitations and boundaries to the system that is explained here. Finally, the transmotor-flywheel powertrain assisted by the ultracapacitor is proposed as an alternative to remedy some of the shortcomings and limitations of the 4WD transmotor-flywheel-based powertrain.

3.1. Transmotor

The transmotor concept is first proposed by Ehsani et al [2]. The transmotor can be described as an electric machine with two mechanical ports and one controllable electrical port. The electrical port may be used to adjust the torque and subsequently, the flow of power between the two mechanical ports. In the other words, the Transmotor can be viewed as an active magnetic clutch that is capable of recovering or injecting slip power, as needed [20]. Various types of transmotor can be designed and prototyped, such as Squirrel Cage Dual Mechanical Port (SCDMP) introduced in [33, 34]. However, since compactness is one of the main criteria in mobile applications, a permanent magnet-based transmotor is chosen for this research. Equations 1-3 express the torques, speeds, and power relationships between the mechanical ports and the electrical port of the transmotor, respectively [21-24]. The magnitudes of the torques on the mechanical shafts are equal, but in opposite directions, as is shown in equations 1-3. therefore, the input/output

powers on the mechanical shafts of the transmotor can only be equal, if the angular velocities of the mechanical shafts are not equal ($P = T\omega$). Let's assume the transmotor is an ideal system (i.e., a lossless system). Since energy is conserved in any system, the power difference between the two mechanical ports may be adjusted by the electrical port (Fig. 5).

Fig. 5 presents a simplified diagram of the PMSM-based transmotor with the inner rotor and outer rotor as the mechanical shafts, while the electrical port (winding) is located on the inner rotor. For a detailed prototype structure, please look at chapter 5.

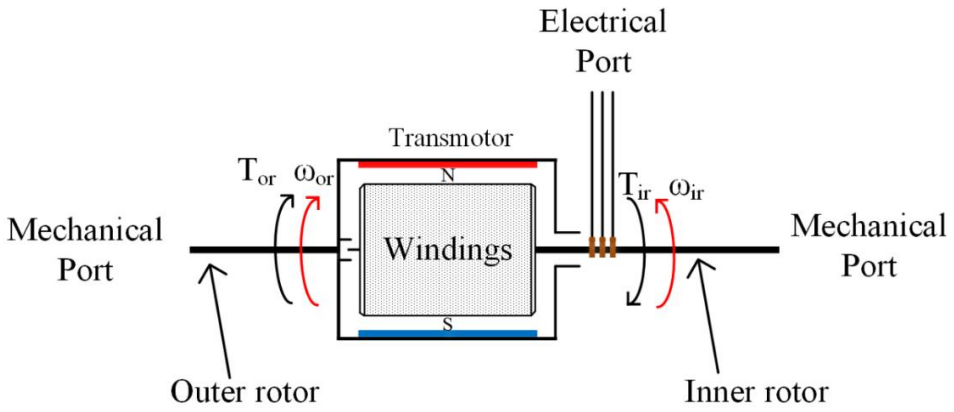

Fig 5. Transmotor as a Three-Port Machine

$$|T_{m1}| = |T_{m2}| \quad (4)$$

$$\omega_e = \omega_{m2} - \omega_{m1} \quad (5)$$

$$P_e = P_{m2} - P_{m1} \quad (6)$$

Equations 7 to 13 express the dynamic response of the transmotor in space vector format, where the d-axis is aligned with the flux. Since both mechanical ports are free to rotate the reference frame of rotation is opted to rotate with the flux resultant angular velocity (ω_e).

$$v_{qir} = R_{ir} i_{qir} + \frac{d\lambda_{qir}}{dt} + N(\omega_e)\lambda_{dir} \quad (7)$$

$$v_{dir} = R_{ir} i_{dir} + \frac{d\lambda_{dir}}{dt} - N(\omega_e)\lambda_{qir} \quad (8)$$

$$\lambda_{qir} = L_{qir} i_{qir} \quad (9)$$

$$\lambda_{dir} = \lambda_m + L_{dir} i_{dir} \quad (10)$$

$$T_{eir} = -T_{eor} = 3N(i_{qir}\lambda_m + (L_{dir} - L_{qir}) i_{dir} i_{qir}) \quad (11)$$

$$T_{eir} = T_{mir} + J_{ir}\frac{d\omega_{ir}}{dt} + B_{ir}\omega_{ir} \quad (12)$$

$$T_{eor} = T_{mor} + J_{or}\frac{d\omega_{or}}{dt} + B_{or}\omega_{or} \quad (13)$$

Fig. 6 presents the power flow in the transmotor in various mechanical angular velocities of the shafts. As is shown, two arbitrary inertias (flywheels A and B in fig.6) are connected to the two mechanical ports of the transmotor with specific relative angular velocity, and the electrical port is connected to a proper bidirectional energy storage media (such as a battery pack, capacitor and...).

a. Fig. 6, Region I (flywheel A to B): The goal is to transfer power from flywheel A to flywheel B. Let's assume the angular velocity in flywheel A is greater than in flywheel B. The excess power of flywheel A, due to the higher angular velocity, needs to be absorbed by the electrical port.
b. Fig. 6, Region I: (flywheel B to A): The goal is to transfer power from flywheel B to flywheel A. Let's assume the angular velocity in flywheel B is greater than in flywheel A. Similarly, the excess power of flywheel B, due to the higher angular velocity, needs to be absorbed by the electrical port.
c. Fig. 6, Region II: (flywheel A to B): The goal is to transfer power from flywheel A to flywheel B. Let's assume the angular velocity in flywheel B is greater than in

flywheel A. The supplied power by flywheel A, due to the lower angular velocity, needs to be compensated by the electrical port.

d. Fig. 6, Region II: (flywheel B to A): The goal is to transfer power from flywheel B to flywheel A. Let's assume the angular velocity in flywheel A is greater than in flywheel B. Similarly, the supplied power by flywheel B, due to the lower angular velocity, needs to be compensated by the electrical port.

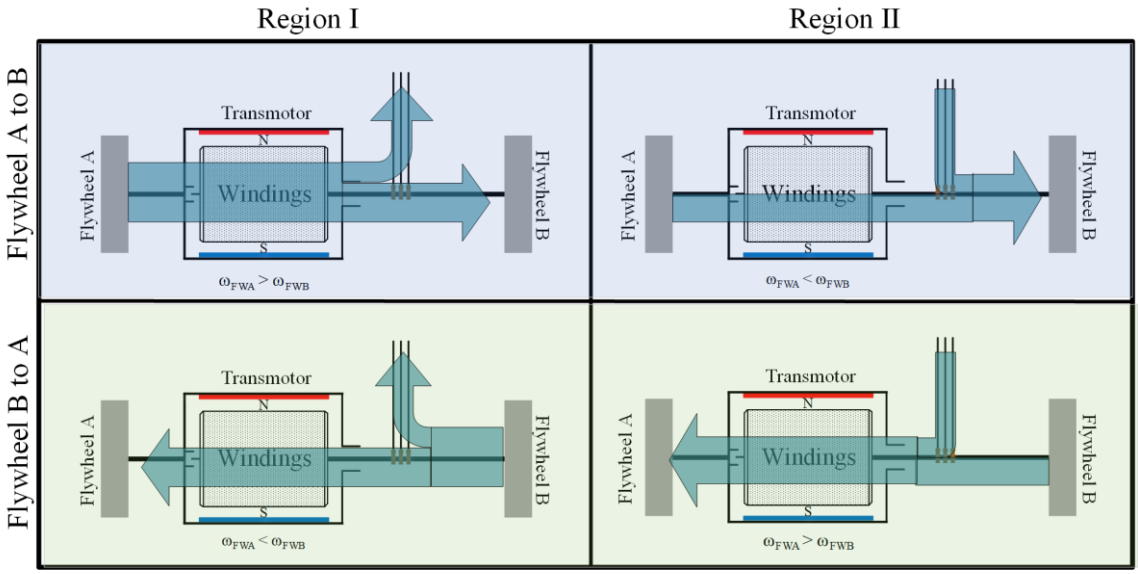

Fig 6. Transmotor's Power Flow in An Ideal Case* (Reprinted with permission from [36])

3.2. Transmotor-Flywheel-Based Powertrain

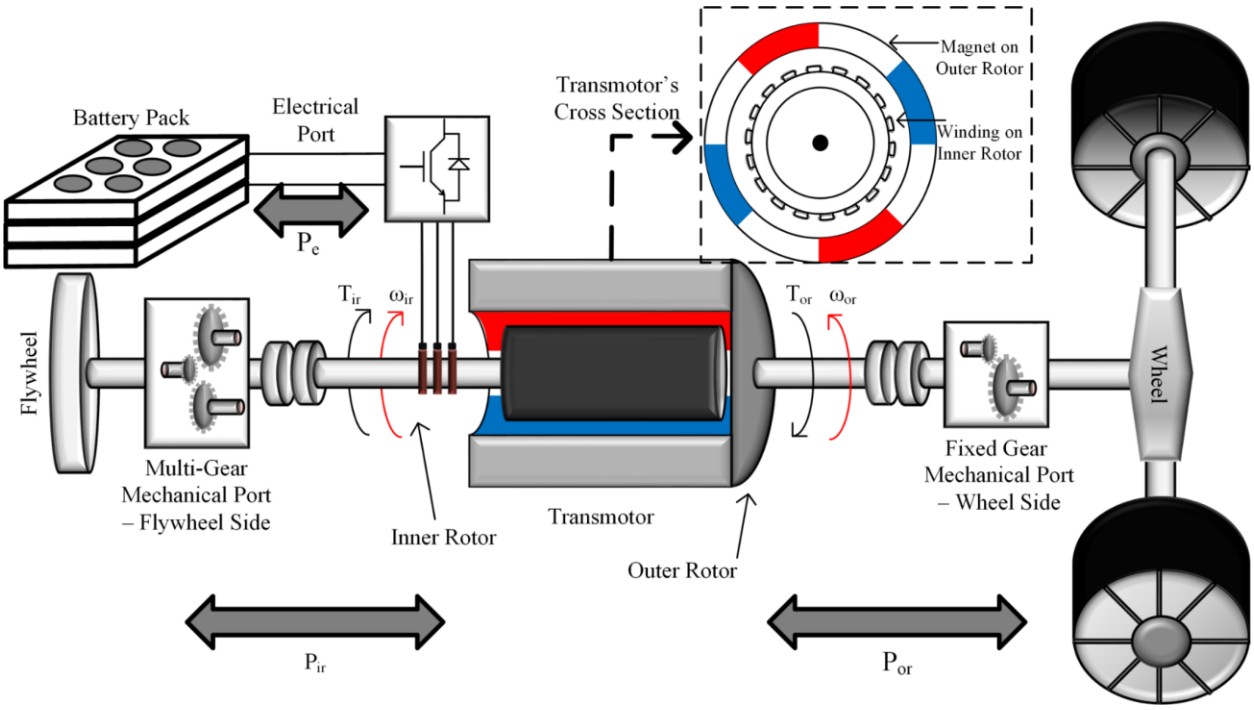

Fig. 7. Transmotor-Flywheel Powertrain 3D Model* (Reprinted with permission from [24])

The transmotor can be utilized as the main propulsion system in a BEV powertrain. The transmotor-flywheel-based powertrain is first proposed in this utilization mode [21]. The transmotor has two mechanical ports and one electrical port, as explained. In the transmotor-flywheel-based powertrain that is utilized as the main propulsion system, one mechanical shaft is connected to a light flywheel (as a power buffer) and the other mechanical shaft is connected to the vehicle's drive shaft with proper gear ratio, as is shown in Fig. 7. The gear connecting the transmotor to flywheel could be a fixed gear or multi-gear as utilized in [24]. The electrical port is connected to the energy storage media, such as a battery pack, via the power processing units (PPU) to control the power flow between the mechanical ports [20].

A transmotor-flywheel-based powertrain's power flow is presented in Fig. 7. Let's assume that the inner rotor, connected to the flywheel, has a higher angular velocity than the outer rotor,

connected to the vehicle drive shaft, and the goal is to accelerate the vehicle. Since, $P_{ir} > P_{or}$, the flywheel extra power is stored by the electrical port and charged to the energy storage media (battery in here), as illustrated in Fig. 8A. Now, in the described powertrain, let's assume the inner rotor, connected to the flywheel, has a lower angular velocity than the outer rotor, connected to the vehicle drive shaft. Since $P_{ir} < P_{or}$, the flywheel power is not adequate, and hence, the electrical port needs to supply the extra demanded power from the energy storage media (battery in here). This is presented in Fig. 8B.

Next, in this powertrain, let's assume the inner rotor, connected to the flywheel, has a lower angular velocity than that of the outer rotor, connected to the drive shaft, and the goal is to decrease the vehicle's speed. Since, $P_{ir} < P_{or}$, the wheel's extra power is stored by the electrical port in the energy storage media (battery in here), as illustrated in Fig. 8C. Finally, assume the same situation in this powertrain, however, the angular velocity of the inner rotor, connected to the flywheel being more than the outer rotor, connected to the drive shaft. Since $P_{ir} > P_{or}$, the wheel's inadequate power needs to be assisted by the electrical port and supplied by the energy storage media (battery in here). This is shown in Fig. 8D. The above power flow of the transmotor-flywheel-based powertrain is presented in Table V.

TABLE V: Transmotor-Based Powertrain Power Flow

Event/Condition	$\omega_{ir} > \omega_{or}$	$\omega_{ir} < \omega_{or}$
Acceleration	$P_{ir} > P_{or}$	$P_{ir} < P_{or}$
	$P_e < 0$	$P_e > 0$
Deceleration	$P_{ir} < P_{or}$	$P_{ir} > P_{or}$
	$P_e < 0$	$P_e > 0$

It is worth mentioning that this powertrain has a unique power flow in cases A and D. In case A, the command is to increase the vehicle's speed, however, the energy storage media is receiving the electrical power. Furthermore, in the case of D, the target is to decrease the vehicle's speed,

however, the battery needs to supply the required electrical power. This behavior is unique to the transmotor as a multiport powertrain that was explained previously.

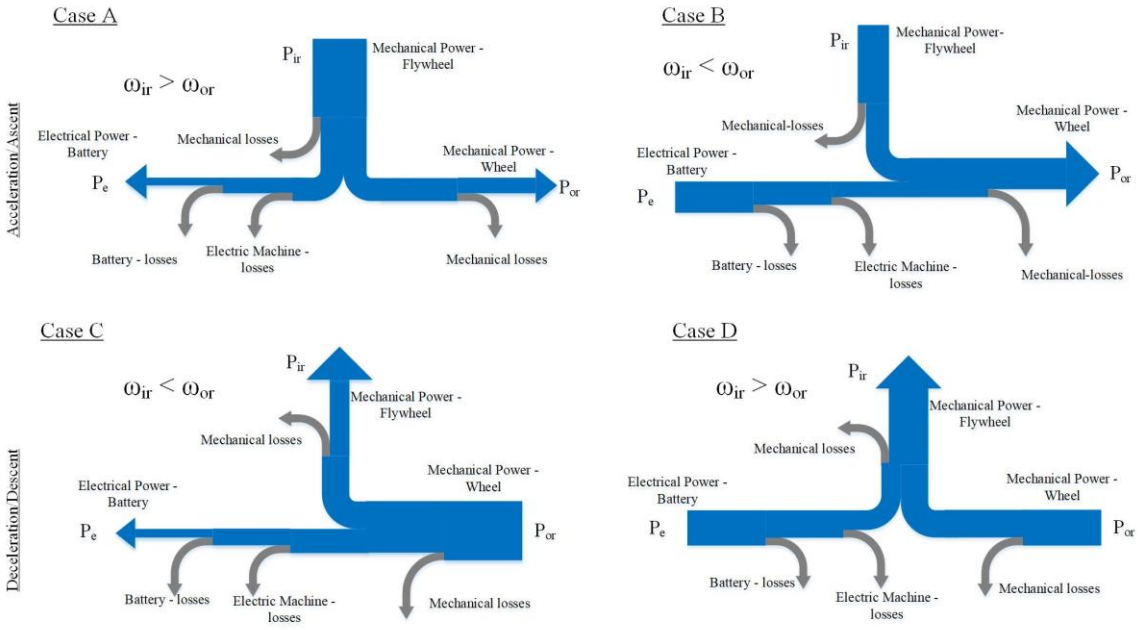

Fig. 8. Transmotor's Power Flow, Including the Electrical and Mechanical Losses * (Reprinted with permission from [24])

3.3. Transmotor-Flywheel-Based Powertrain Modes of Operation

As is shown in Fig. 9, the transmotor-flywheel-based powertrain can have the following operation modes:

I) High performance mode

In this operation mode, depicted in Fig. 9-I, the transmotor can transfer more than its electrical rating and the explained power flow is valid in this mode. Clutch 1 and clutch 2 are engaged and lock 1 and lock 2 are disengaged in order to have access to the flywheel (power buffer) and battery simultaneously.

II) Conventional electric motor mode:

In this operation mode, lock 1 and clutch 2 are engaged, and clutch 1 and lock 2 are

disengaged as is shown in Fig. 9-II. In this mode, the flywheel is not engaged and is free disengaged as is shown in Fig. 9-II. In this mode, the flywheel is not engaged and is free to rotate, however, the relayed shaft is locked. Thus, it let the transmotor operate similarly to the conventional electrical motor (two-port electric machine). In the other words, the transmotor in this mode of operation is similar to the conventional electric motor.

III) Flywheel charging mode:

In this operation mode, lock 2 and clutch 1 are engaged, and clutch 2 and lock 1 are disengaged as is shown in Fig. 9-III. In the other words, the wheel is locked, and the flywheel is engaged. In this mode, the flywheel speed can be adjusted as needed. The flywheel speed could decline during the vehicle acceleration and deceleration due to the various associated losses such as electrical and mechanical losses. This mode can be used while the vehicle is at standstill behind the stop sign or at full stops in the various driving cycles.

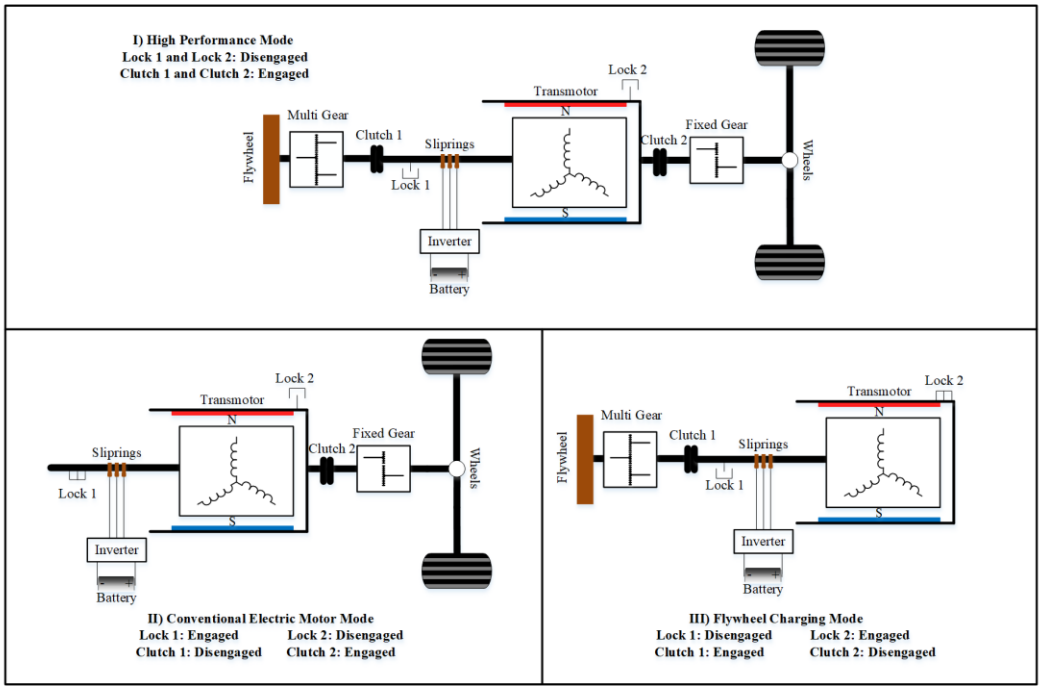

Fig. 9. The Transmotor-Based Powertrain Modes*(Reprinted with permission from [24])

In chapters 4 and 5, the high-performance mode is assumed, in general, to emphasize the maximum improvement of the transmotor-flywheel-based powertrains assisted by the ultracapacitor.

3.4. Transmotor-Flywheel-Based Powertrain Torque-Speed Characteristics

The transmotor-flywheel-based powertrain allows us to have access to the maximum torque at any electric motor, and subsequently vehicle's speed. In the other words, it is possible to have access to the maximum torque at any feasible vehicle's speed. Furthermore, it is possible to reduce or eliminate the need for the field weakening approach at a higher angular velocity in the powertrain equipped with the transmotor. These features are possible because the transmotor's shafts rotate in the same direction, and hence, the back-emf voltage can be limited at various angular velocities.

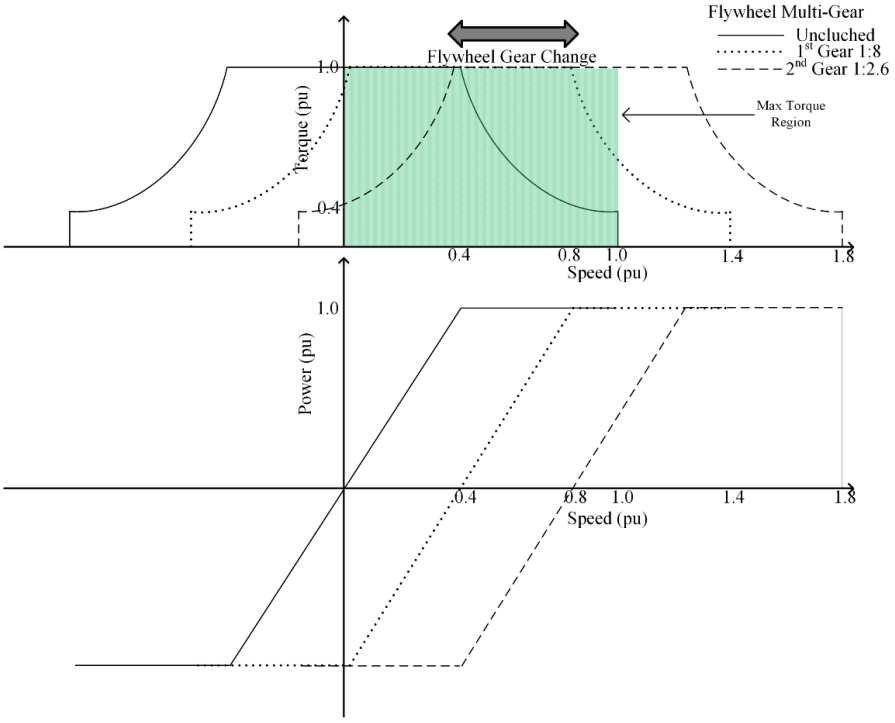

Fig. 10. Torque-Speed Characteristic of the Transmotor's Electrical Port* (Reprinted with permission from [24])

Let’s assume the flywheel is disengaged and free to rotate and the transmotor’s shaft is locked. Then, the torque-speed characteristics of the transmotor will be similar to the conventional electric motors (i.e., Permanent Magnet Synchronous Machine in current design). Thus, the transmotor’s maximum torque is accessible from the standstill to the natural speed (around half of the maximum angular velocity). In order to increase the electric motor's angular velocity from this point toward the maximum angular velocity, the field weakening approach would be required that limits the output torques of the transmotor. However, when the flywheel is engaged to the transmotor’s shaft, the induced voltage on the winding (located on the outer rotor) could be manipulated as needed, and hence, the field weakening could be avoided. Fig. 10 presents a representation of this phenomenon that can be realized by assuming that the torque-speed characteristics of the transmotor are relocating to a higher speed range.

It is possible to connect the flywheel to the transmotor via a fixed or multi-gear. Fig 7 is an example of two gear interfaces between the flywheel and the transmotor’s shaft. In this example, the first gear (1:8) is covering the low-speed range, and the second gear (1:2.6) is covering the high-speed range. Thus, it is possible to cover the entire speed range (from standstill to maximum speed). It is noteworthy to mention that it is feasible to utilize only a fixed gear to interface the flywheel and the transmotor. The multi-gear is used in fig. 7 to demonstrate the torque-speed characteristic of the transmotor-flywheel-based powertrain.

Having access to the maximum torque in any given angular velocity has the following benefits:

1. Vehicle performance improvement: Since the torque-speed profile of the transmotor moves to the right (high speed) while the flywheel is engaged, the operating point of the powertrain changes. Thus, the region with the maximum torque becomes accessible at higher angular velocities.

2. Regenerative braking improvement (especially at a higher vehicle's speed): This is achievable due to the possibility of recovering a higher amount of energy at higher vehicle speeds. This feature is beside the more efficient nature of the transmotor in recovering the vehicle's kinetic energy during the braking.
3. Vehicle gradeability improvement: Since the maximum torque is available in the transmotor-flywheel-based powertrain at any given speed, better gradeability is achievable. In the other words, it is viable to climb a steep grade or recover energy higher energy moving down a hill. It is worth mentioning that this feature is limited to the flywheel inertia max angular velocity and cannot be used for a long period of time on a steep grade (both in regenerative mode and performance mode).

3.5. Transmotor-Based Powertrain Advantages and Disadvantages

The transmotor-flywheel-based powertrain has the following main properties that can be utilized in various applications, such as transportation:

1. Availability of the max torque at any given angular velocity: As explained, due to the transmotor-flywheel system torque-speed characteristic, it is possible to have access to the maximum torque at any given angular velocity. This feature enables us to have a higher performance and gradeability at higher vehicle's speed.
2. Transferring power more than the transmotor's electrical rating: It is feasible to transfer more mechanical power between the transmotor's shafts than its electrical rating [19]. This property can be realized when both transmotor's shafts rotate in the same direction. By this utilization approach, the air gap voltage can be limited to a lower range, hence, the required electrical power is reduced. For instance, a transmotor-flywheel-based powertrain with an electrical rating of 100% can transfer about 200% of mechanical power to the driving

shaft. This feature heavily depends on the powertrain design and the required vehicle's performance.

3. Higher overall efficiency: Since the inner rotor and outer rotor are magnetically coupled, it is feasible to transfer power directly between the two transmotor shafts, with a lower electromechanical energy conversion requirement. Therefore, the overall efficiency of the transmotor-flywheel-based powertrain will be better than the conventional electric motors. This property is explained extensively in [21].
4. Low average electrical power utilization: When the power is transferred between the two shafts of the transmotor, some of the mechanical energy transfers magneto-mechanically in the air gap without the need for energy conversion to the electrical or chemical domain. Therefore, the required average electrical power utilization is less than the total transferred power. This property mainly depends on the speed difference of the transmotor's shafts (the inner rotor and the outer rotor). For instance, if the transmotor's shafts have the same angular velocity, the electrical power utilization, in theory, is equal to zero. Nima et al. have mathematically proved this feature in [23].

However, implementing the transmotor-flywheel-based powertrain can have some drawbacks that are addressed as follow:

1. Slip rings and brushes: Both members of the transmotor are free to rotate, so in order to have contact with the windings (located on the inner rotor or the outer rotor) could be challenging. The utilized transmotor, in this research, has the winding on the inner rotor. In order to have access to the electrical port, brushes, and slip rings are required. Please refer to Chapter 5 for further explanation.

2. Mechanical implementation: One of the essential components of the transmotor-flywheel-based powertrain is the flywheel. The flywheel in this powertrain has some inertia, and subsequently some mass, and it needs to rotate in the vehicle, which is a moving object. According to the gyroscopic effect, a rotating object connected to the transmotor's shaft produces a torque perpendicular to the shaft that needs to be considered in the design. In order to alleviate this, it is recommended to utilize a low-weight flywheel that is limited to subcritical speed to reduce the effect. Furthermore, if higher inertia is required or the flywheel need to rotate at higher angular velocity various approach can be considered. For instance, it is possible to reduce this effect by designing two counter-rotating flywheels connected to a transmotor's shaft.

3.6. 4WD Transmotor-Flywheel-Based Powertrain

According to Fig. 11, the 4WD transmotor-flywheel-based powertrain is made of a conventional electric motor (PMSM in here), and a transmotor-flywheel system. The combination of a transmotor-flywheel system and a PMSM could provide an enhanced performance, which depends on the relative speed of the transmotor's shafts speed at the given vehicle's speed. This could enable us to limit the energy storage media (battery in here) utilization. If the transmotor's shaft connecting to the flywheel has higher angular velocity than the shaft connected to the driveshaft, (i.e., $\omega_{FW} \geq \omega_{W}$), the two electric machines (the transmotor and PMSM) will have an opposite mode of operation. In the other words, when the PMSM is in generating mode, the transmotor is in motoring mode, and vice versa. Table VI summarizes the modes of operation for the 4WD transmotor-flywheel-based powertrain.

The 4WD transmotor-flywheel-based powertrain can operate in zero battery utilization mode if the requirement is met. In the other words, it is possible, in some instances, to deliver

the required electrical power directly from one electric motor to the other one. In this mode, if the vehicle is accelerating, the PMSM will operate in motoring mode and the transmotor will operate in the generating mode. Hence, some of the required mechanical power will be transferred from the flywheel to the rear wheel's magneto-mechanically in a very highly efficient manner. Since the wheel-side speed is lower than the flywheel-side speed, the slip power (the electrical power produces due to the transmotor's shaft speed) is transferred to the PMSM. The slip power, then, is absorbed by the PMSM that is in motoring mode and converted to mechanical power that helps the vehicle acceleration. In order to transfer the entire electrical power to the PMSM, proper torque control is required. In the other words, the higher torque could be inaccessible which will be explained in the next section. It is noteworthy to mention that the battery does not need to supply any electrical energy in a chemical form that could noticeably increase the system's overall efficiency.

Similarly, if all the requirements are met, the transmotor will operate in motoring mode, and the PMSM will be in generating mode, during the vehicle's deceleration. Similar to the vehicle's acceleration, a portion of the recovered kinetic energy will be magneto-mechanically transferred from the rear wheels to the flywheel in a highly efficient manner. Since the transmotor shaft connected to the flywheel is higher than the rear wheel speed ($\omega_{FW} \geq \omega_W$), the kinetic energy recovered from the vehicle's braking is lower than the power absorbed by the flywheel. Therefore, the electrical energy needs to be supplied to the transmotor electrical port. This power can be supplied by the PMSM that is connected to the front shaft if the proper torque control is applied. However, the higher torque could be inaccessible which will be elaborate on later. It is noteworthy to mention that the battery does not need to store any electrical energy in a chemical form that could noticeably increase the system's overall efficiency (Fig.11b)

TABLE VI: Transmotor and PMSM Modes of Operation*				
Mode	Acceleration		Deceleration	
Speed	$\omega_{FW} \geq \omega_W$	$\omega_{FW} < \omega_W$	$\omega_{FW} \geq \omega_W$	$\omega_{FW} < \omega_W$
Transmotor	Gen.	Mot.	Mot.	Gen.
PMSM	Mot.	Mot.	Gen.	Gen.

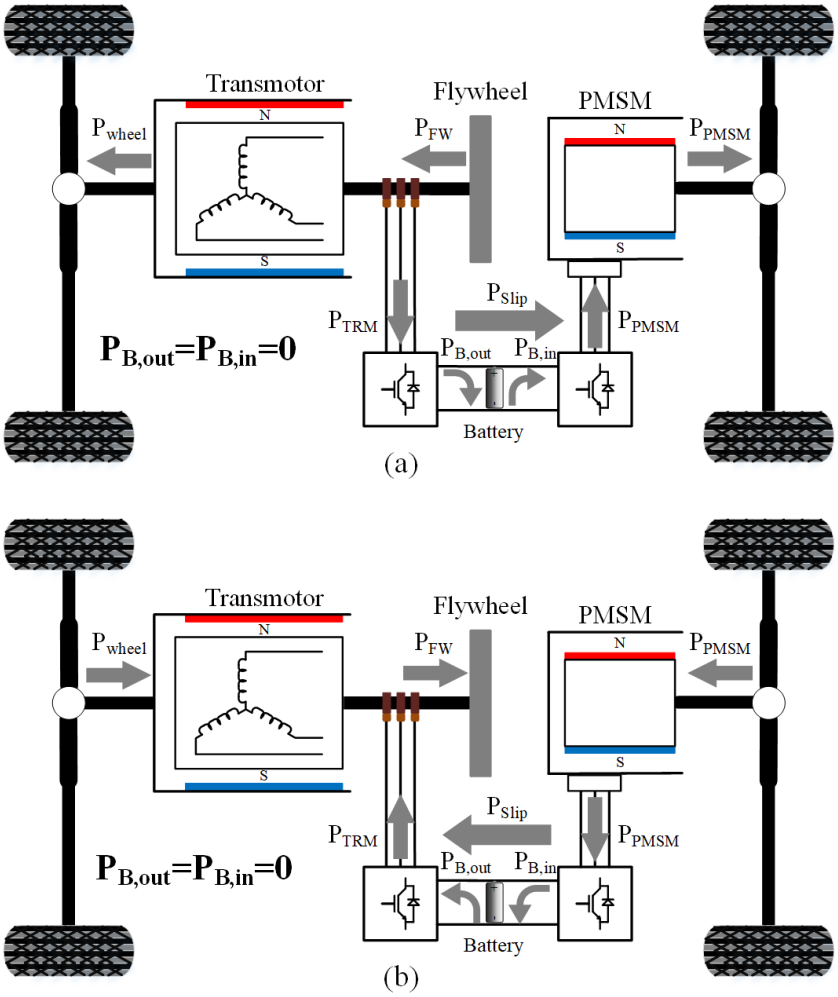

Fig. 11. 4WD Transmotor-Based Powertrain. (a) Acceleration, (b) Deceleration* (Reprinted with permission from [23])

In order to present the vehicle's acceleration and regenerative braking of the 4WD transmotor-flywheel-based powertrain in the zero-battery utilization mode, equations 14-20 need to be valid

to guarantee zero battery utilization mode. The goal, as explained, is to directly transfer power from the PMSM electrical port to the transmotor electrical port in a correct proportion and vice versa [3]. To simplify the equations, mechanical or electrical losses are not included.

$$P_{FW} = P_{TRM} + P_{PMSM} \quad (14)$$

$$T_{TRM}\omega_{FW} = T_{TRM}\omega_{W} + T_{PMSM}\omega_{W} \quad (15)$$

$$T_{Total} = T_{TRM} + T_{PM_{SM}} \quad (16)$$

$$K_1 = \frac{\omega_W}{\omega_{FW}} \quad (17)$$

$$K_2 = 1 - \frac{\omega_W}{\omega_{FW}} = 1 - K_1 \quad (18)$$

$$T_{TRM} = K_1 T_{Total} \quad (19)$$

$$T_{PMSM} = K_2 T_{Total} \quad (20)$$

3.7. Transmotor-Flywheel 4WD Powertrain Boundaries and Limitations

Only if the transmotor's shaft connected to the flywheel has a greater angular velocity than the transmotor's shaft connected to the flywheel, zero-battery utilization is feasible (Fig. 11). Otherwise, the operation modes of the transmotor and PMSM are the same, and either they both inject power to the electrical port or the need to be supplied by the energy storage media (battery in here). If the driving cycle in the immediate future is predictable, the flywheel speed can be adjusted accordingly, but in manual driving that could be challenging.

Furthermore, the torque input/output of the PMSM and transmotor's need to be in a way that transferred power from one electric motor to the other one is equal. In the other words, the total maximum torque of both machines is not available, which could reduce the vehicle's performance in zero-battery utilization mode. For instance, let's assume the transmotor and PMSM as the same rated torque equal to 1pu, as is shown in equations 21 and 22.

$$0pu < T_{PMSM} < 1pu \quad (21)$$

$$0pu < T_{TRM} < 1pu \quad (22)$$

If the torque of these two electrical machines were independent, the total torque would be limited to 2pu, as is shown in equation 23.

$$0pu < T_{total} < 2pu \quad (23)$$

However, since the torque of the transmotor and PMSM need to be in a way that the electrical power exchanged between the two electric motors is equal, the total output torque cannot be any number between 0 and 2pu (equations 24 and 25).

$$T_{PMSM} = K_1 T_{Total}, 0 < K_1 < 1 \quad (24)$$

$$T_{TRM} = (1 - K_1)\, T_{Total}, 0 < K_1 < 1 \quad (25)$$

Therefore, the total torque can be presented as following equations (equations 26 and 27).

$$T_{total} = \frac{1}{1 - K_1} T_{TRM}, 0 < K_1 \leq 0.5 \quad (26)$$

$$T_{total} = \frac{1}{K_1} T_{PMSM}, 0.5 \leq K_1 < 1 \quad (27)$$

Fig. 12 presents the explained torque constraint. The x-axis is the possible value of the K_1, and the y-axis is the total available torque under zero battery utilization mode. According to fig. 12, the maximum torque (2 pu) is only available at K_1=0.5, when the transmotor's shaft's angular velocity connected to the wheel is twice the other shaft. In the worst-case scenario, if K_1 is equal to 0 or 1, only half of the total torque is available (1 pu).

The torque constraint is only valid if the powertrain works in zero-battery utilization mode. If it is desired to switch from this mode to conventional mode, the vehicle can retain its full performance. However, while zero-battery utilization mode can help the overall efficiency and

battery state of health, the battery power rating needs to be designed for the worst-case scenario. Therefore, the battery power rating, while utilized less intensively, need to be the same as the conventional electric vehicles.

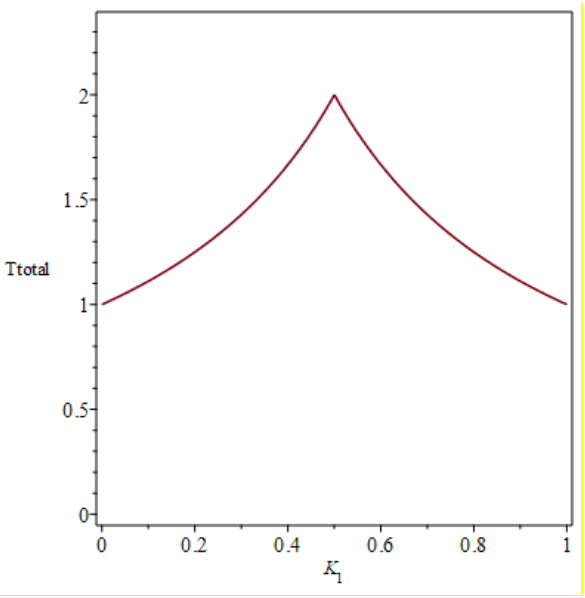

Fig. 12: The Transmotor-Based 4WD Powertrain Total Available Per-Unit Torque Limit with Respect to K_1^* (Reprinted with permission from [23])

It is worth mentioning that in the 4wd transmotor-flywheel-based powertrain, two electric motors and more power electronic components are required which could affect the initial vehicle cost and limit the applications to a large vehicle.

3.8. Transmotor-Flywheel Powertrain Assisted by An Ultracapacitor

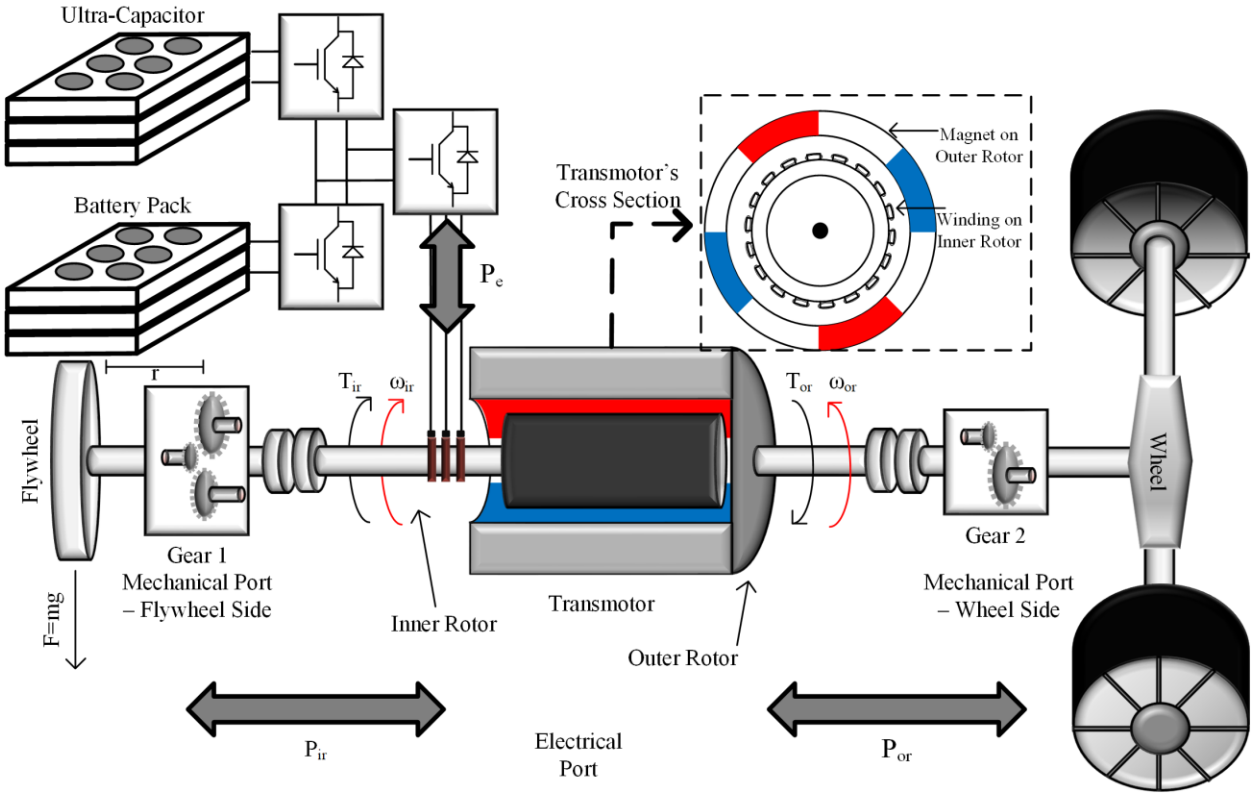

Fig. 13. The Proposed Transmotor-Based Powertrain Assisted by an Ultracapacitor (Reprinted with permission from [36])

Alternatively, it is feasible to improve the transmotor-flywheel powertrain by adding a small ultracapacitor pack between the transmotor's electrical port and battery pack to manage the high-power demand during the vehicle's acceleration or deceleration. Fig. 13 presents the transmotor-flywheel powertrain enhanced by an ultracapacitor. The flywheel-transmotor-wheel connection is similar to what is reviewed in this chapter. However, as mentioned, the ultracapacitor is placed between the battery pack and the transmotor's electrical port (fig. 14). The voltage of the ultracapacitor and the DC-bus are controlled at all times via DC/DC converters. The ultracapacitor voltage needs to be in a specific range. If exceeding the maximum voltage it could damage the component, especially the ultracapacitors, and if the voltage is bellowing the minimum, the DC-bus , and consequently, the powertrain performance could be affected. It is noteworthy to

mention that the ultracapacitor set point needs to be dynamically corrected according to the speed difference between the flywheel and the driveshaft (transmotor's mechanical ports).

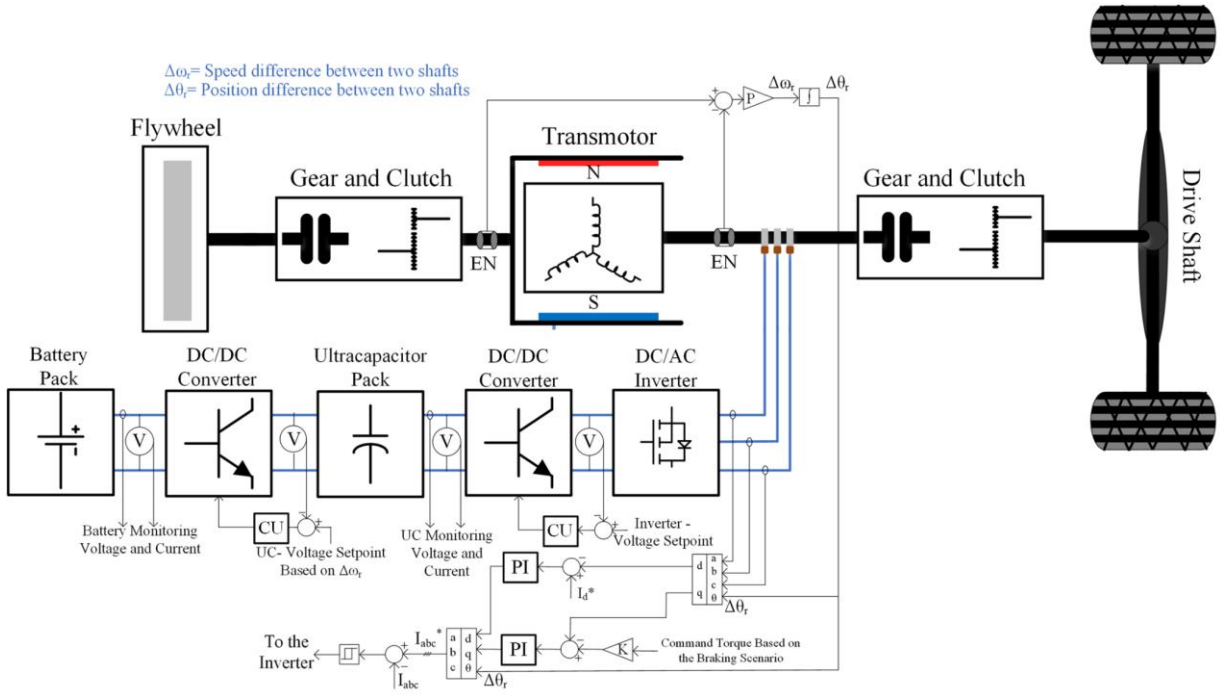

Fig 14: Transmotor-Flywheel Powertrain Assisted with Ultracapacitor's Control Diagram* (Reprinted with permission from [36])

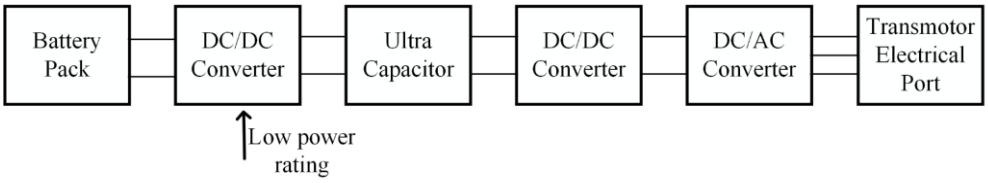

Fig 15: Transmotor-Flywheel Powertrain Assisted by an Ultracapacitor* (Reprinted with permission from [36])

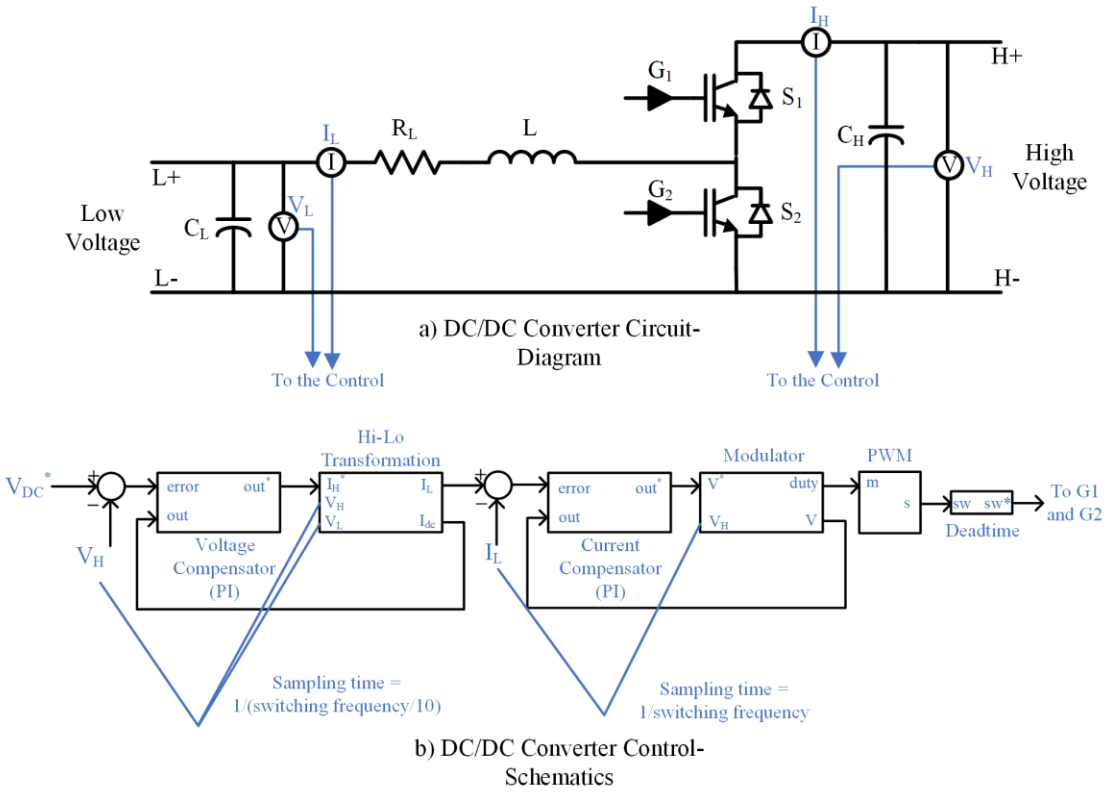

Fig 16: DC/DC Converter Utilized in This Simulation: a) Circuit Diagram b) Control Schematics* (Reprinted with permission from [36])

For instance, when the transmotor's shaft has the same angular velocity, the ultracapacitor voltage has to be set to its maximum, and the ultracapacitor voltage has to be set to near its minimum when the speed difference between the transmotor's shaft is the largest. In the case of the multi-gear utilization in the flywheel transmotor interface, the ultracapacitor voltage will follow the same logic, and it mainly depends on the flywheel referred speed to the transmotor side.

Various configurations can be considered for connecting the ultracapacitor to the battery pack and the electric motor, as reviewed in [3, 26]. Each of these configurations is associated with its advantages and drawbacks. In the proposed powertrain, the cascaded configuration, type I, is chosen to connect the ultracapacitor to the system, as is shown in Fig 15. This topology lets us

have precise control over the battery and ultracapacitor power flow that improve the system performance and the life of the battery pack. However, due to the required complex control approach and sophisticated power electronic structure, it could be more expensive and challenging in comparison to the available interfaces.

The DC/DC converter connecting the battery pack and ultracapacitor has the same power rating as the battery pack power rating. However, as was mentioned, in the transmotor-flywheel powertrain, assisted by an ultracapacitor, the maximum power rating of the battery could be reduced significantly. Thus, the DC/DC converter between the battery pack and the ultracapacitor has a low power rating. Moreover, in this topology, it is possible to use a battery pack with a lower voltage rating that could reduce the cost and ease the manufacturing process and reduce battery failure. The detailed utilized DC/DC converter topology is presented in fig. 16.

Let us assume the vehicle is at standstill, and the flywheel speed is set to its initial value, which usually is adjusted to be near its maximum speed. Now assume, the driver decides to increase the vehicle speed. At the beginning of the vehicle acceleration process, since the vehicle drive shaft, angular velocity is lower than the flywheel's angular velocity, the power provided by the flywheel is greater than the power that the drive shaft can absorb, so the extra energy should be absorbed by the electrical port (Region I in Fig. 17). If the driver continues to accelerate the vehicle, at some point, the drive shaft speed exceeds the flywheel speed, and subsequently, the power provided by the flywheel to the drive shaft will be inadequate. Thus, the electrical port needs to inject energy into the system (Region II in Fig. 17). The same explanation provided for vehicle acceleration applies to vehicle braking. During the vehicle braking, when the drive shaft speed is greater than the flywheel speed, the power provided by the drive shaft is greater than the amount that the

flywheel can absorb, and thus, the extra energy needs to be absorbed by the electrical port (Region I in Fig. 17).

As the vehicle speed decreases, the electrical power that the drive shaft can provide will be less than the amount of energy that the flywheel can absorb, and thus, the electrical port should inject energy into the system (Region II in Fig. 17).

Due to this complementary behavior of the power flow in the transmotor-flywheel powertrain, a power buffer (power source) with a high-power density and low energy density, such as an ultracapacitor pack, can be used. It is noteworthy to mention that the high energy density storage media such as battery or fuel cell is still required to provide energy in sustained low power conditions, such as cruising over a long time.

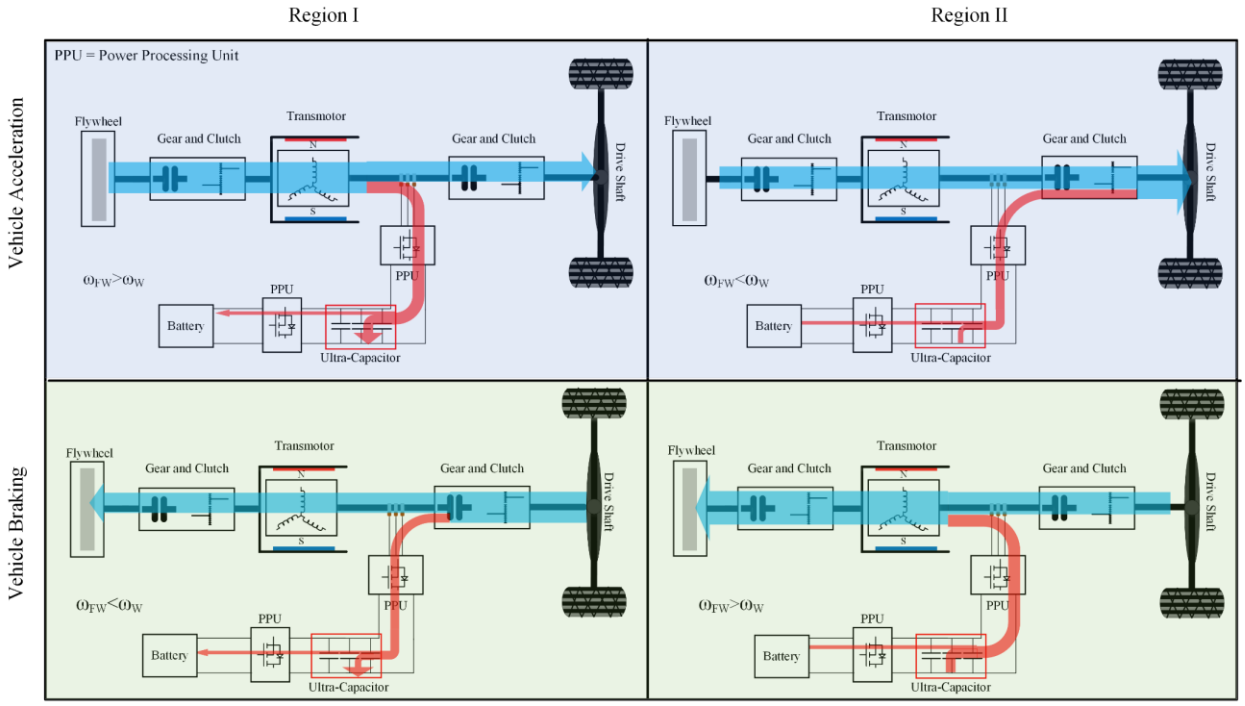

Fig 17: Transmotor-Flywheel Powertrain Assisted by an Ultracapacitor- Power Flow *(Reprinted with permission from [36])

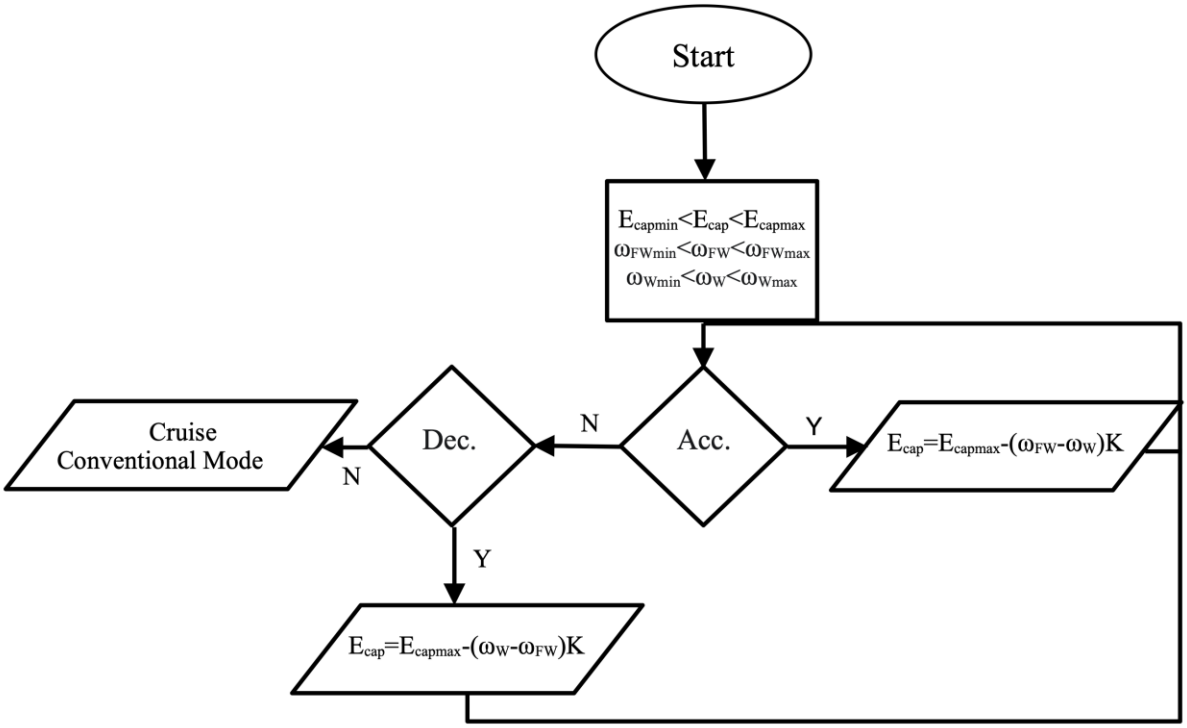

Fig 18. Transmotor-Flywheel Powertrain Assisted by an Ultracapacitor - Voltage Setpoint

The ultracapacitor size can be further optimized by proper voltage control depending on the vehicle's current speed and the flywheel speed. Fig. 18 presents a flowchart that how we can control the ultracapacitor and flywheel in various situations. It is assumed that the capacitor voltage (E_{cap}), flywheel (ω_{FW}), and wheel (ω_{W}) referred speed to the transmotor have lower (min) and upper limit (max).

If the goal is to increase the vehicle's speed, then the capacitor voltage should be adjusted by equation 28. If the goal is to decelerate the vehicle, then equation 29 needs to be utilized as is shown in Fig 14. K is a constant related to the powertrain parameter with the V/rpm unit.

$$E_{cap} = E_{capmax} - \left(\omega_{FW} - \omega_{W} \right) K \tag{28}$$

$$E_{cap} = E_{capmax} - \left(\omega_{W} - \omega_{FW} \right) K \tag{29}$$

4. SIMULATION OF BRAKING SCENARIOS

This chapter provides a series of simulations to compare the Chevrolet bolt powertrain, the transmotor-flywheel powertrain [36], and the transmotor-flywheel powertrain assisted by ultracapacitor in various vehicle braking scenarios.

In these braking scenarios, it is assumed that the vehicle's initial speed is 60 mph, and the target is to reach the full stop at a designated time to emulate various braking intensities. All the competing powertrain technologies are utilized in such a way to absorb the maximum possible kinetic energy of the vehicle. If the electrical (regenerative) braking is not sufficient, the mechanical brake will be engaged, and the remained vehicle kinetic energy will be dissipated in the form of heat.

4.1. Simulation Environment

The simulated braking scenarios in this chapter are implemented by utilizing a software package, PLECS from Plexim Company. Fig. 19 and Fig. 14 show the control diagram of the transmotor-flywheel and the transmotor-flywheel assisted by an ultracapacitor, respectively.

Space vector theory is utilized in order to control the torque and speed of the vehicle. The position difference of the shafts is estimated by the encoders installed on the transmotor's shaft, and it is utilized to refer the three phases (abc) to synchronous frame (dq) as mentioned in Chapter 3. The hysteresis control strategy is chosen in order to regulate the DC/AC converter connected to any of the mentioned powertrain technology. However, it is possible to utilize space vector PWM or other methods to implement the current regulation.

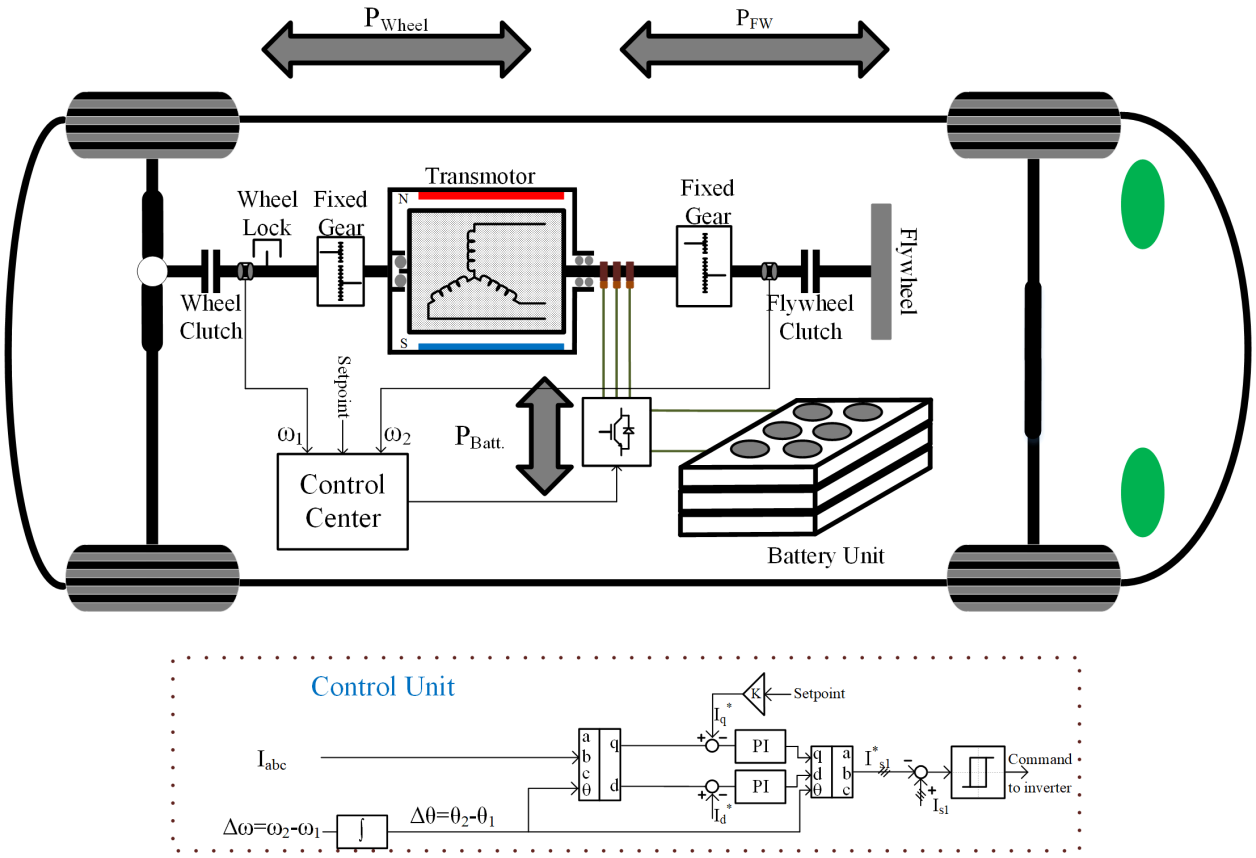

Fig 19. Transmotor-Flywheel Powertrain Assisted by an Ultracapacitor-Control Diagram

As shown in Fig. 19, the speed of both shafts needs to be measured and the speed differentiation is used to control the I_q and I_d. Furthermore, the three-phase current of the inner rotor is measured to control the transmotor power flow. The speed of the flywheel should also be considered in order to effectively manage it as a power buffer (power source).

For the transmotor-flywheel assisted by an ultracapacitor same approach as the transmotor-flywheel powertrain can be adopted. However, the voltage of the ultracapacitor, the angular velocity of the flywheel speed as well as the vehicle speed needs to be considered. That's why, as shown in Fig. 15, two DC/DC converters are also considered in the control schematics.

The voltage and the current of the battery and ultracapacitor pack need to be monitored at all times, as shown in Fig. 14. The DC/DC converter circuit schematic and control diagram utilized

in this study is exhibited in Fig. 16. The current control mode is adopted to have precise control over voltage and current of the individual energy storage media (main and auxiliary energy storage medias) [34].

4.2. The Braking Scenarios

In this subsection, the Chevrolet Bolt, the transmotor-flywheel [21-24], and the transmotor-flywheel powertrain enhanced by the ultracapacitor powertrain, are compared in various braking scenarios. the vehicle's initial speed is set to be 60 mph, and the target of the scenario is to reach a full stop in 4, 8, 12, and 16 seconds, respectively. This initial condition is chosen to emulate various braking scenarios, from harsh to mild vehicle braking, from a high vehicle speed.

Fig. 20 presents the maximum braking power required for a 1600 kg vehicle that has an initial speed equal to 60 mph. For instance, if the target is to stop the vehicle in 4 seconds, the maximum power required to achieve this braking requirement is about 280 kW. The majority of the kinetic energy of the vehicle can be recuperated if the power rating of the vehicle powertrain (including the energy storage media power rating) is greater or equal to this number.

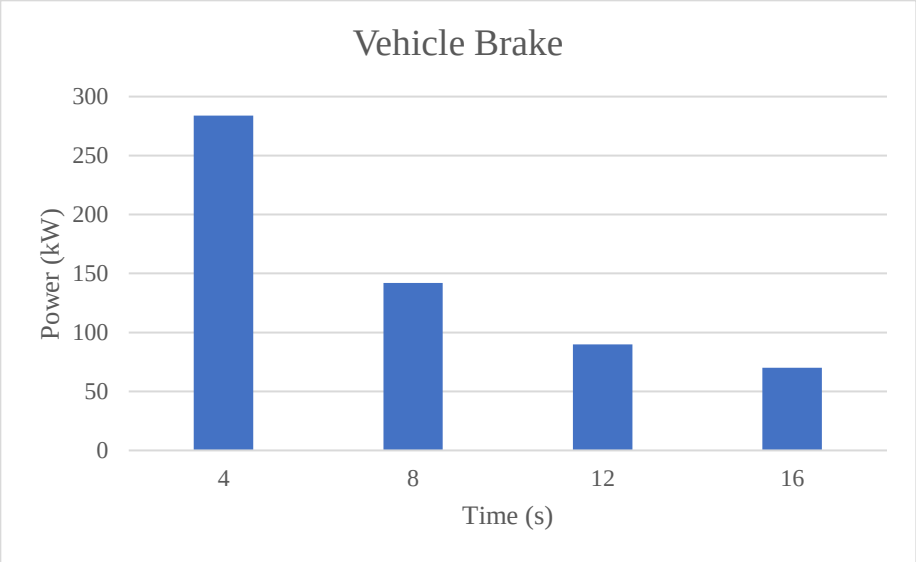

Fig 20. Maximum Required Power to Stop A 1600 kg Vehicle Moving 60 mph in the Given Time

Tables VII, VIII, and IX present the stock Chevrolet bolt, the transmotor-flywheel equipped vehicle, and the car with the transmotor-flywheel assisted by an ultracapacitor technology, respectively. All the vehicles in this simulation have a mass of around 1600 kg. However, the electric propulsion system and/or energy storage media are different. The Chevrolet Bolt, representing a conventional BEV, is equipped with a 150 kW Permanent Magnet Synchronous Motor (PMSM), and a 160kW battery pack as main storage media. In the transmotor-flywheel powertrain, the PMSM is replaced by a 150 kW transmotor, and the second mechanical shaft of the transmotor is connected to a 16 Kg flywheel as an auxiliary energy storage media (power source). Finally, the transmotor-flywheel assisted by an ultracapacitor powertrain has the same transmotor that was utilized in the transmotor-flywheel powertrain, but a small ultracapacitor pack is added to the electrical port. Hence, the battery pack is utilized as the main energy storage media and the flywheel and ultracapacitor as auxiliary storage media (power sources). As a result of utilizing two power sources in this powertrain, the battery pack is only needed in cases of low power demands, and thus, the power rating has reduced significantly (from 160 kW to 30 kW).

Table VII: Chevrolet Bolt Powertrain Parameters		
General Information		
Parameter	Unit	Value
Total vehicle mass	kg	1620
Maximum torque on the wheels	Nm	2500
Electric Motor (PMSM) /Battery		
Electrical power rating	kW	150
Battery power rating	kW	(-70, 160)

Table VIII: Transmotor-Flywheel Powertrain Parameters		
General Information		
Parameter	Unit	Value
Total vehicle mass	kg	1640
Maximum torque on the wheel	Nm	2500
Electric Motor (Transmotor)/Battery		
Electrical power rating	kW	150
Battery Power rating	kW	(-70, 160)
Power Buffer(s)		
Flywheel		
Inertia	Kgm^2	1
Mass	Kg	16
Max. Angular Velocity	rpm	16000
Max. Energy	MJ	1.2

Table IX: Transmotor-Flywheel Powertrain Assisted by an Ultracapacitor Parameters		
General Information		
Parameter	Unit	Value
Total vehicle mass	Kg	1660
Maximum torque on the wheel	Nm	2500
Electric Motor (Transmotor)/Battery		
Electrical power rating	kW	150
Battery Power rating	kW	(-15, 30)
Battery pack voltage	V	150
Battery pack current	A	167
Power Buffers		
Ultracapacitor		
Parameter	Unit	Value
Capacitance	F	6
Voltage	V	300
Mass	Kg	15
Flywheel		
Inertia	Kgm^2	1
Mass	Kg	16
Max. Angular Velocity	rpm	16000
Max. Energy	MJ	1.2

4.3. Detailed Simulation Result of The Braking Scenarios

4.3.1. Braking Scenario: 60-0 mph in 16 seconds

Fig. 21 presents a simplified rendition of the vehicle. "F_{brake}", "T_{brake}", "V", and "P" are the vehicle braking force, braking torque, speed and braking power, respectively. Fig. 22 presents the values of the required F_{brake}, T_{brake}, V and P to reduce the vehicle speed from 60 mph to full stop in 16 seconds to emulate the mild braking scenario. A braking force equal to 2.59 kN is required to meet the braking scenario. The braking force, as the wheel radius of the vehicle is 35 cm, can be estimated to be around 850 Nm. In this braking scenario, 568kJ kinetic energy needs to be processed in 16 seconds. It is noteworthy to mention that not all of this energy is recoverable as some of it will be consumed for loads such as air drag and rolling resistance. Thus, only 493 kJ of the 568 kJ is recoverable in this braking scenario.

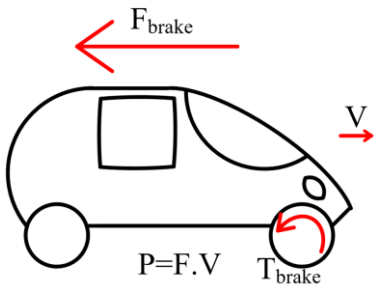

Fig. 21. Simplified Rendition of the Vehicle During a Braking Episode

Fig. 23 presents the regenerative braking capability of each powertrain technology in the described braking scenario. As is shown in Fig. 23, the Chevrolet Bolt powertrain is able to recover about 81% of the total available vehicle kinetic energy (400 kJ) during this braking scenario. Furthermore, the transmotor-flywheel powertrain can recuperate about 419 kJ in this braking scenario which is about 83% of the total available vehicle kinetic energy. Finally, the transmotor-flywheel powertrain equipped with the ultracapacitor can recover about 452 kJ in this braking scenario which is roughly about 92% of the total available vehicle kinetic energy.

In the case of the first two powertrains, Chevrolet bolt, and transmotor-flywheel powertrains, a full-size battery is required in their design. However, the battery power rating in the case of the transmotor-flywheel powertrain equipped with the ultracapacitor can be reduced by about 80%. Thus, the battery charging and discharging rate can be reduced to around -15 kW and 30 kW, respectively.

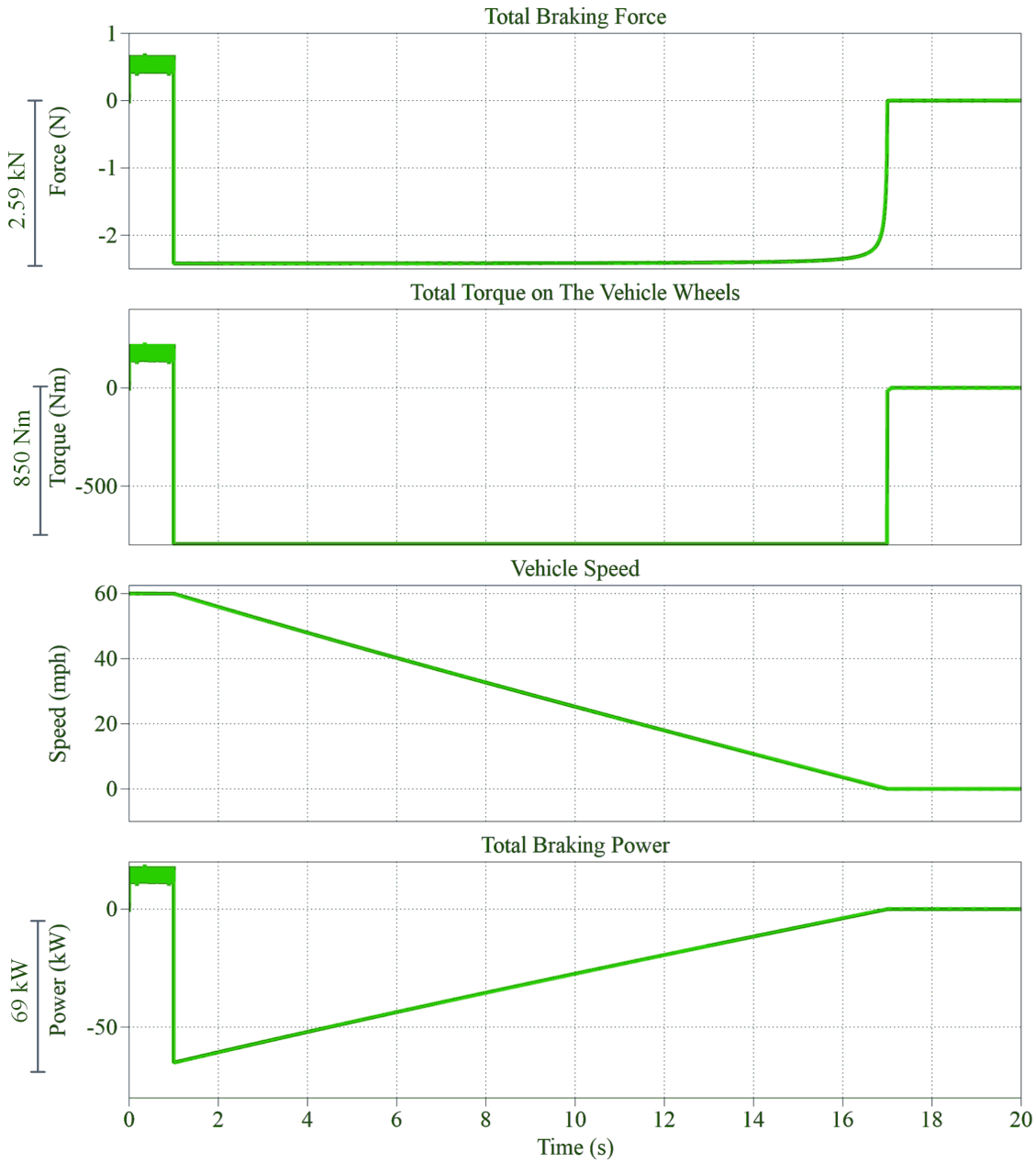

Fig 22. Required Force and Torque to Stop the Vehicle with an Initial Speed of 60 mph in 16 Seconds

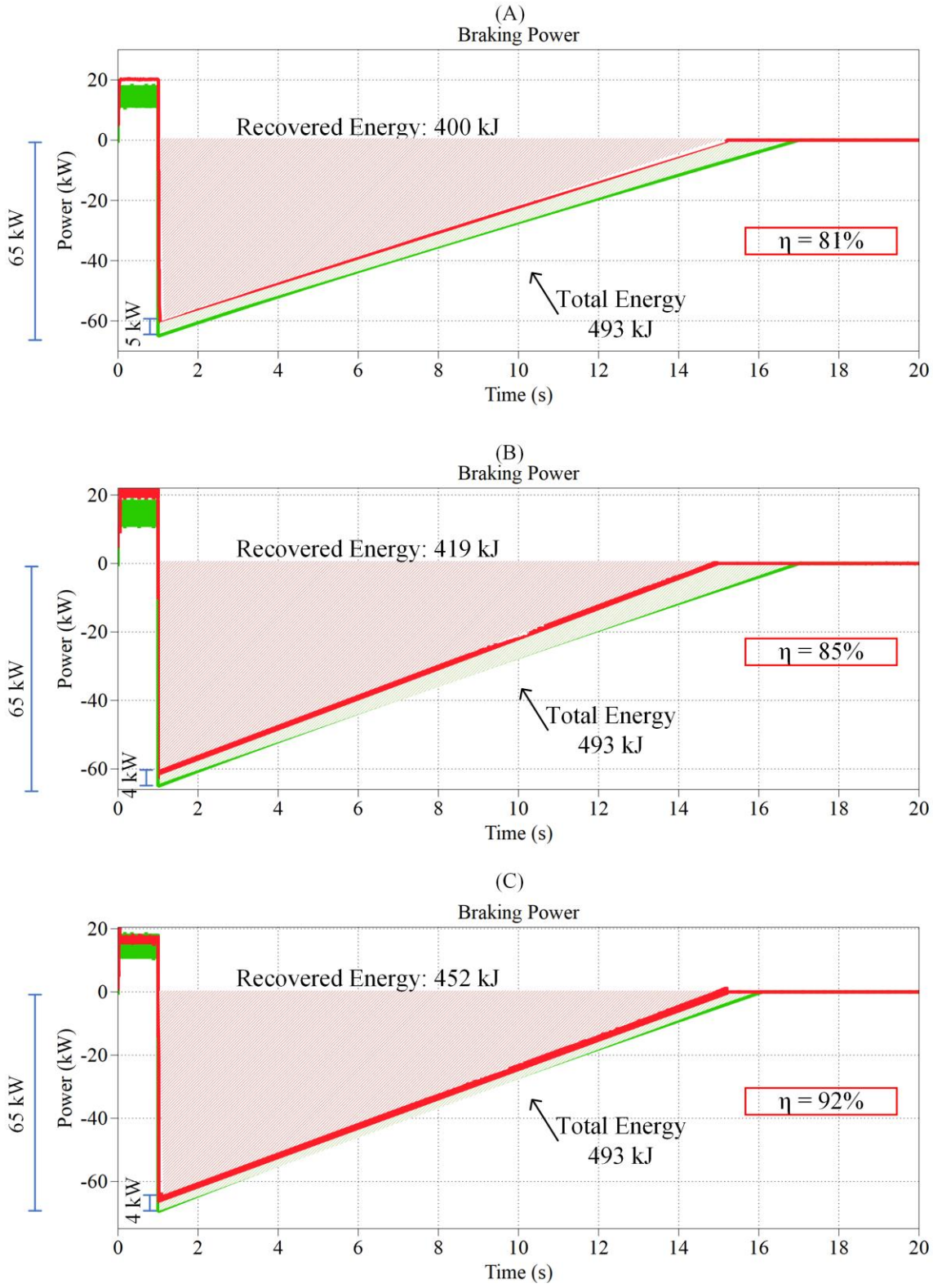

Fig. 23. The Energy and Power Management of Each Powertrain in the Described Braking Scenario Simulation: (A) Chevrolet Bolt Powertrain (B) Transmotor-Flywheel Powertrain (C) Transmotor-Flywheel Powertrain Assisted by an Ultracapacitor (16 Seconds)

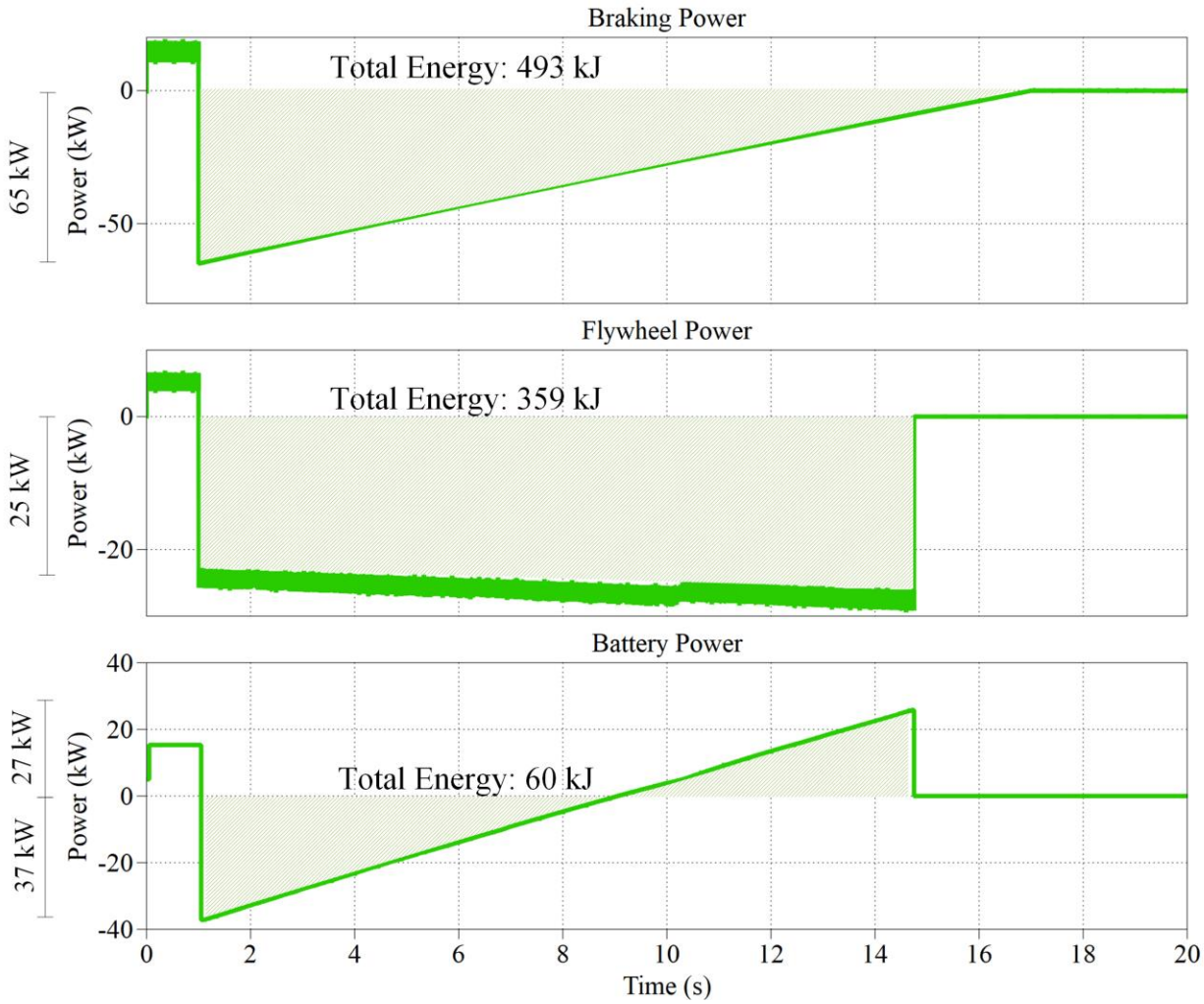

Fig 24. Detailed Energy and Power Management of the Transmotor-Flywheel Powertrain (16 Seconds)

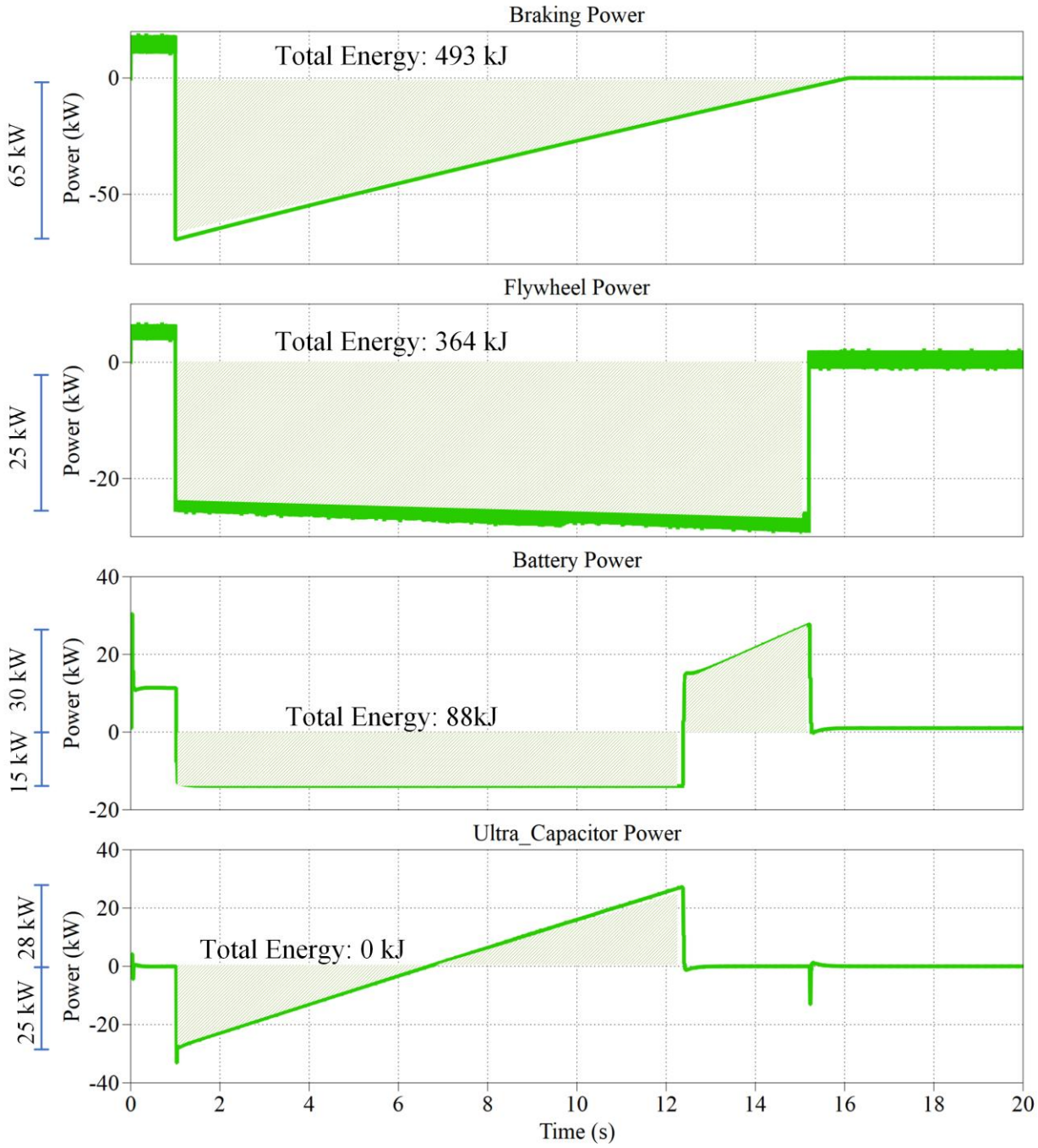

Fig 25. Detailed Energy and Power Management of the Proposed Powertrain (16 Seconds)

Fig. 24 exhibits the power and energy distribution associated with the transmotor-flywheel powertrain, including the battery (main energy storage media) and the flywheel (auxiliary energy storage media) during the braking scenario. As is shown in Fig. 24, around 359 kJ of the total recoverable energy (493 kJ) is stored in the power source (flywheel), while the battery

momentarily absorbs 140 kJ, and then supplied about 80 kJ of the stored energy back to the transmotor. It is worth mentioning that a full-size battery is still needed (160 kW) to process the electrical power. During this process, the flywheel speed changes from 13.4 krpm to 15.6 krpm.

Fig. 25 shows the power and energy distribution associated with the transmotor-flywheel powertrain assisted by an ultracapacitor, including the battery (main energy storage media), ultracapacitor (power source 1), and flywheel (power source 2) during the braking scenarios. As is shown in Fig 25, about 364 kJ is restored to the flywheel during the braking scenario. The battery power is designed to be limited to -15 kW and 30 kW. During this braking scenario about 88 kJ is absorbed by the battery. However, the ultracapacitor mainly processes the high electrical power demands which reach 25 kW in the mild braking scenario. The utilized ultracapacitor does not need to have high energy density as it is mainly used as a power buffer. For instance, in this braking scenario, the maximum energy cycled by the ultracapacitor is 78 kJ. During this process the flywheel speed changes from 13.4 krpm to 15.60 krpm.

Fig. 26 presents the ultracapacitor voltage change of the transmotor-flywheel assisted by ultracapacitor technology. During the first six seconds of the braking scenario (1-7 seconds), because the driveshaft side speed is more than the flywheel side speed ($\omega_w > \omega_{Fw}$), the ultracapacitor stores energy, and hence, the ultracapacitor voltage increases from 200 V to 258 V (Region I). However, when the drive shaft speed subceed the flywheel speed ($\omega_w < \omega_{Fw}$) the ultracapacitor begins to supply power into the system. Thus, the ultracapacitor voltage returns back to its initial voltage (200 V) (Region II). Finally, from 12.5 to 14.5 seconds, the ultracapacitor stops supplying the energy, and battery start providing the energy to preserve the ultracapacitor voltage.

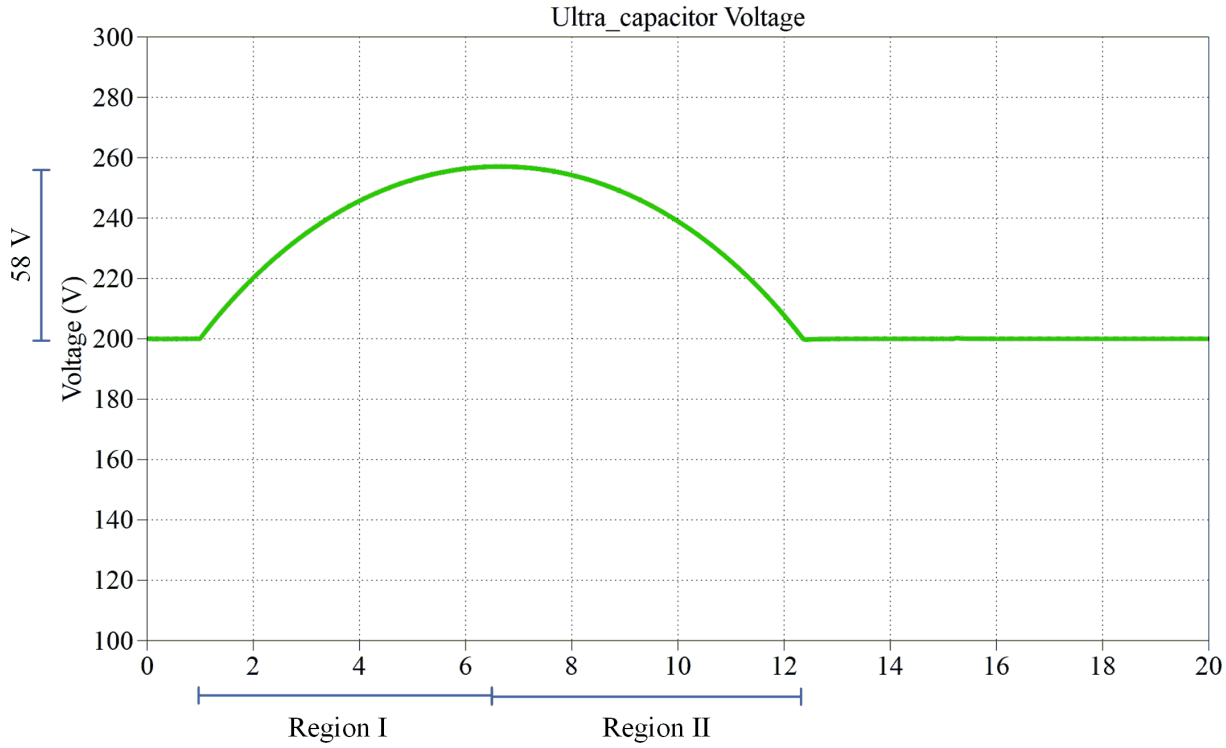

Fig 26. Ultracapacitor Voltage Variation in the Proposed Powertrain (16 Seconds)

4.3.2. Braking Scenario: 60-0 mph in 12 seconds

Fig. 21 presents a simplified rendition of the vehicle. "F_{brake}", "T_{brake}", "V", and "P" are the vehicle braking force, braking torque, speed, and braking power, respectively. Fig. 27 presents the values of the required F_{brake}, T_{brake}, V, and P to reduce the vehicle speed from 60 mph to full stop in 12 seconds to emulate a mild to moderate braking scenario. A braking force equal to 3.32 kN is required to meet the braking scenario. The braking force, as the wheel radius of the vehicle is 35 cm, can be estimated to be around 1093 Nm. In this braking scenario, 568kJ kinetic energy needs to be processed in 12 seconds. It is noteworthy to mention that not all of this energy is recoverable as some of it will be consumed for loads such as air drag and rolling resistance. Thus, only 512 kJ of the 568 kJ is recoverable.

Fig. 28 presents the regenerative braking capability of each powertrain technology in the described braking scenario. As is shown in Fig. 28, the Chevrolet Bolt powertrain is able to recover about 78% of the total available vehicle kinetic energy (400 kJ) during this braking scenario. Furthermore, the transmotor-flywheel powertrain can recuperate about 438 kJ in this braking scenario which is about 86% of the total available vehicle kinetic energy. Finally, the transmotor-flywheel powertrain equipped with the ultracapacitor can recover about 470 kJ in this braking scenario which is roughly about 92% of the total available vehicle kinetic energy.

In the case of the first two powertrains, Chevrolet bolt, and transmotor-flywheel powertrains, a full-size battery is required in their design. However, the battery power rating in the case of the transmotor-flywheel powertrain equipped with the ultracapacitor can be reduced by about 80%. Thus, the battery charging and discharging rate can be reduced to around -15 kW and 30 kW, respectively.

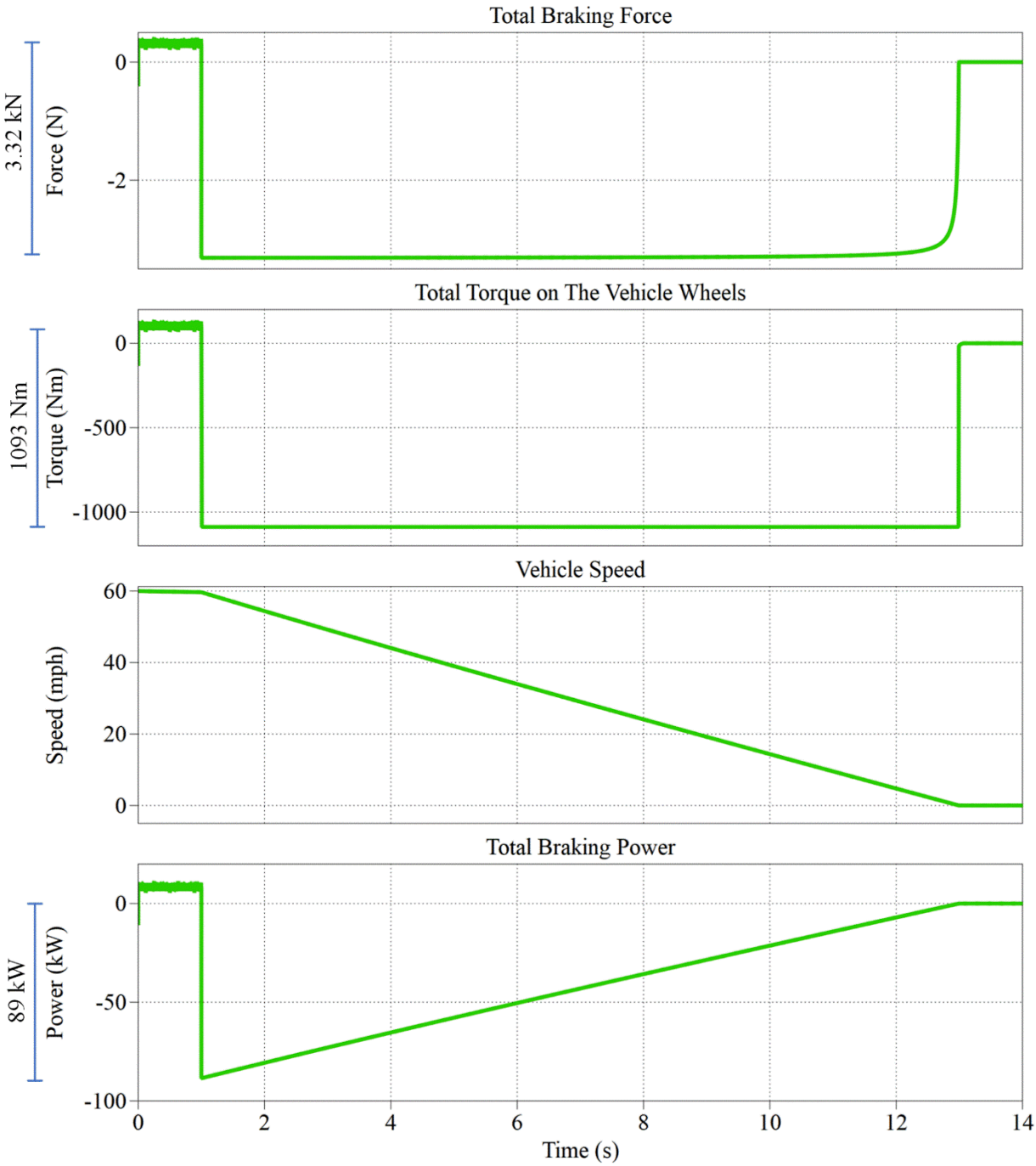

Fig 27. Required Force and Torque to Stop the Vehicle with an Initial Speed of 60 mph in 12 Seconds

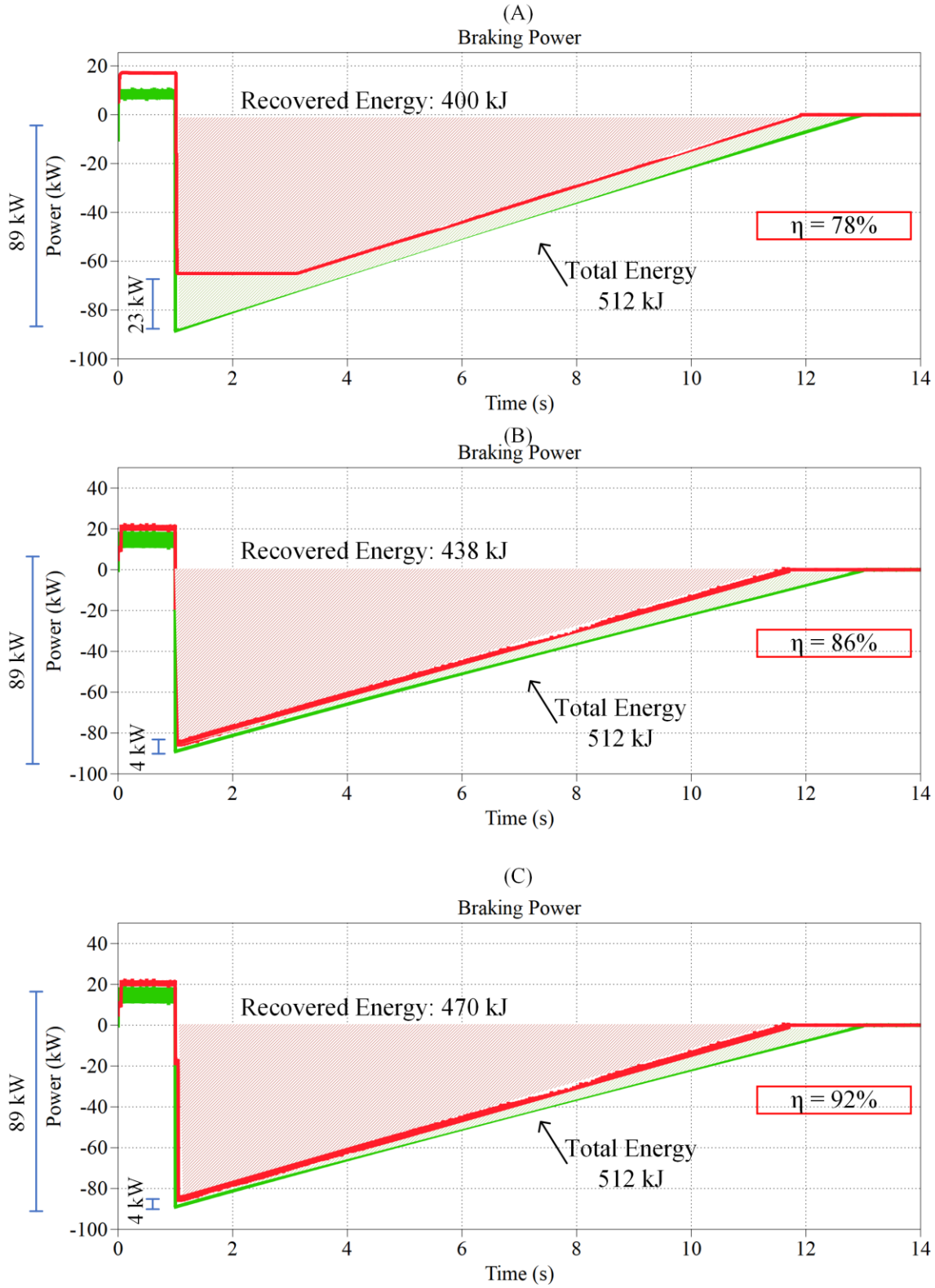

Fig. 28. The Energy and Power Management of Each Powertrain in the Described Braking Scenario Simulation: (A) Chevrolet Bolt Powertrain (B) Transmotor-Flywheel Powertrain (C) Transmotor-Flywheel Powertrain Assisted by an Ultracapacitor (12 Seconds)

Fig. 29 exhibits the power and energy distribution associated with the transmotor-flywheel powertrain, including the battery (main energy storage media) and the flywheel (auxiliary energy storage media) during the braking scenario. As is shown in Fig. 29, around 380 kJ of the total recoverable energy (512 kJ) is stored in the power source (flywheel), while the battery momentarily absorbs 168 kJ, and then supplied about 110 kJ of the stored energy back to the transmotor. It is worth mentioning that a full-size battery is still needed (160 kW) to process the electrical power. During this process, the flywheel speed changes from 13.4 krpm to 15.7 krpm.

Fig. 30 shows the power and energy distribution associated to the transmotor-flywheel powertrain, assisted by ultracapacitor, including the battery (main energy storage media), ultracapacitor (power source 1), and flywheel (power source 2) during the braking scenarios. As is shown in Fig. 30, about 348 kJ is restored to the flywheel during the braking scenario. The battery power is designed to be limited to -15 kW and 30 kW. During this braking scenario about 122 kJ is absorbed by the battery. However, the ultracapacitor mainly processes the high electrical power demands which reach 42 kW in the mid-harsh braking scenario. The utilized ultracapacitor does not need to have high energy density as it is mainly used as a power source. For instance, in this braking scenario, the maximum energy cycled by the ultracapacitor is 97 kJ. During this process, the flywheel speed changes from 13.4 krpm to 15.6 krpm.

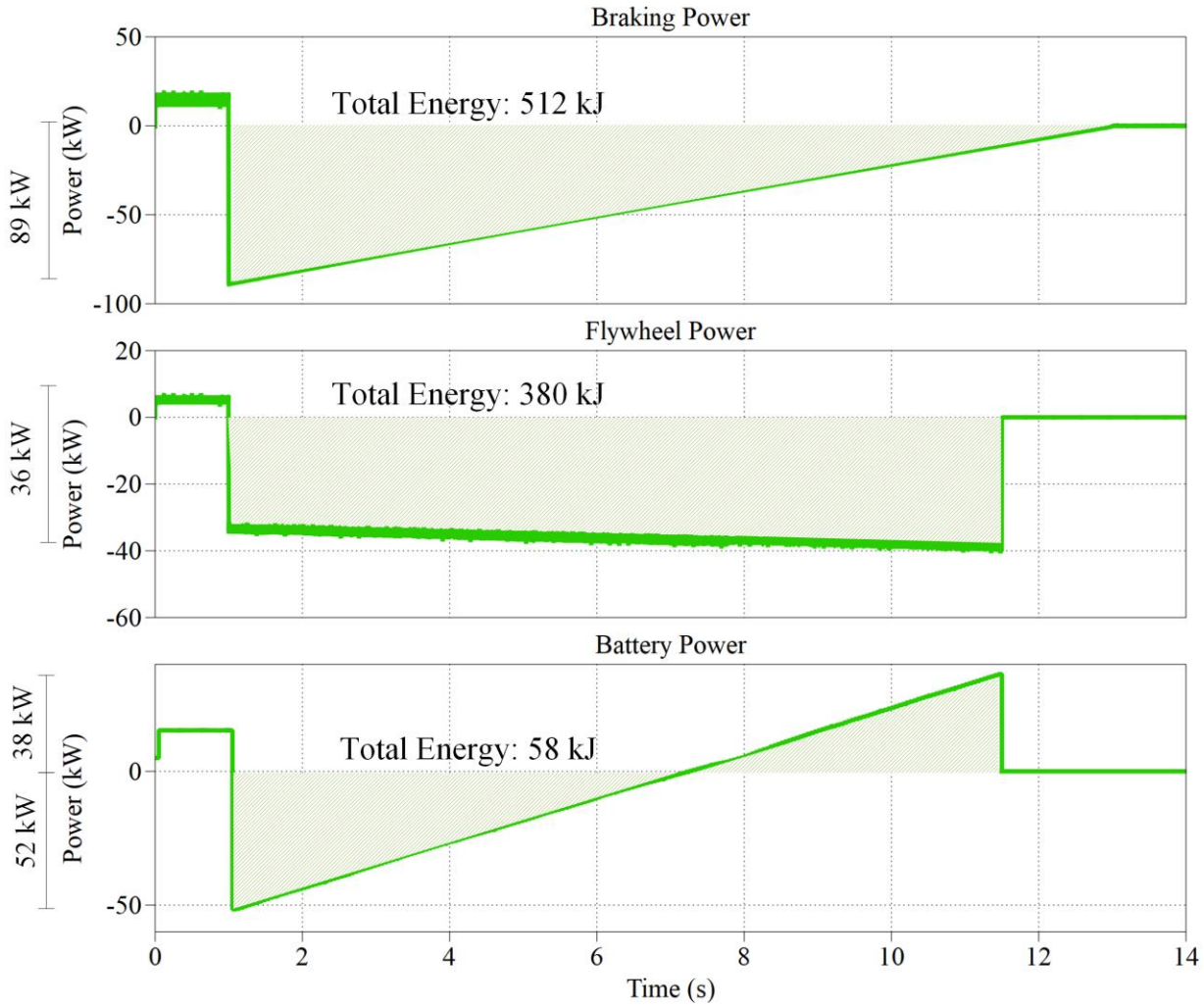

Fig 29. Detailed Energy and Power Management of the Transmotor-Flywheel Powertrain (12 Seconds)

Fig. 31 presents the ultracapacitor voltage change of the transmotor-flywheel assisted by ultracapacitor technology. During the first five seconds of the braking scenario (1-6 seconds), because the driveshaft side speed is more than the flywheel side speed ($\omega_w > \omega_{Fw}$), the ultracapacitor stores energy, and hence, the ultracapacitor voltage increases from 200 V to 273 V (Region I). However, when the drive shaft speed subceed the flywheel speed ($\omega_w < \omega_{Fw}$) the ultracapacitor begins to supply power to the system. Thus, the ultracapacitor voltage returns back to its initial voltage (200 V) (Region II). The battery does not need to supply any power during this braking scenario as the ultracapacitor charge/discharge is symmetrical. Note that because of this

complementary power flow behavior of this topology, the needed ultracapacitor in this technology is relatively small. The utilized ultracapacitor pack for this design has 6F capacitance and 300 V maximum which has a total mass of around 16 kg.

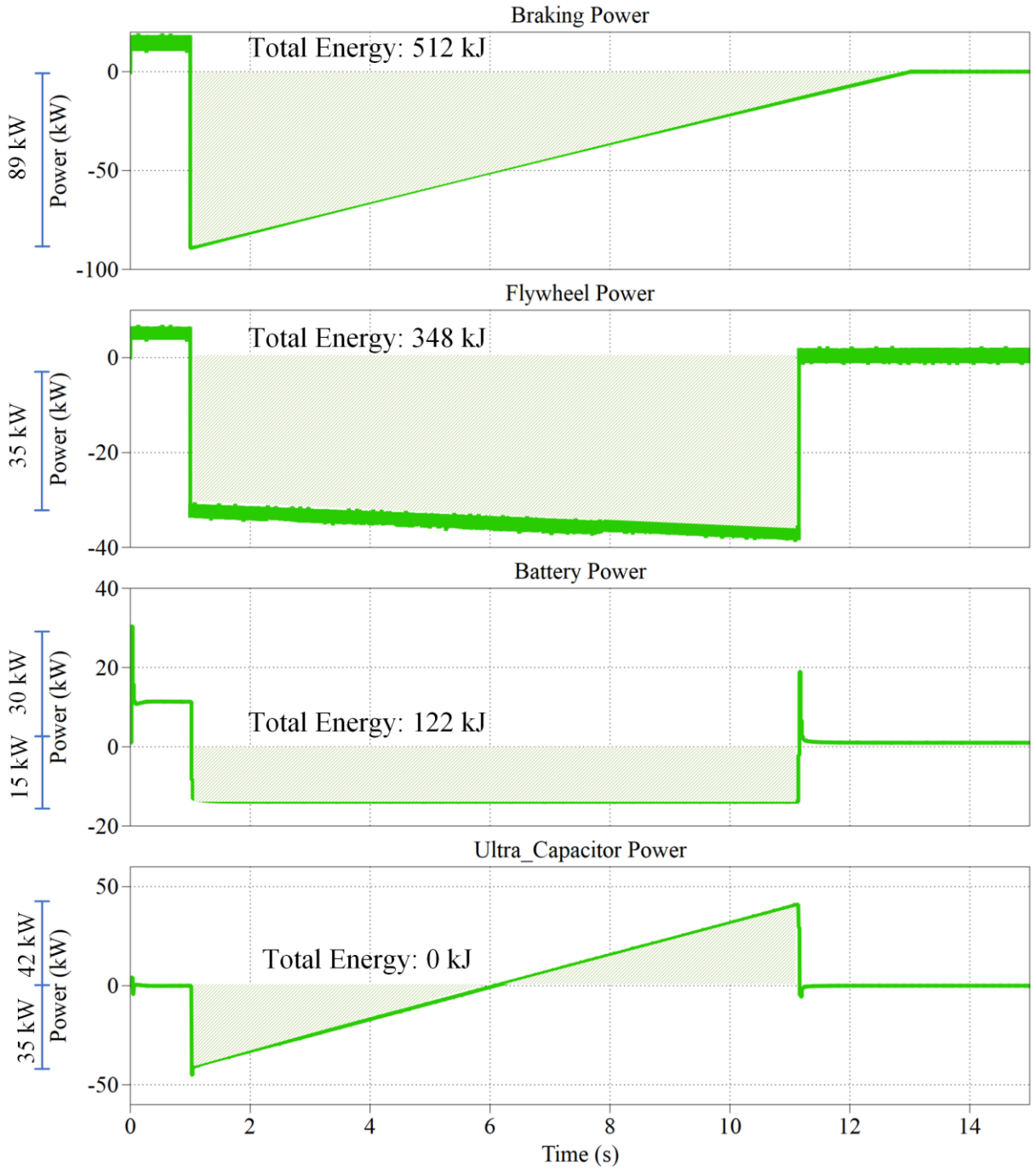

Fig 30. Detailed Energy and Power Management of the Proposed Powertrain (12 Seconds)

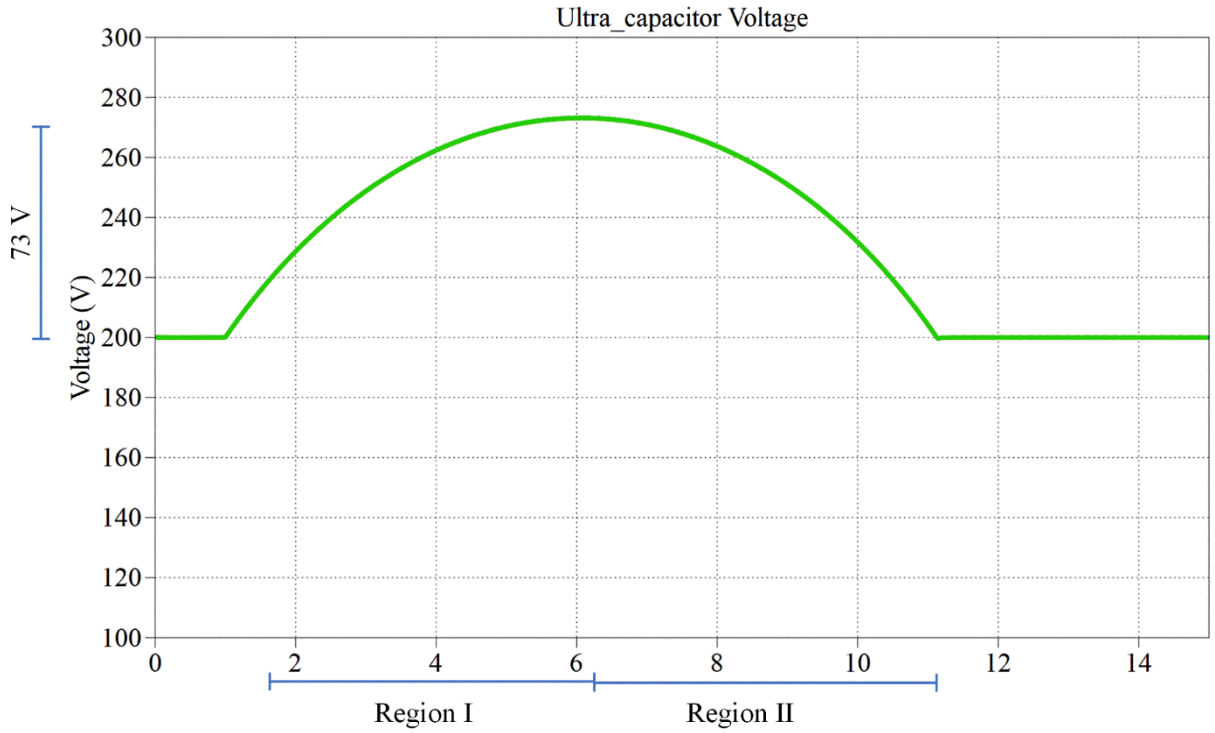

Fig 31: Ultracapacitor Voltage Variation in the Proposed Powertrain (12 Seconds)

4.3.3. Braking Scenario: 60-0 mph in 8 seconds

Fig. 21 presents a simplified rendition of the vehicle. "F_{brake}", "T_{brake}", "V", and "P" are the vehicle braking force, braking torque, speed, and braking power, respectively. Fig.32 presents the values of the required F_{brake}, T_{brake}, V, and P to reduce the vehicle speed from 60 mph to full stop in 8 seconds to emulate the moderate to harsh braking scenario. A braking force equal to 5.11 kN is required to meet the braking scenario. The braking force, as the wheel radius of the vehicle is 35 cm, can be estimated to be around 1680 Nm. In this braking scenario, 568 kJ kinetic energy needs to be processed in 8 seconds. It is noteworthy to mention that not all of this energy is recoverable as some of it will be consumed for loads such as air drag or rolling resistance. Thus, only 531 kJ of the 568 kJ is recoverable.

Fig. 33 presents the regenerative braking capability of each powertrain technology in the described braking scenario. As is shown in Fig. 33, the Chevrolet Bolt powertrain is able to recover

about 62% of the total available vehicle kinetic energy (331 kJ) during this braking scenario. Furthermore, the transmotor-flywheel powertrain can recuperate about 404 kJ in this braking scenario which is about 76% of the total available vehicle kinetic energy. Finally, the transmotor-flywheel powertrain equipped with the ultracapacitor can recover about 478 kJ in this braking scenario which is roughly about 90% of the total available vehicle kinetic energy.

In the case of the first two powertrains, Chevrolet bolt and transmotor-flywheel powertrains, a full-size battery is required in their design. However, the battery power rating in the case of the transmotor-flywheel powertrain equipped with the ultracapacitor can be reduced by about 80%. Thus, the battery charging and discharging rate can be reduced to around -15 kW and 30 kW, respectively.

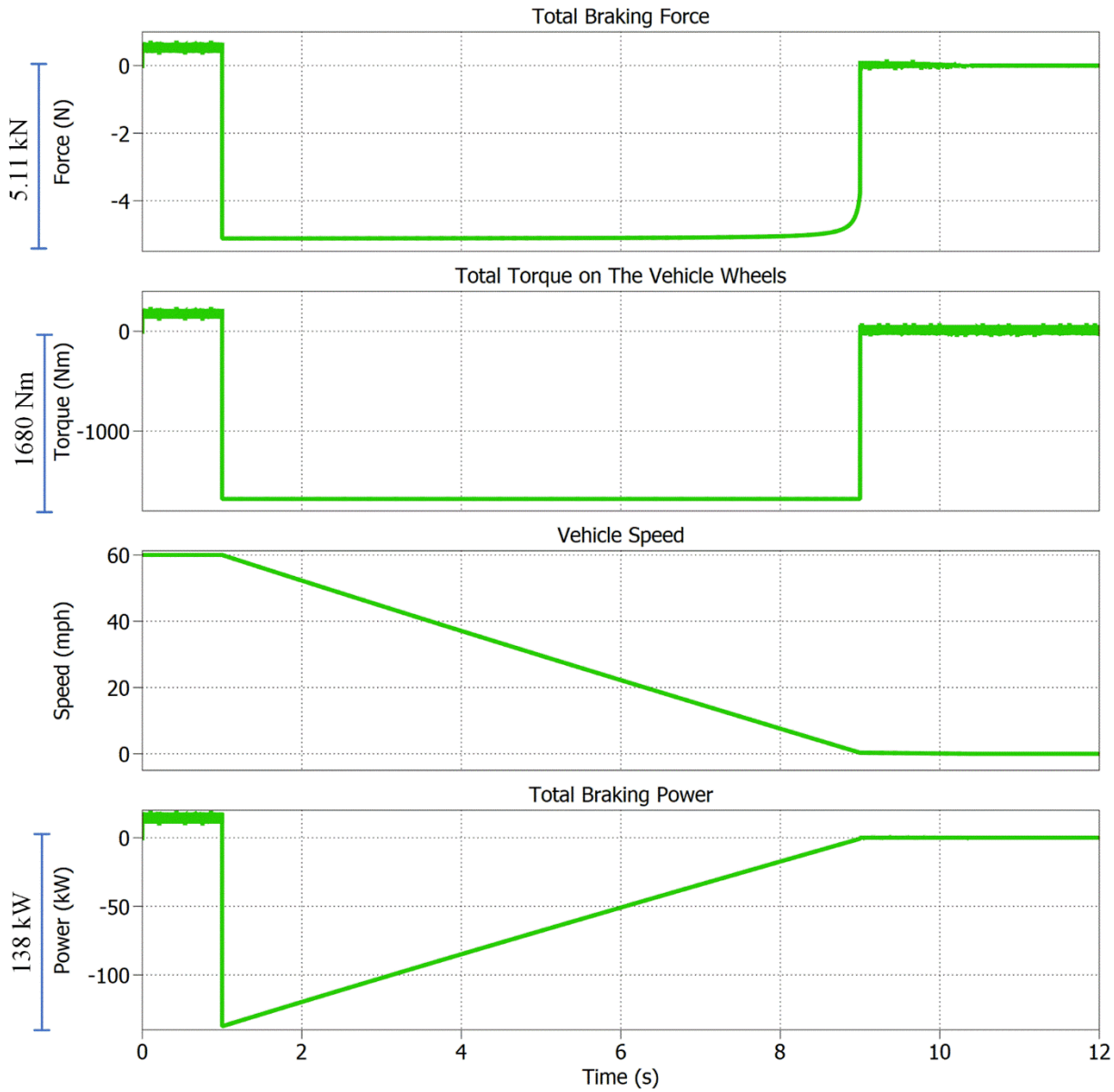

Fig 32. Required Force and Torque to Stop the Vehicle with an Initial Speed of 60 mph in 8 Seconds

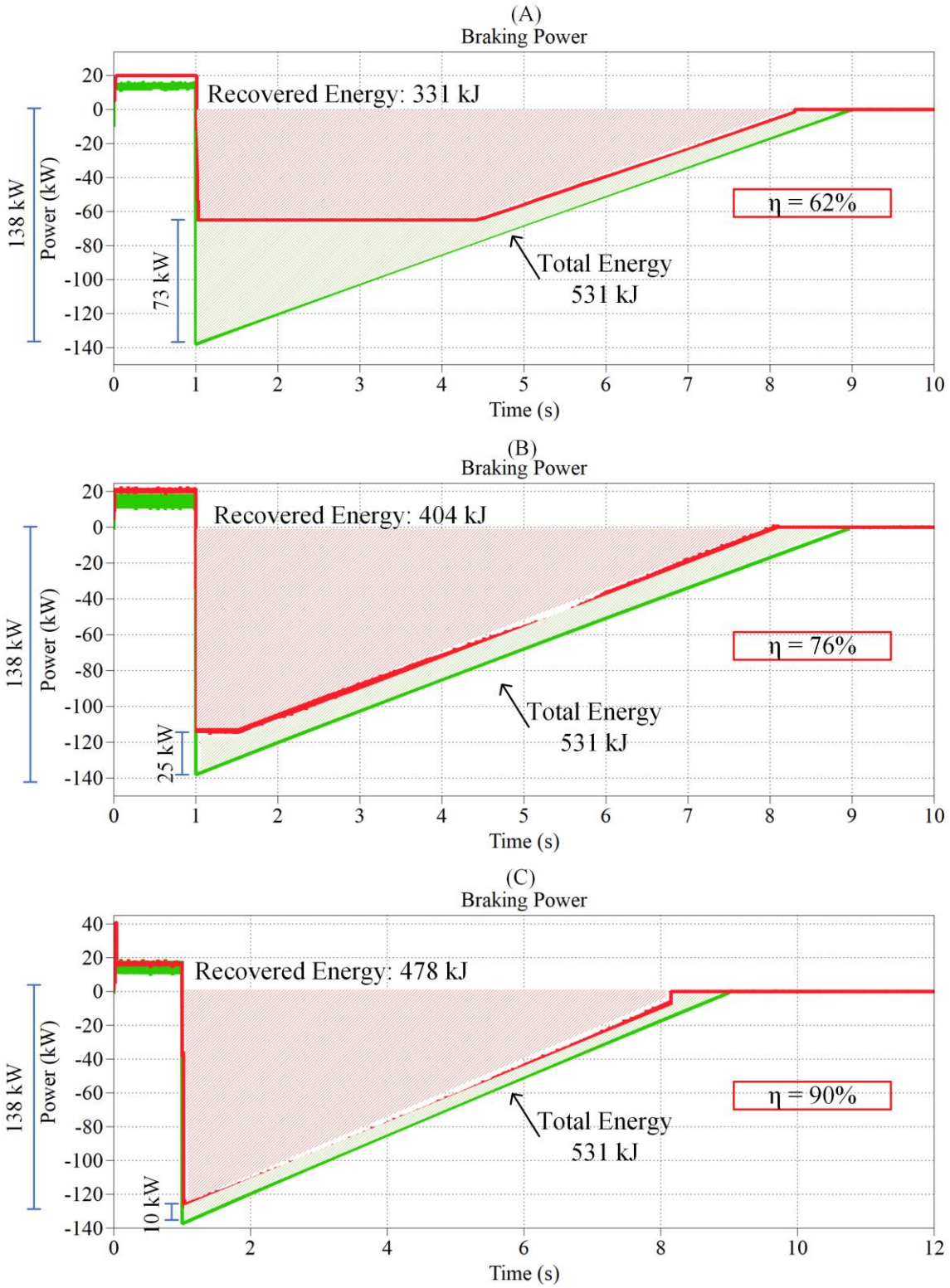

Fig. 33. The Energy and Power Management of Each Powertrain in the Described Braking Scenario Simulation: (A) Chevrolet Bolt Powertrain (B) Transmotor-Flywheel Powertrain (C) Transmotor-Flywheel Powertrain Assisted by an Ultracapacitor (8 Seconds)

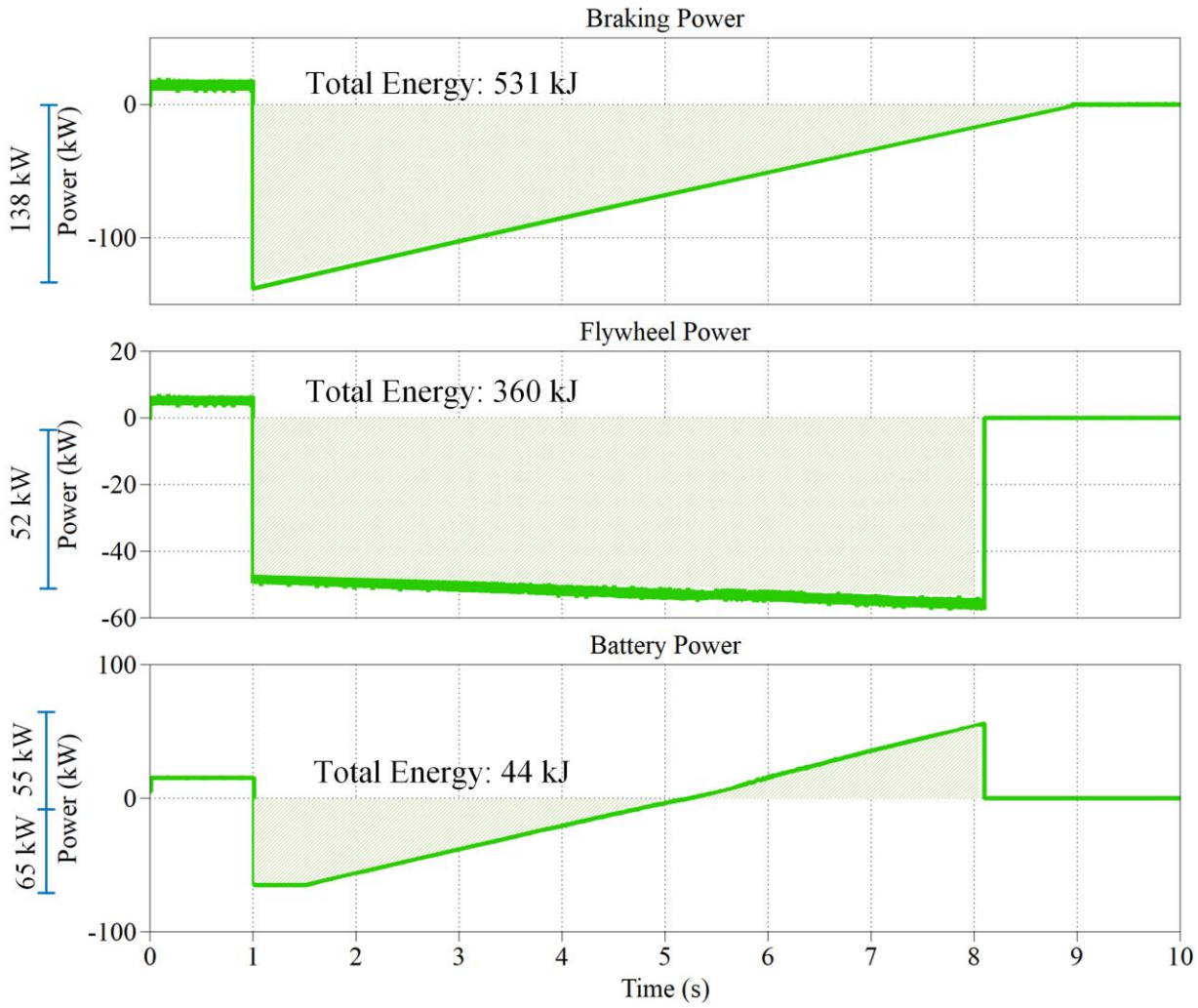

Fig 34. Detailed Energy and Power Management of the Transmotor-Flywheel Powertrain (8 Seconds)

Fig. 34 exhibits the power and energy distribution associated with the transmotor-flywheel powertrain, including the battery (main energy storage media) and the flywheel (auxiliary energy storage media) during the braking scenario. As is shown in Fig. 34 around 360 kJ of the total recoverable energy (531 kJ) is stored in the power source (flywheel), while the battery momentarily absorbs 124 kJ, and then supplied about 80 kJ of the stored energy back to the transmotor. It is worth mentioning that a full-size battery is still needed (160 kW) to process the electrical power. During this process, the flywheel speed changes from 13.4 krpm to 15.6 krpm.

Fig. 35 shows the power and energy distribution associated with the transmotor-flywheel powertrain, assisted by ultracapacitor, including the battery (main energy storage media), ultracapacitor (power source 1), and flywheel (power source 2) during the braking scenarios. As is shown in Fig 35, about 370 kJ is restored to the flywheel during the braking scenario. The battery power is designed to be limited to -15 kW and 30 kW. During this braking scenario about 108 kJ is absorbed by the battery. However, the ultracapacitor mainly processes the high electrical power demands which reach 67 kW in the mid-harsh braking scenario. The utilized ultracapacitor does not need to have high energy density as it is mainly used as a power buffer. For instance, in this braking scenario, the maximum energy cycled by the ultracapacitor is 115 kJ. During this process, the flywheel speed changes from 13.4 krpm to 15.7 krpm.

Fig. 36 presents the ultracapacitor voltage change of the transmotor-flywheel assisted by ultracapacitor technology. During the first four seconds of the braking scenario (1-5 seconds), because the driveshaft side speed is more than the flywheel side speed ($\omega_w > \omega_{Fw}$), the ultracapacitor stores energy, and hence, the ultracapacitor voltage increases from 200 V to 285 V (Region I). However, when the drive shaft speed subceed the flywheel speed ($\omega_w < \omega_{Fw}$) the ultracapacitor begins to supply power to the system. Thus, the ultracapacitor voltage returns back to its initial voltage (200 V) (Region II). The battery needs to absorb some power between 8.3 seconds to 9.3 seconds as the ultracapacitor charge/discharge is not symmetrical. Note that because of this complementary power flow behavior of this topology, the needed ultracapacitor in this technology is relatively small. The utilized ultracapacitor pack for this design has 6F capacitance and 300 V maximum which has a total mass of around 16 kg.

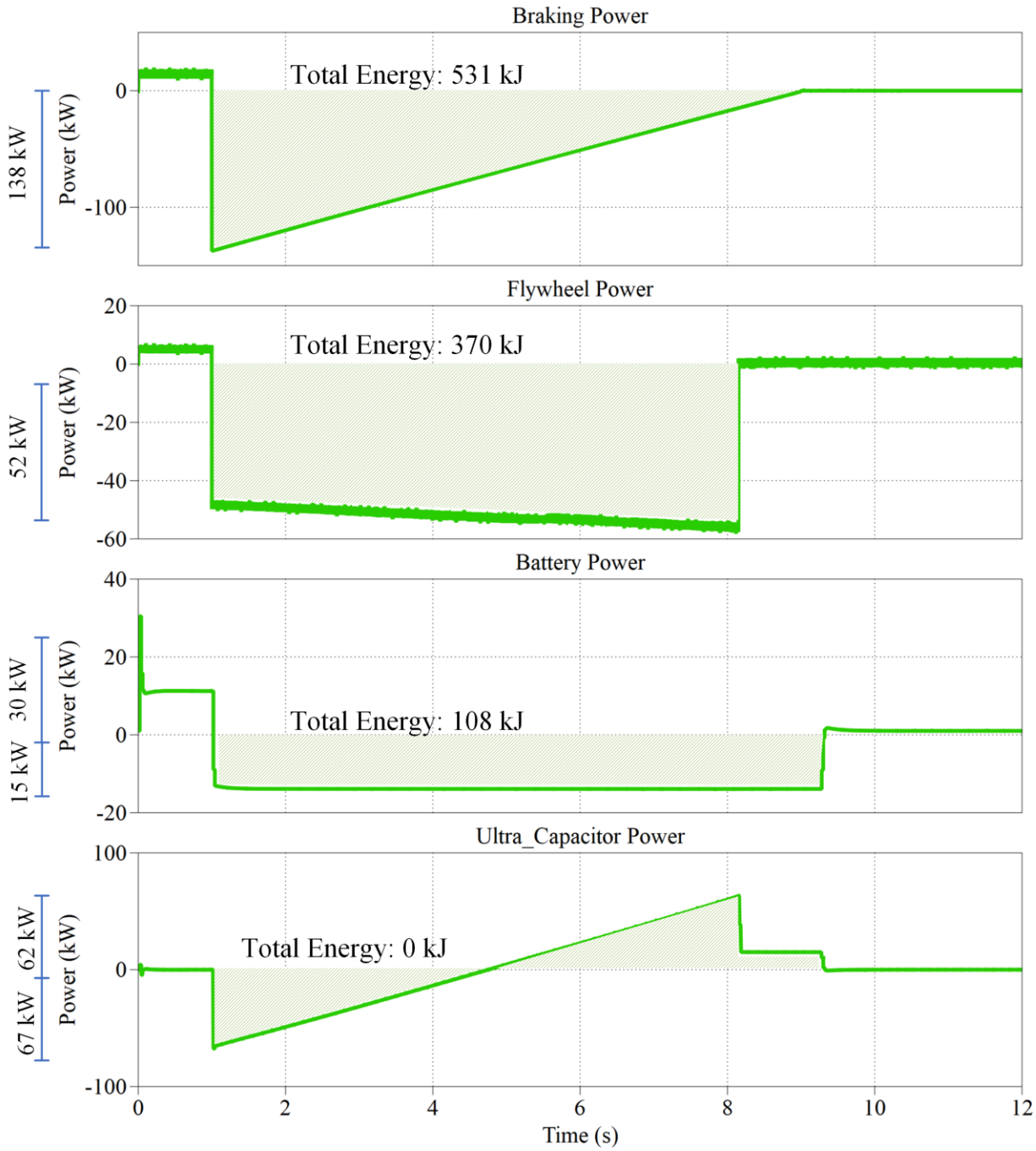

Fig 35. Detailed Energy and Power Management of the Proposed Powertrain (8 Seconds)

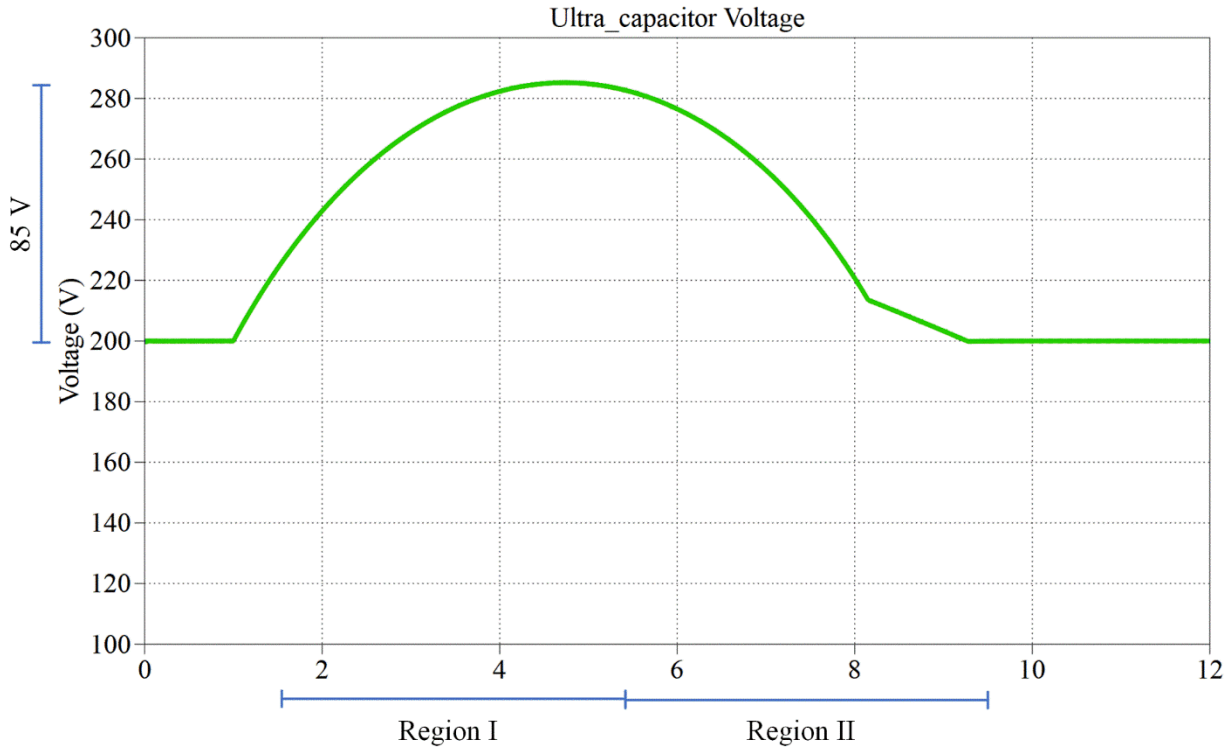

Fig 36: Ultracapacitor Voltage Variation in the Proposed Powertrain (8 Seconds)

4.3.4. Braking Scenario: 60-0 mph in 4 seconds

Fig. 21 presents a simplified rendition of the vehicle. "F_{brake}", "T_{brake}", "V", and "P" are the vehicle braking force, braking torque, speed, and braking power, respectively. Fig. 37 presents the values of the required F_{brake}, T_{brake}, V, and P to reduce the vehicle speed from 60 mph to full stop in 4 seconds to emulate the harsh braking scenario. A braking force equal to 10.49 kN is required to meet the braking scenario. The braking force, as the wheel radius of the vehicle is 35 cm, can be estimated to be around 3438 Nm. In this braking scenario, 568kJ kinetic energy needs to be processed in 4 seconds. It is noteworthy to mention that not all of this energy is recoverable as some of it will be consumed for loads such as air drag and rolling resistance. Thus, only 550 kJ of the 568 kJ is recoverable.

Fig. 38 presents the regenerative braking capability of each powertrain technology in the described braking scenario. As is shown in Fig. 38, the Chevrolet Bolt powertrain is able to recover about 32% of the total available vehicle kinetic energy (176 kJ) during this braking scenario. Furthermore, the transmotor-flywheel powertrain can recuperate about 274 kJ in this braking scenario which is about 50% of the total available vehicle kinetic energy. Finally, the transmotor-flywheel powertrain equipped with the ultracapacitor can recover about 330 kJ in this braking scenario which is roughly about 60% of the total available vehicle kinetic energy.

In the case of the first two powertrains, Chevrolet bolt and transmotor-flywheel powertrains, a full-size battery is required in their design. However, the battery power rating in the case of the transmotor-flywheel powertrain equipped with the ultracapacitor can be reduced by about 80%. Thus, the battery charging and discharging rate can be reduced to around -15 kW and 30 kW, respectively.

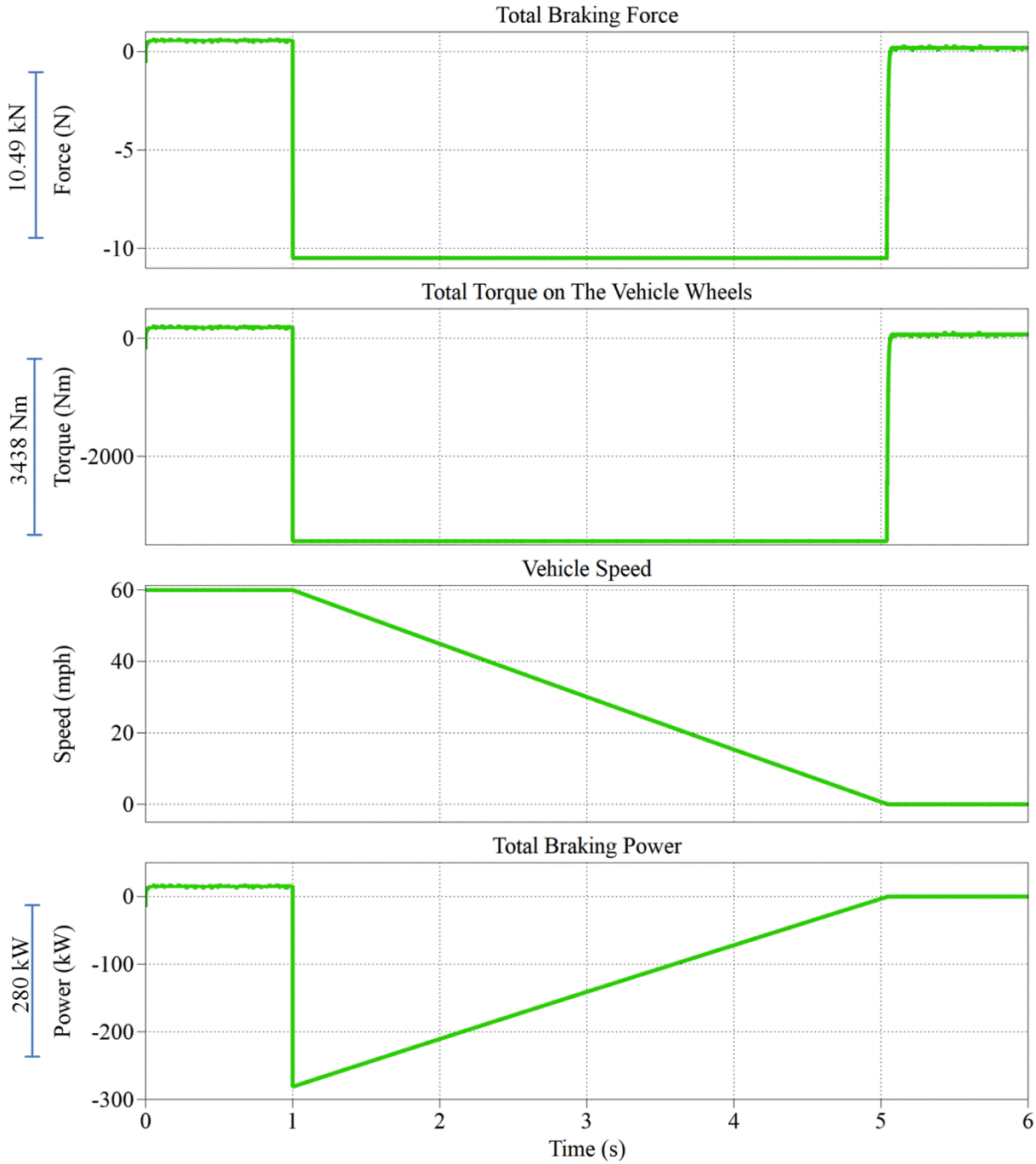

Fig 37. Required Force and Torque to Stop the Vehicle with an Initial Speed of 60 mph in 4 Seconds

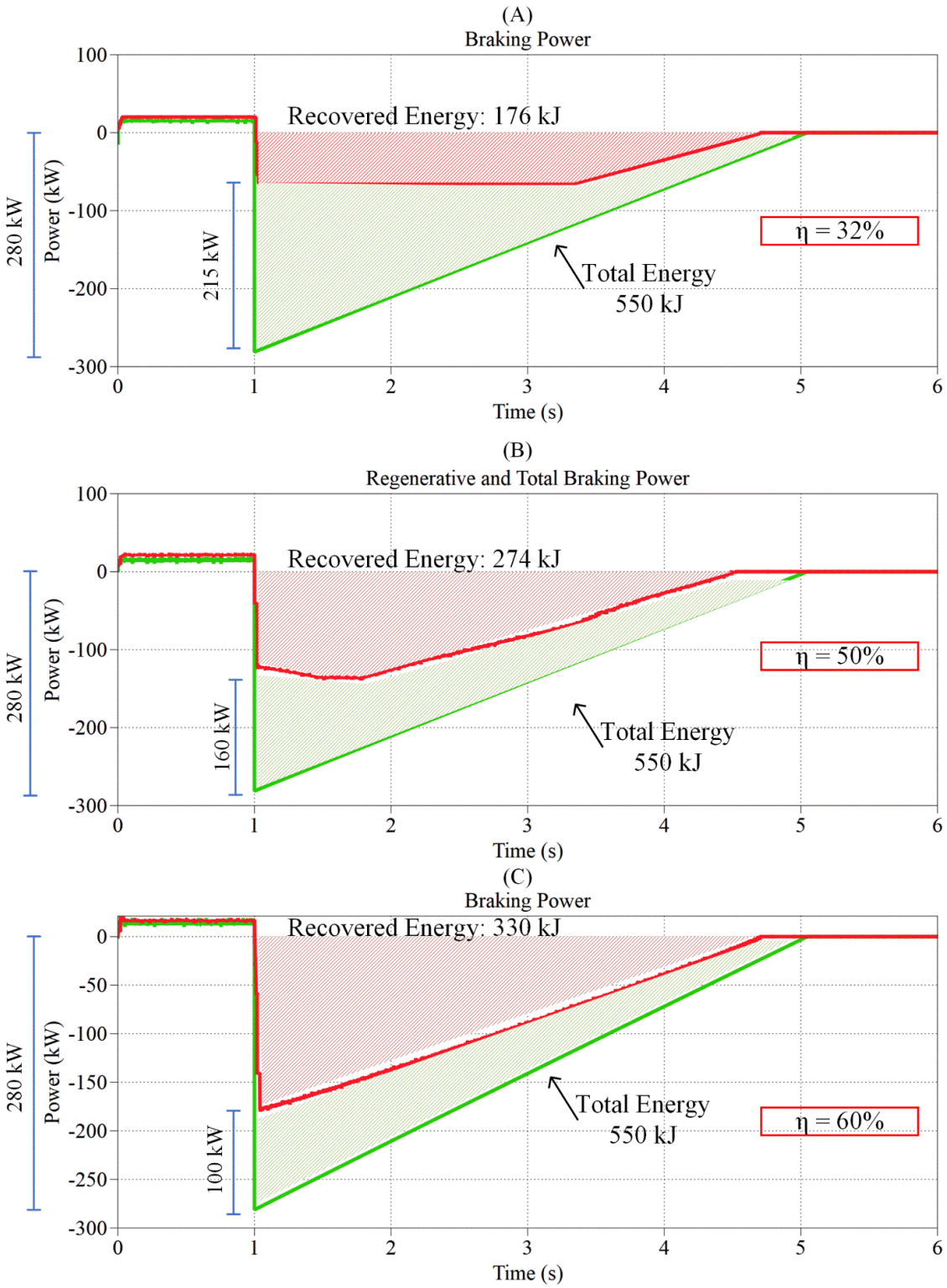

Fig. 38. The Energy and Power Management of Each Powertrain in the Described Braking Scenario Simulation: (A) Chevrolet Bolt Powertrain (B) Transmotor-Flywheel Powertrain (C) Transmotor-Flywheel Powertrain Assisted by an Ultracapacitor (4 Seconds)

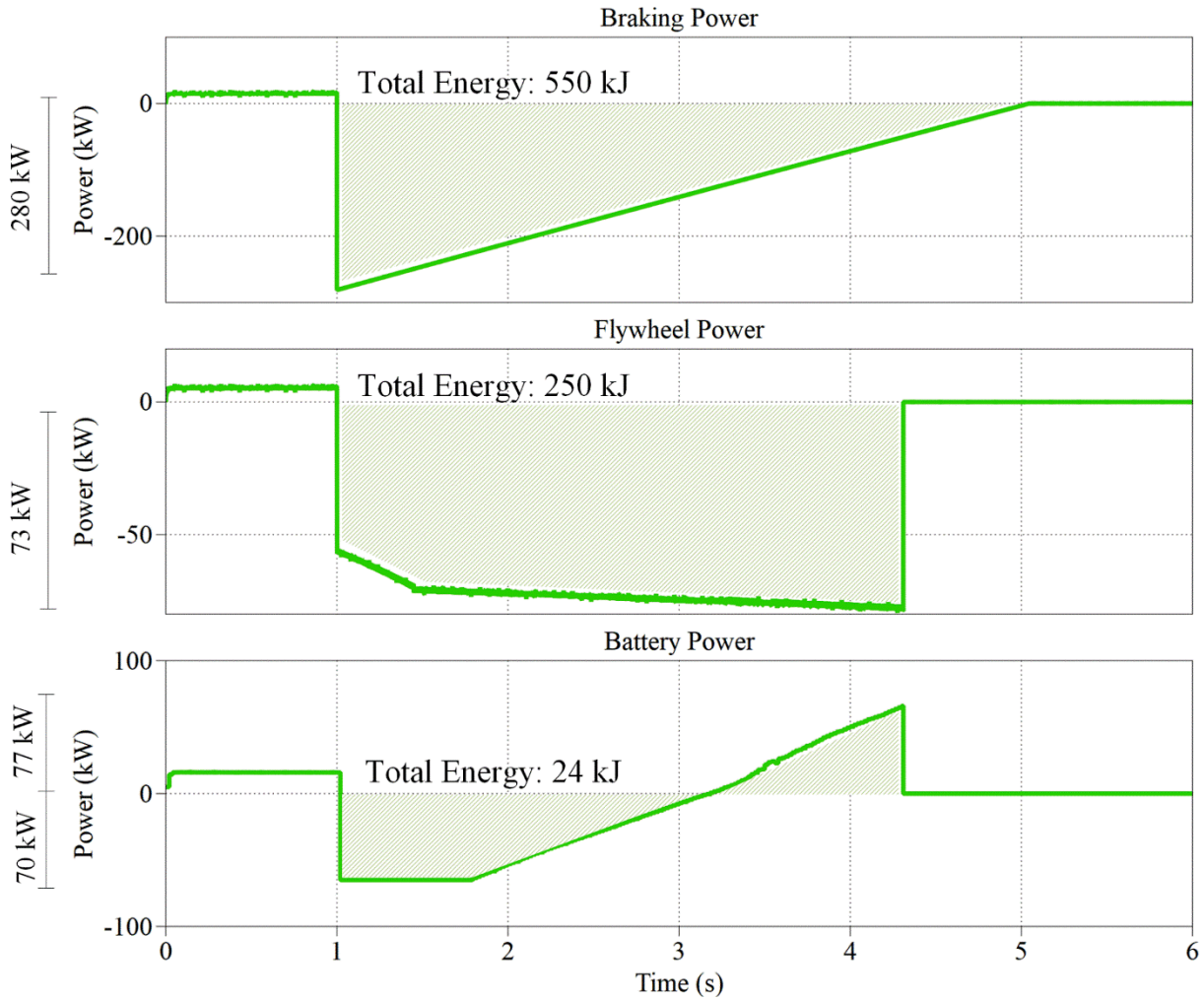

Fig 39. Detailed Energy and Power Management of the Transmotor-Flywheel Powertrain (4 Seconds)

Fig. 39 exhibits the power and energy distribution associated with the transmotor-flywheel powertrain, including the battery (main energy storage media) and the flywheel (auxiliary energy storage media) during the braking scenario. As is shown in Fig. 23, around 250 kJ of the total recoverable energy (550 kJ) is stored in the power buffer (flywheel), while the battery momentarily absorbs 80 kJ, and then supplied about 56 kJ of the stored energy back to the transmotor. It is worth mentioning that a full-size battery is still needed (160 kW) to process the electrical power. During this process, the flywheel speed changes from 13.35 krpm to 14.96 krpm.

Fig. 40 shows the power and energy distribution associated with the transmotor-flywheel powertrain, assisted by ultracapacitor, including the battery (main energy storage media),

ultracapacitor (Power buffer 1), and flywheel (power buffer 2) during the braking scenarios. As is shown in Fig 40, about 297 kJ is restored to the flywheel during the braking scenario. The battery power is designed to be limited to -15 kW and 30 kW. During this braking scenario about 33 kJ is absorbed by the battery. However, the ultracapacitor mainly processes the high electrical power demands which reach 105 kW in the harsh braking scenario. The utilized ultracapacitor does not need to have high energy density as it is mainly used as a power buffer. For instance, in this braking scenario, the maximum energy cycled by the ultracapacitor is 88 kJ. During this process, the flywheel speed changes from 13.35 krpm to 15.28 krpm.

Fig. 41 presents the ultracapacitor voltage change of the transmotor-flywheel assisted by ultracapacitor technology. During the first two seconds of the braking scenario (1-3 seconds), because the driveshaft side speed is more than the flywheel side speed ($\omega_w > \omega_{Fw}$), the ultracapacitor stores energy, and hence, the ultracapacitor voltage increases from 200 V to 269 V (Region I). However, when the drive shaft speed subceed the flywheel speed ($\omega_w < \omega_{Fw}$) the ultracapacitor begins to supply power to the system. Thus, the ultracapacitor voltage returns back to its initial voltage (200 V) (Region II). The battery needs to absorb some power between 4.8 seconds to 5 seconds and recharge the ultracapacitor to its initial voltage between 5 to 5.4 seconds as the ultracapacitor charge/discharge is not symmetrical. The ultracapacitor needs to be greater than 180 V in this design, and if it reaches 180 V or less, the regenerative braking needs to be disengaged. However, by the proper design, this situation can be averted. Note that because of this complementary power flow behavior of this topology, the needed ultracapacitor in this technology is relatively small. The utilized ultracapacitor pack for this design has 6F capacitance and 300 V maximum which has a total mass of around 16 kg.

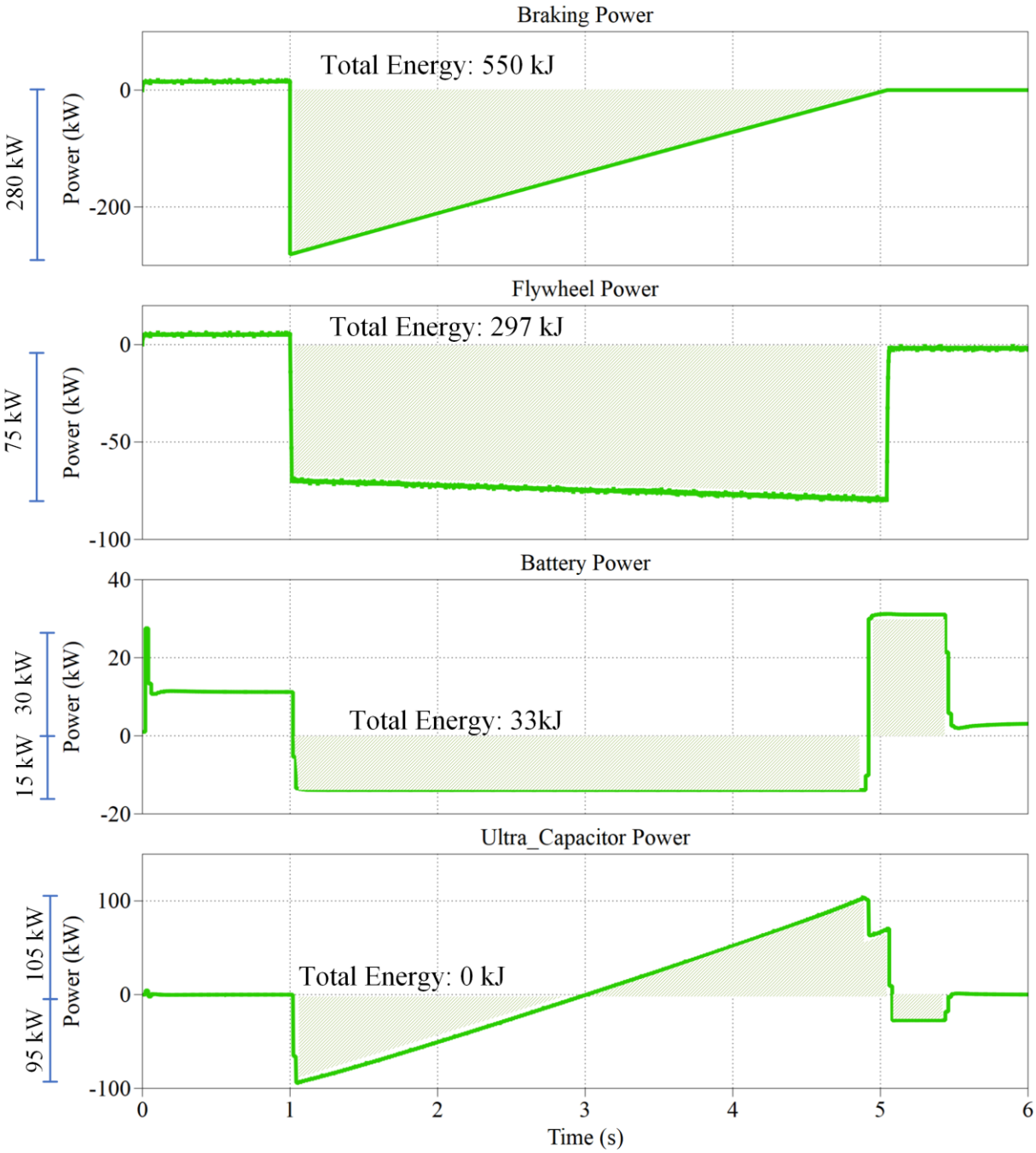

Fig 40: Detailed Energy and Power Management of the Proposed Powertrain (4 Seconds)

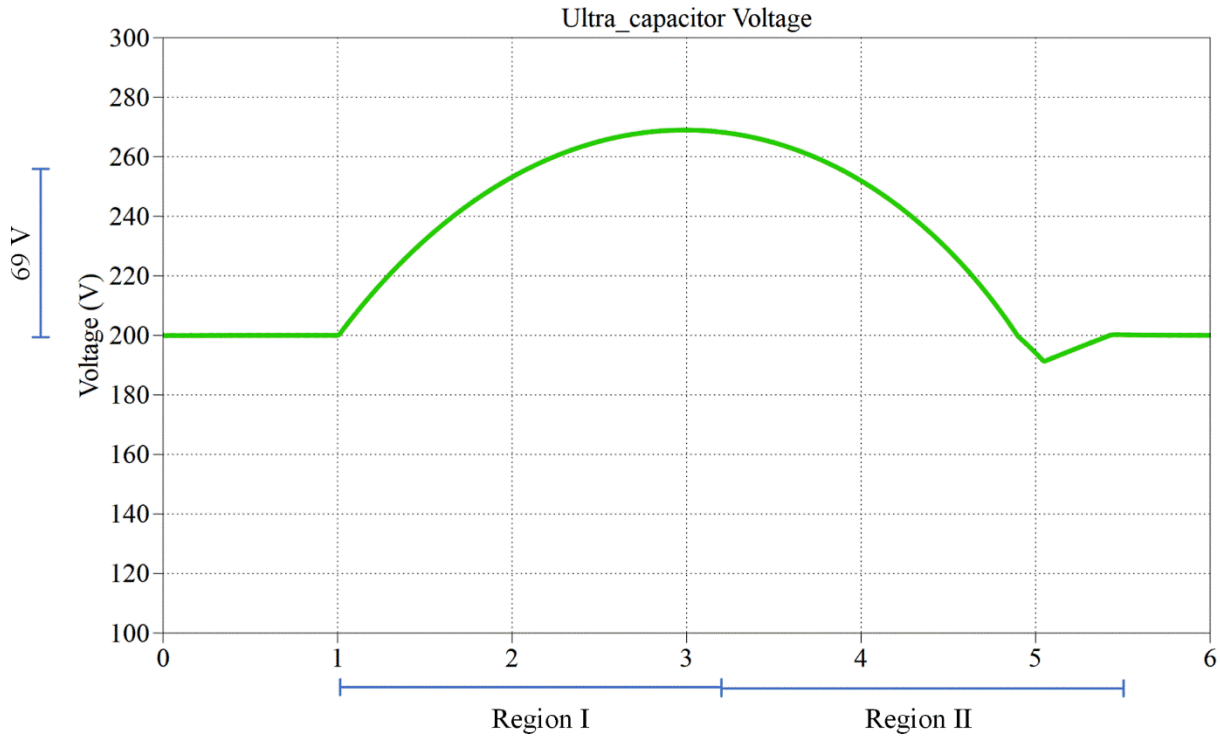

Fig 41: Ultracapacitor Voltage Variation in the Proposed Powertrain (4 Seconds)

4.3.5. Fuel Cell as The Prime Energy Storage Media

Tables X presents the transmotor-flywheel powertrain assisted by an ultracapacitor and equipped with the Fuel Cell (FC) technology as the main energy storage media instead of the Li-ion battery of the previous 4.2. The assumed parameters are similar to the original transmotor-flywheel powertrain assisted by an ultracapacitor, but the required ultracapacitor is increased by 25% (8F instead of 6F), but the same flywheel and transmotor are utilized. Furthermore, the mass of the ultracapacitor is increased from 16 kg to 20 kg and considered in the simulations. The main reason that a larger ultracapacitor is required in this design is the lack of FC onboard rechargeability.

Table X: Transmotor-Flywheel Powertrain Assisted by an Ultracapacitor Parameters (Fuel Cell)		
General Information		
Parameter	Unit	Value
Total vehicle mass	Kg	1670
Maximum torque on the wheel	Nm	2500
Electric Motor (Transmotor)/Battery		
Electrical power rating	kW	150
Battery Power rating	kW	(0, 30)
Battery pack voltage	V	150
Battery pack current	A	167
Power Buffers		
Ultracapacitor		
Parameter	Unit	Value
Capacitance	F	8
Voltage	V	300
Mass	Kg	20
Flywheel		
Inertia	Kgm^2	1
Mass	Kg	16
Max. Angular Velocity	rpm	16000
Max. Energy	MJ	1.2

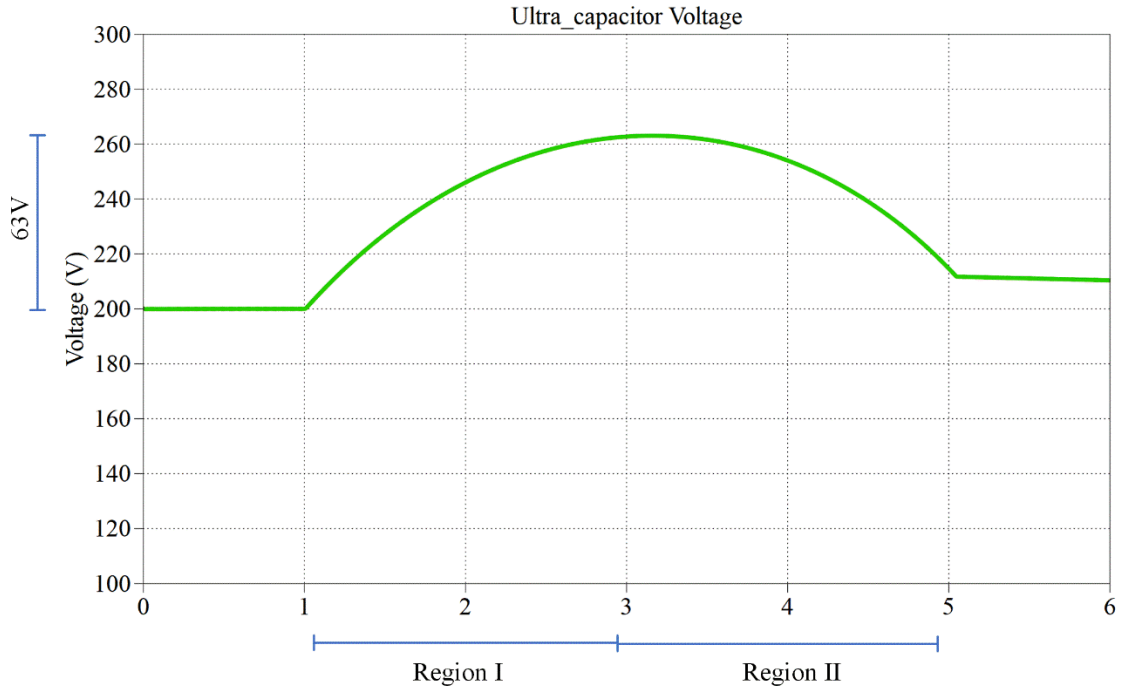

Fig 42. Ultracapacitor Voltage Variation in the Proposed Powertrain equipped with Fuel Cell (60 to mph in 4 Seconds)

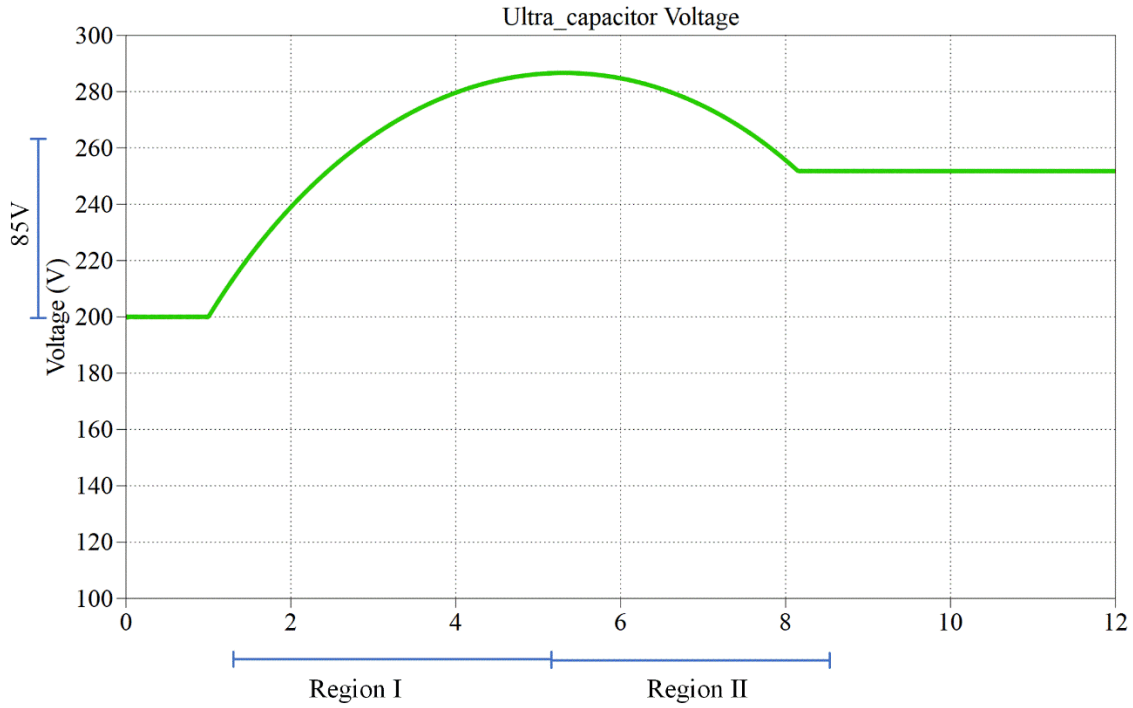

Fig 43. Ultracapacitor Voltage Variation in the Proposed Powertrain equipped with Fuel Cell (60 to mph in 8 Seconds)

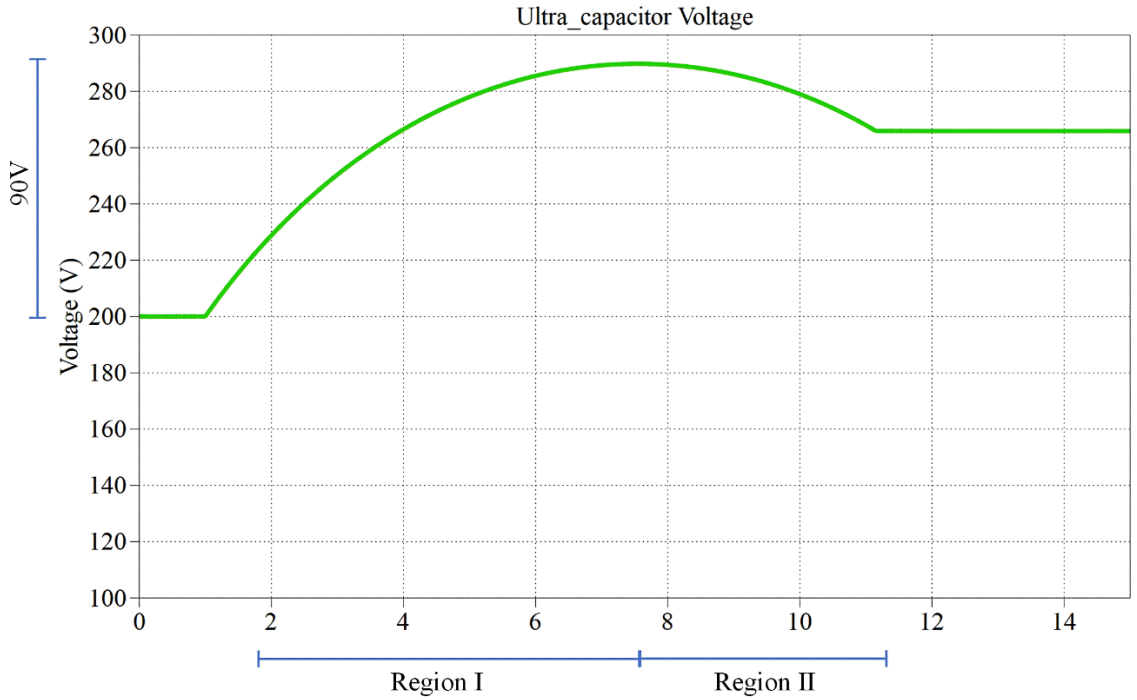

Fig 44. Ultracapacitor Voltage Variation in the Proposed Powertrain equipped with Fuel Cell (60 to mph in 12 Seconds)

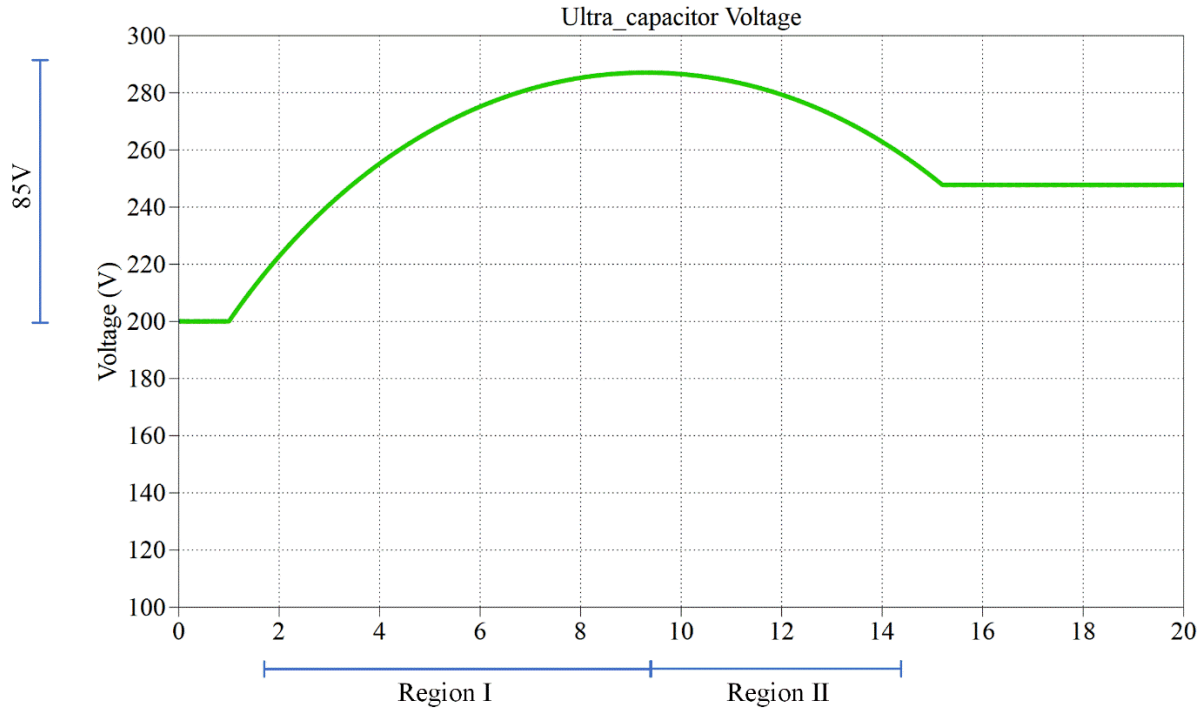

Fig 45. Ultracapacitor Voltage Variation in the Proposed Powertrain equipped with Fuel Cell (60 to mph in 16 Seconds)

Fig. 42-45 present the ultracapacitor voltage variation in different braking scenarios. As the results suggest, the voltage of the capacitor will always be in the acceptable range. Furthermore, since the FC cannot be charged from the ultracapacitor, the extra voltage stored in the ultracapacitor cannot be returned to the main energy storage media and need to be processed in other ways, such as Transmotor stand-alone mode or adjusting the flywheel speed if necessary. It is noteworthy to mention that since the entire high-demand load is managed by the ultracapacitor/flywheel, the main storage media (FC) does not require to have a fast response to the load. Hence, the proposed technology could be a suitable combination with FC or any similar technology with high energy density, but poor power density or with sluggish response to the various loads.

4.4. Harsh, Mid-levels and Mild Braking Scenario Analysis

Table XI and Fig. 46 compare the Chevrolet Bolt, transmotor-flywheel and transmotor-flywheel assisted by ultracapacitor technology (with Li-ion or FC) in four different braking scenarios of harsh, mid-levels, and mild braking in a simulation environment as discussed in detail in chapter. It is assumed that the vehicle's initial speed is 60 mph, and the vehicle mass is around 1600 kg in these simulations. In the harsh, moderate to harsh, mild to moderate, and mild braking scenarios, the goal is to reduce the vehicle speed from its initial speed (60 mph) to stand still in 4, 8, 12, and 16 seconds, respectively.

In case of the harsh braking scenario, the Chevrolet Bolt, transmotor-flywheel, transmotor-flywheel assisted by ultracapacitor (Li-ion), and transmotor-flywheel assisted by ultracapacitor (FC) powertrains could recover 32%, 50%, 60% and 62% of the vehicle kinetic energy, respectively.

In the case of the first mid-level braking scenario, the Chevrolet Bolt, transmotor-flywheel, transmotor-flywheel assisted by ultracapacitor (Li-ion), and transmotor-flywheel assisted by ultracapacitor (FC) powertrains could recover 78%, 86%, 92% and 94% of the vehicle kinetic energy, respectively.

In the case of the second mid-level braking scenario, the Chevrolet Bolt, transmotor-flywheel, transmotor-flywheel assisted by ultracapacitor (Li-ion), and transmotor-flywheel assisted by ultracapacitor (FC) powertrains could recover 62%, 76%, 90% and 92% of the vehicle kinetic energy, respectively.

In case of the mild braking scenario, the Chevrolet Bolt, transmotor-flywheel, transmotor-flywheel assisted by ultracapacitor (Li-ion), and transmotor-flywheel assisted by ultracapacitor (FC) powertrains could recover 81%, 85%, 92% and 94% of the vehicle kinetic energy, respectively.

While the regenerative braking system of conventional electric vehicles (such as the Chevrolet Bolt) has a noticeable effect on vehicle range in less harsh scenarios, it becomes significantly less effective in harsher braking scenarios. It is worth mentioning that transmotor-flywheel assisted by ultracapacitor (FC edition) has a higher regenerative capability than transmotor-flywheel assisted by ultracapacitor (Li-ion edition) due to the larger ultracapacitor and relies solely on the flywheel/ultracapacitor as the power puffer that inherently has a higher total efficiency.

Table XI: Percentage of Recovered Energy in The Breaking Scenarios (60 mph to stand still)

Vehicle Types	Braking Scenario			
	Harsh (in 4s)	Mid-harsh (in 8s)	Mid-harsh (in 12s)	Mild (in 16s)
Chevrolet Bolt	32%	62%	78%	81%
Transmotor-Flywheel powertrain	50%	76%	86%	85%
Transmotor-Flywheel assisted by ultracapacitor (Li-ion Battery)	60%	90%	92%	92%
Transmotor-Flywheel assisted by ultracapacitor (Fuel Cell)	63%	92%	94%	94%

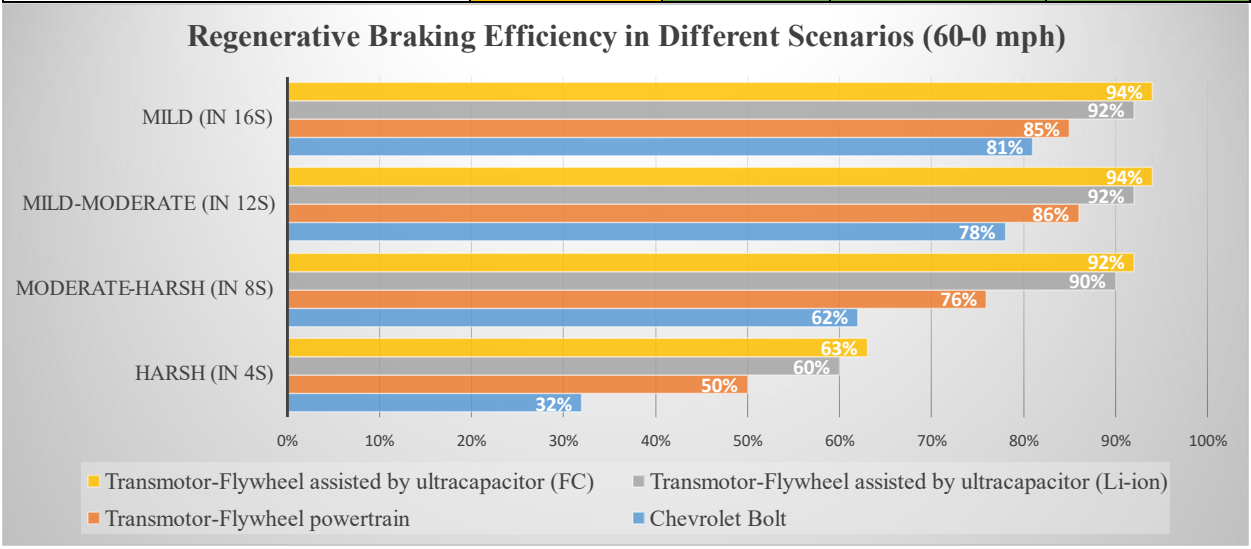

Fig 46. Percentage of Recovered Energy in The Vehicle's Breaking Scenario (60 mph to Stand Still) in Various Braking Scenarios

Table XII presents various energy storage media that can be utilized with the transmotor-flywheel assisted by the ultracapacitor. The provided simulation in chapter 4.2, utilized the Li-ion technology battery. The Li-ion batteries have a specific energy of 150-350 Wh/kg, and overall efficiency of 80%. The Fuel Cell technology can provide 3 times more specific energy, but the overall efficiency is lower (40%) which could provide around twice more vehicle range. Alternatively, a small engine series with a small electric motor can be utilized as the main energy storage media that can increase the vehicle range by 20 times, but the vehicle is not emission-free anymore.

Flywheel and ultracapacitor technologies are suitable to be utilized as power sources, but they have a significantly lower specific energy that makes them not suitable as the main energy storage media in transportation applications.

Table XII: Energy Storage Media Technology			
Main Energy Storage Media			
Energy Storage tech.	Specific Energy (Wh/kg)	Efficiency (%)	Range Improvement (pu)
Li-ion Battery tech.	150-350	80	1
Fuel Cell tech.	750	40	2
Small Engine tech.	13000	20-30	20
Auxiliary Energy Storage Media (Power Buffer)			
Energy Storage tech.	Specific Energy (Wh/kg)	Efficiency (%)	Range Improvement (pu)
Ultracapacitor tech	5	95	NA
Flywheel (Subcritical) tech	25	98	NA

Table XIII presents the main energy storage media utilized in this chapter. The battery power is limited in the case of the Transmotor-flywheel powertrain assisted by an ultracapacitor.

Table XIII: Primary Energy Storage Media Power Rating Utilized in the Simulation		
	Battery Power Rating (kW)	Max Charging Rate (kW)
Chevrolet Bolt	160	-70
Transmotor-Flywheel	160	-70
Transmotor-Flywheel assisted by ultracapacitor (Li-ion)	30	-15
Transmotor-Flywheel assisted by ultracapacitor (FC)	30	0

4.5. Simulation Implementation

Fig. 47, 48, and 49 present the simulation implementation of the Chevrolet Bolt, transmotor-flywheel powertrain, and transmotor-flywheel assisted with ultracapacitor, respectively.

As is shown in these figures, the “Calc.” block calculates the braking force, torque, and power as we as the vehicle speed. The calculated data are presented in the “Vehicle Braking Data” scope. Furthermore, the total braking power and energy of all utilized energy storage media, both individually and in combined form, are evaluated in the “Power and Energy” block.

The air drags and rolling resistance are estimated in “Air drag, Rolling Resistance and Gradeability” and applied to the vehicle's wheel as a nonrecoverable mechanical load. “Mechanical Brake” calculated the required assistance from the mechanical brake to meet the braking demand.

The “Energy storage media” block includes all the energy storage media included in the powertrains, such as battery pack, ultracapacitor pack, and DC/DC converters, …. Moreover, the “Motor Drive” block includes the PI controller, field weakening estimation, hysteresis control, and ….

It is noteworthy to mention that, in these simulations, all the electrical and mechanical loads and losses are considered to have a better overall system efficiency evaluation.

Mechanical loads and losses: (1) Air drags (2) Rolling resistance (3) Gear losses.

Electrical losses: (1) Energy storage medias (2) Converters and inverters (3) Electric motor efficiency (4) Required power for cooling the battery, UC, and electric motor.

Fig 50. presents the transmotor implementation in the simulation environment. In part A, the three-phase system (abc) to the synchronous reference frame (dq) and vice versa is converted. Part B presents the equivalent circuit of the transmotor in the synchronous reference frame. In parts C and D, the electromagnetic torque, and E_{qd} are calculated. Finally, Part E is the mechanical equation implementation of the transmotor.

Fig 51. presents the motor drive implementation in the simulation environment. In part A, the three-phase system (abc) to the synchronous reference frame (dq) and vice versa is calculated. Part B presents the required PI controller to control the vehicle speed and torque. In part C, the field weakening is calculated, and logic is implemented.

Fig. 52. presents the energy storage media interface in the case of the transmotor-flywheel assisted with ultracapacitor as explained in Chapter 2. Furthermore, the battery and ultracapacitor power and energy are calculated in this block.

Fig. 53. presents the energy's storage media, inverter, and motor drive interface in the simulation implementation.

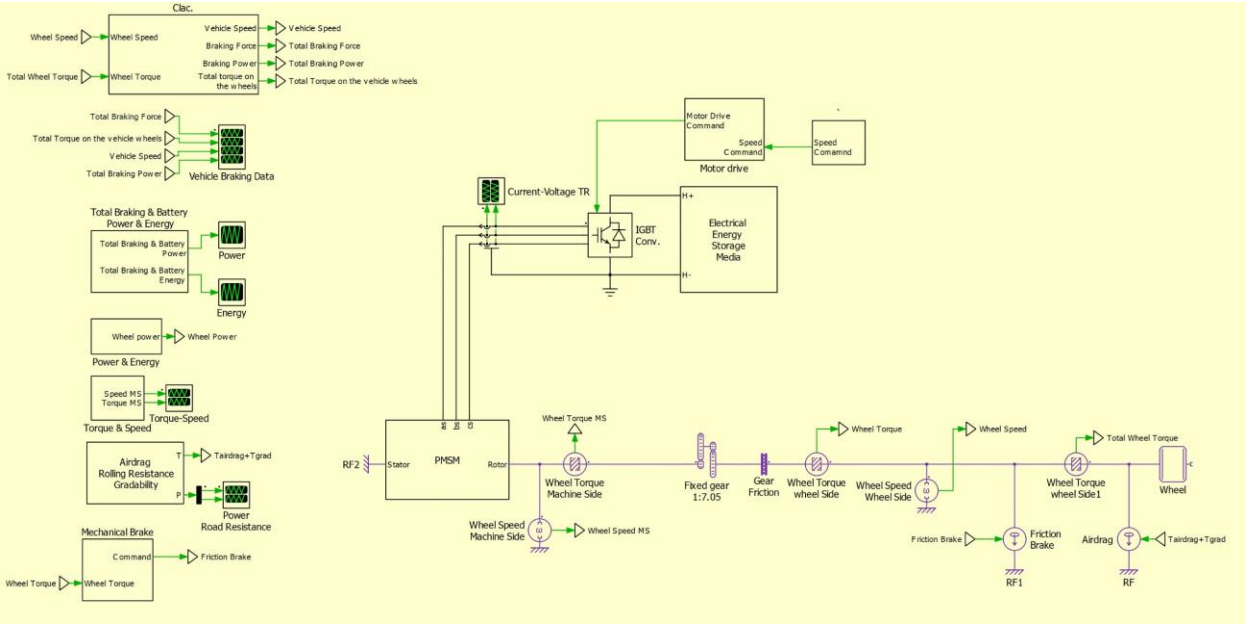

Fig 47. Simulation Environment (Chevrolet Bolt)

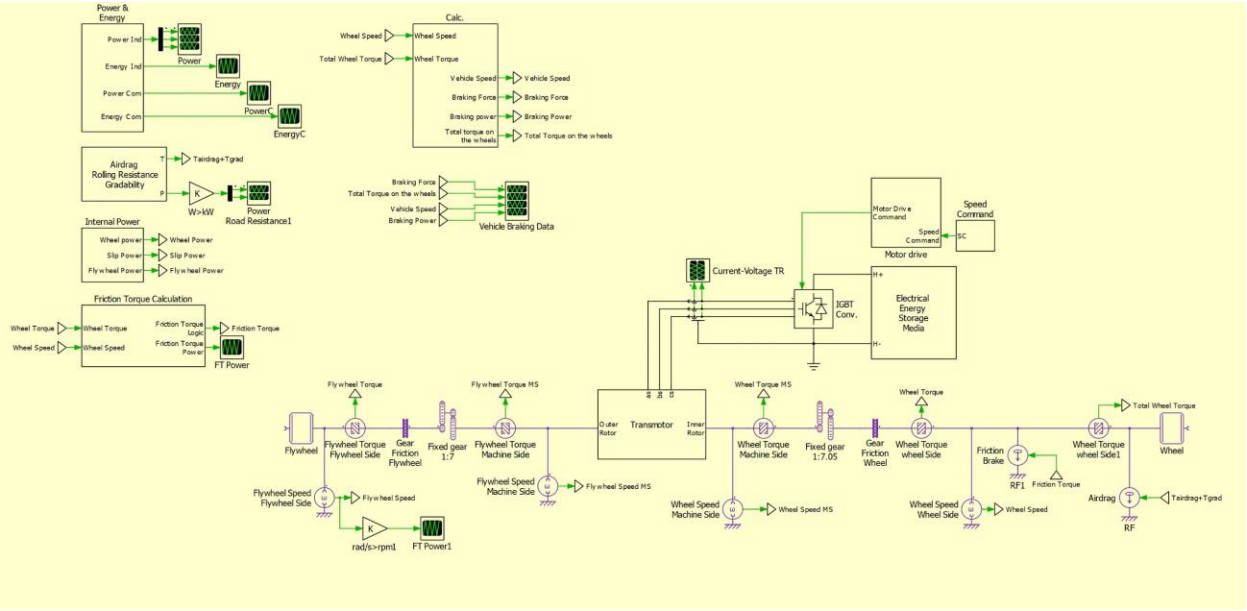

Fig 48. Simulation Environment (Transmotor-Flywheel Powertrain)

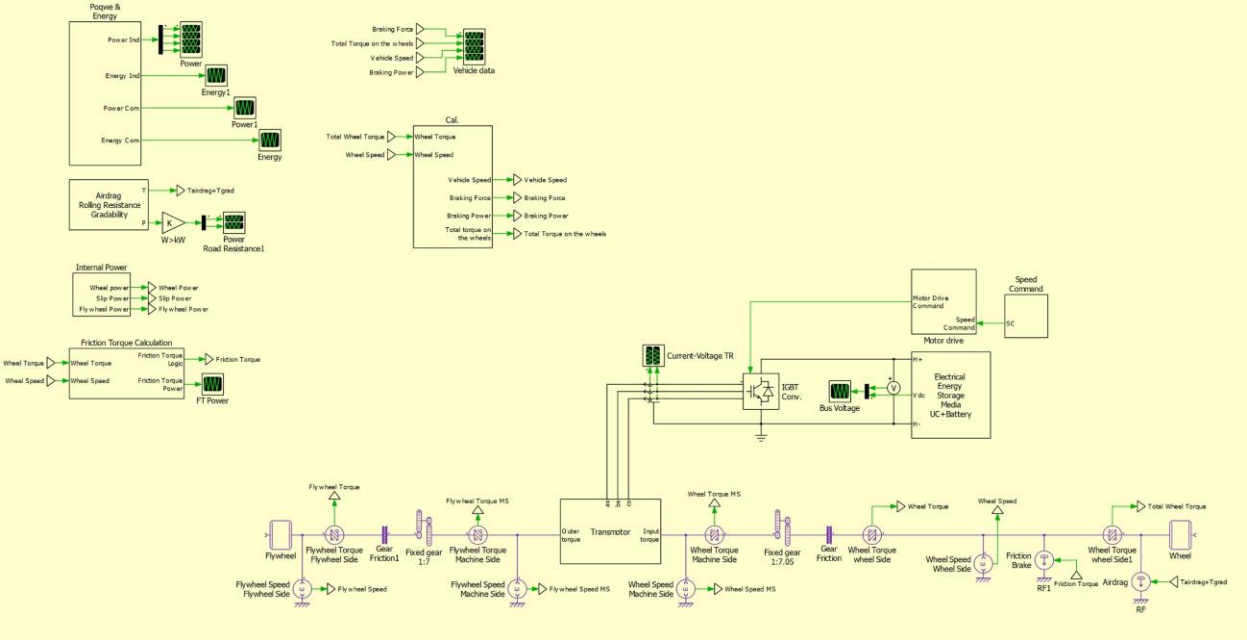

Fig 49. Simulation Environment (Transmotor-Flywheel Assisted by an Ultracapacitor Powertrain)

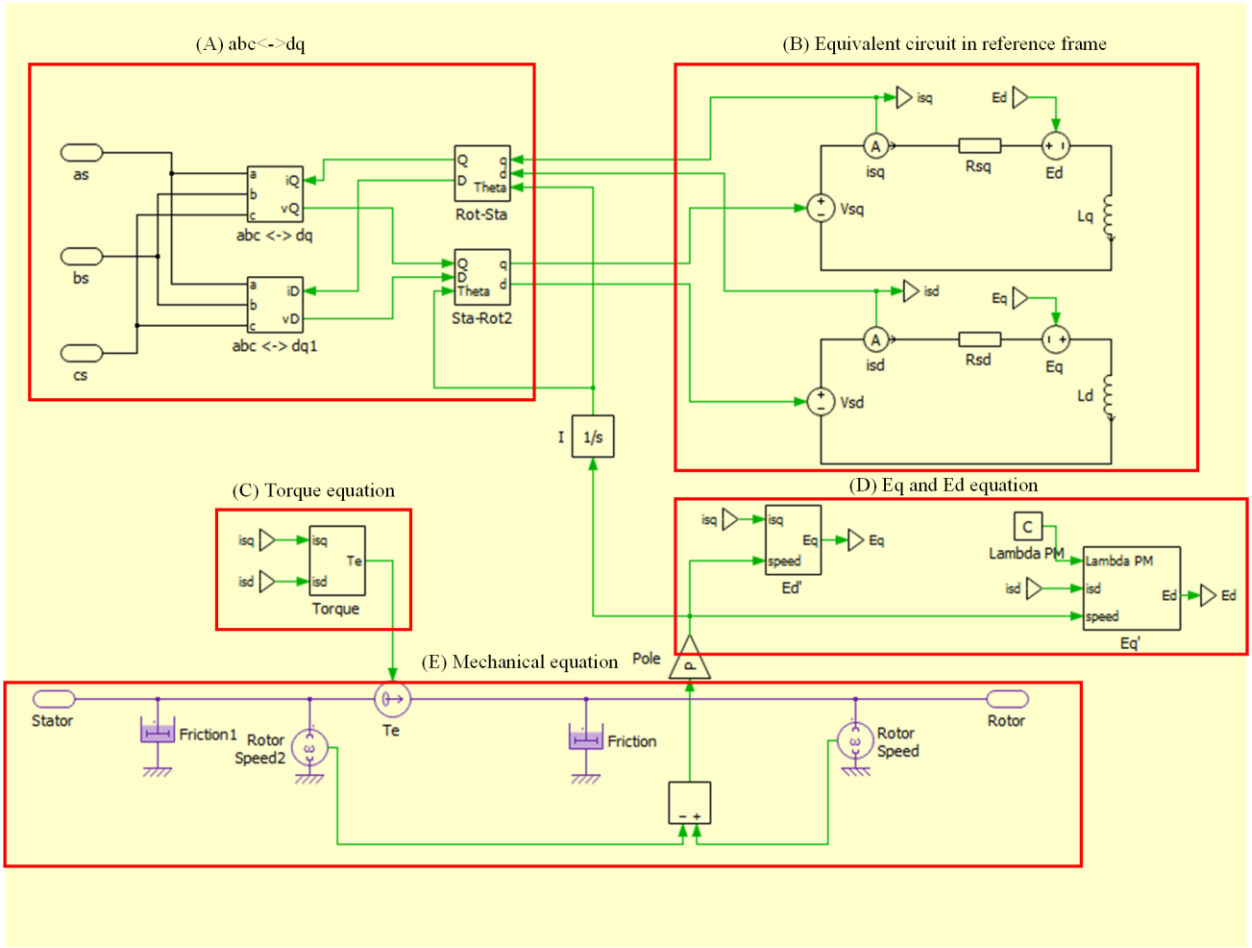

Fig. 50: Simulation Environment (Transmotor Implementation)

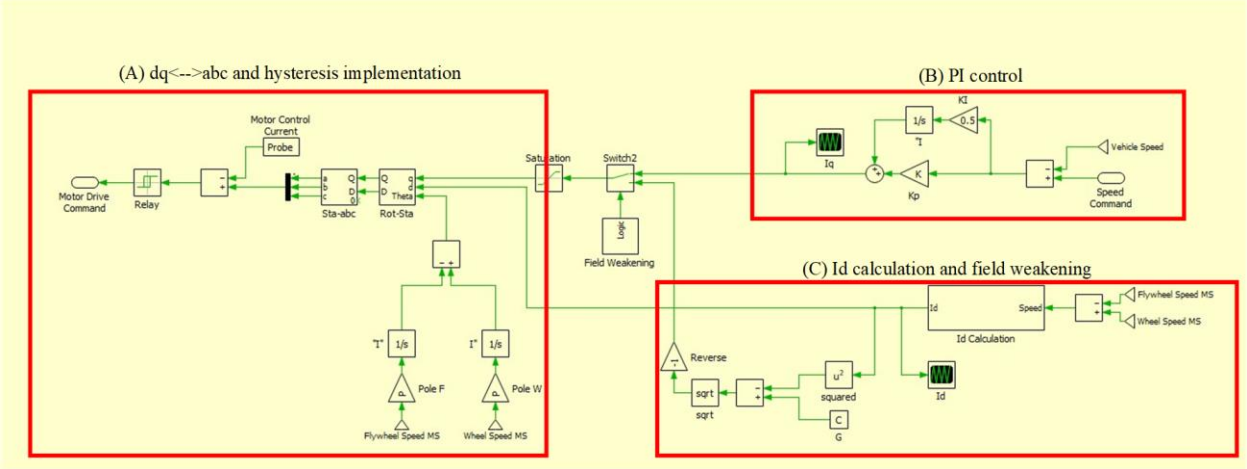

Fig. 51: Simulation Environment (Motor drive Implementation)

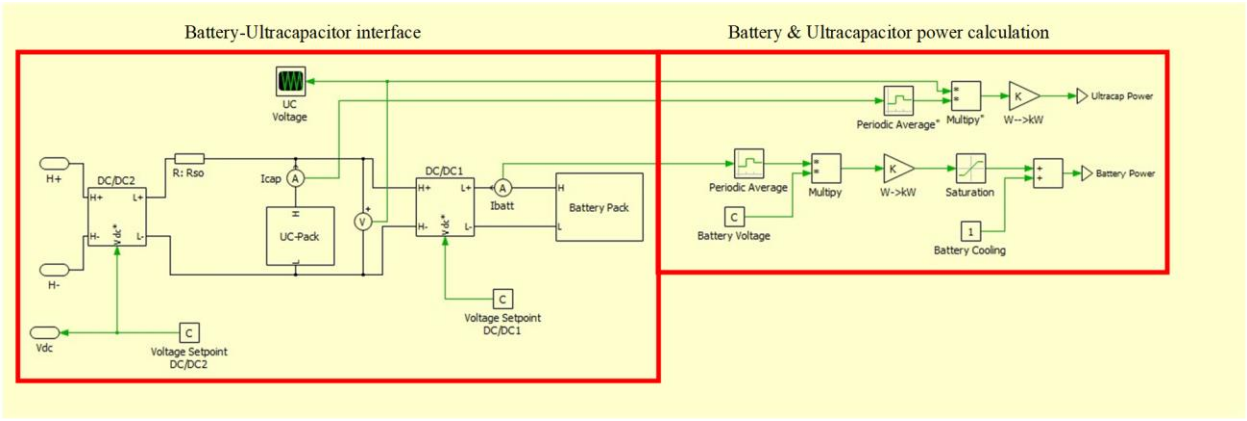

Fig. 52. Simulation Environment (Battery-Ultracapacitor Implementation)

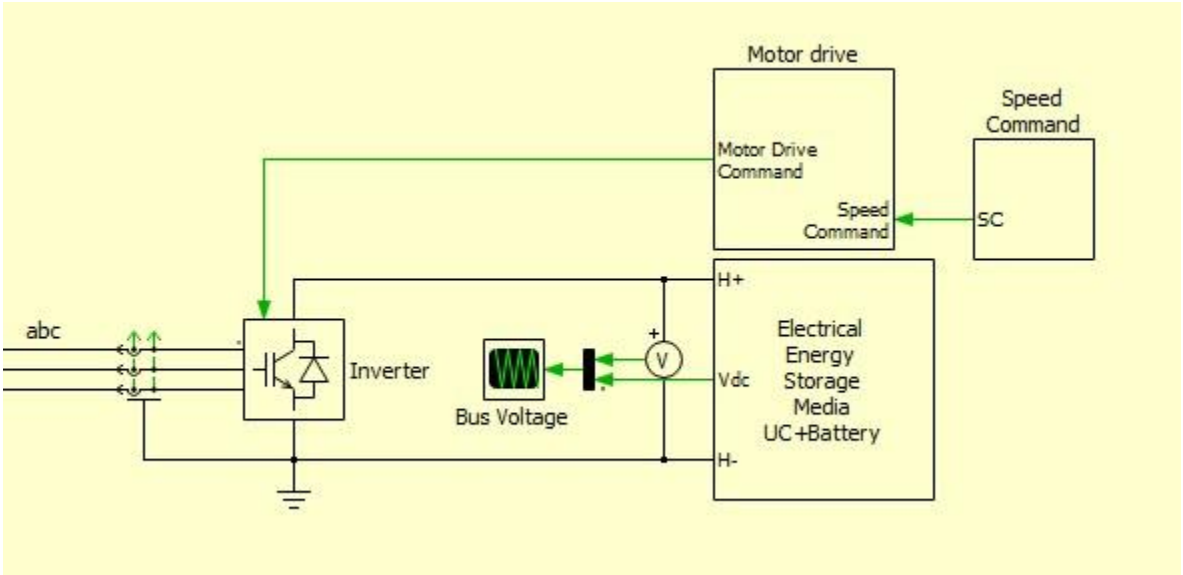

Fig. 53. Simulation Environment Energy storage media interface and control)

5. EXPERIMENTAL SETUP AND EMULATION RESULTS

5.1. Experimental Setup

This chapter presents an emulation result related to the previous chapter (Simulation of Braking Scenarios). The emulation is tested on an experimental setup shown in Fig. 54. The experimental setup consists of two flywheels, the transmotor, a power processing unit, a small added capacitor, and a controllable DC power supply.

1. **Flywheel A&B**: A pair of identical flywheels are utilized to emulate the estimated vehicle inertia and the flywheel (as a power buffer) in this setup. Each flywheel has an inertia of 0.08 kg.m2. There is no gear between the flywheels and the transmotor shafts to simplify the experiment.
2. **Transmotor**: The parameters of the utilized transmotor in this setup are presented in Table XIV. This setup is used only for model verification and control strategy implementation, and hence, is not needed to be the same size as the previous chapter.
3. **Motor controller (Power Processing Unit)**: A motor controller from Texas instrument is utilized to control the transmotor. The detailed picture of the motor drive with its various sections is shown in Fig. 55. In this emulation, only the Microcontroller (TMDSCNCD28335) and inverter are utilized, and the required DC voltage is supplied directly by a controllable DC power supply unit.
4. **Added Capacitor**: The initial capacitance of the Motor controller from Texas Instrument is 1650µF. The DC link capacitor is increased by some added capacitor to be 2750µF to emulate the ultracapacitor in the vehicle powertrain.
5. **Controllable DC Supply**: A controllable DC supply is utilized to provide the DC voltage of the motor controller. In this emulation, the DC supply voltage is adjustable based on the

difference between the flywheel's angular velocity (emulating the flywheel's angular velocity and the vehicle speed).

Table XIV: Utilized Prototype Parameters (Transmotor)	
R_{ir} (Ω)	8.16
L_{dir} (mH)	54
L_{qir} (mH)	54
λ_m (wb)	0.85
Rated torque (Nm)	6.3
Rated speed (rpm)	1100
Rated power (W)	725
Number of pole pairs	2
Outer Rotor Inertia($kg.m^2$)	0.017
Inner Rotor Inertia ($kg.m^2$)	0.009
Friction (Nm.s/rad)	0.005

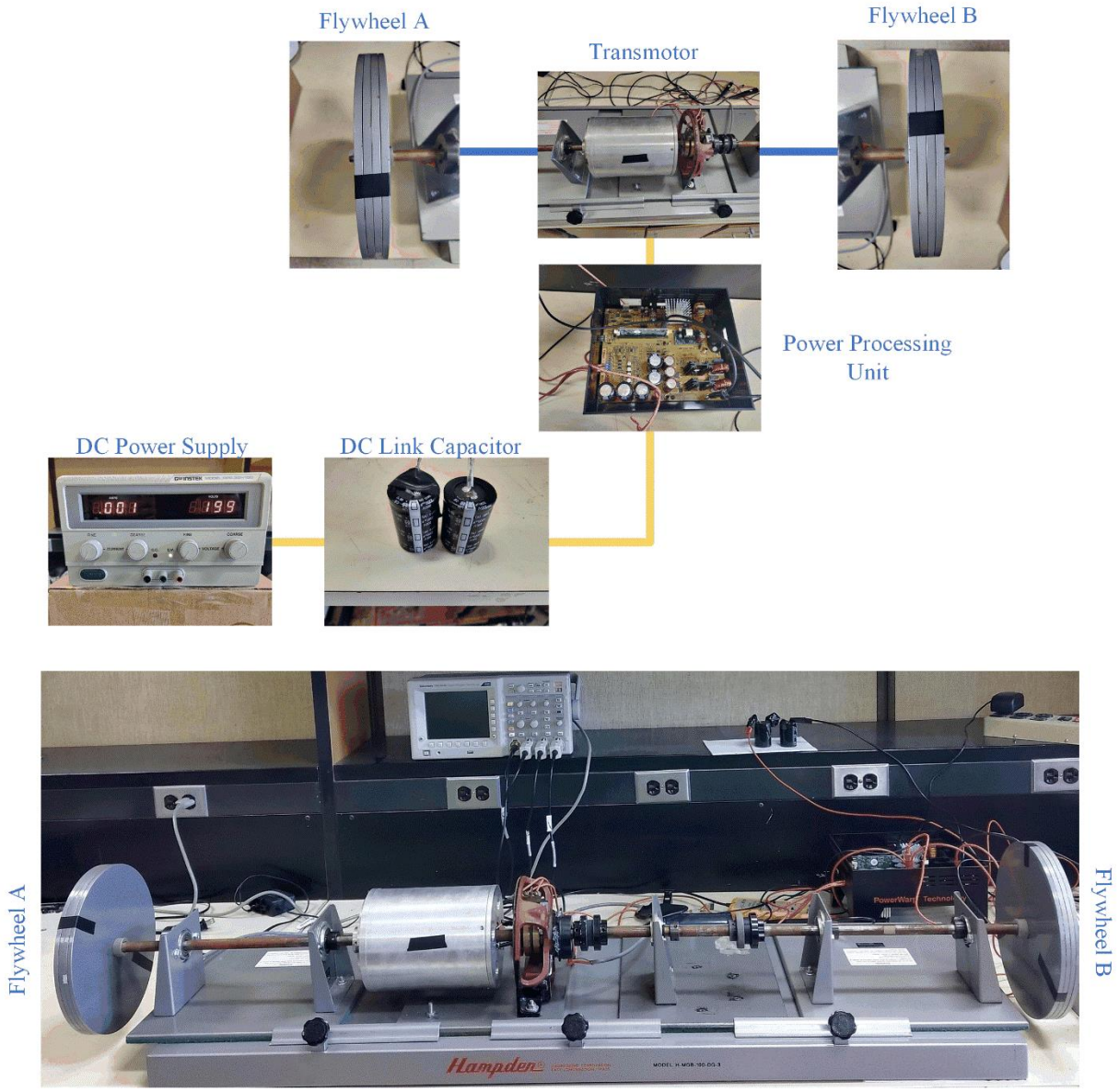

Fig. 54. Physical Connection Between the Component in The Designed Prototype

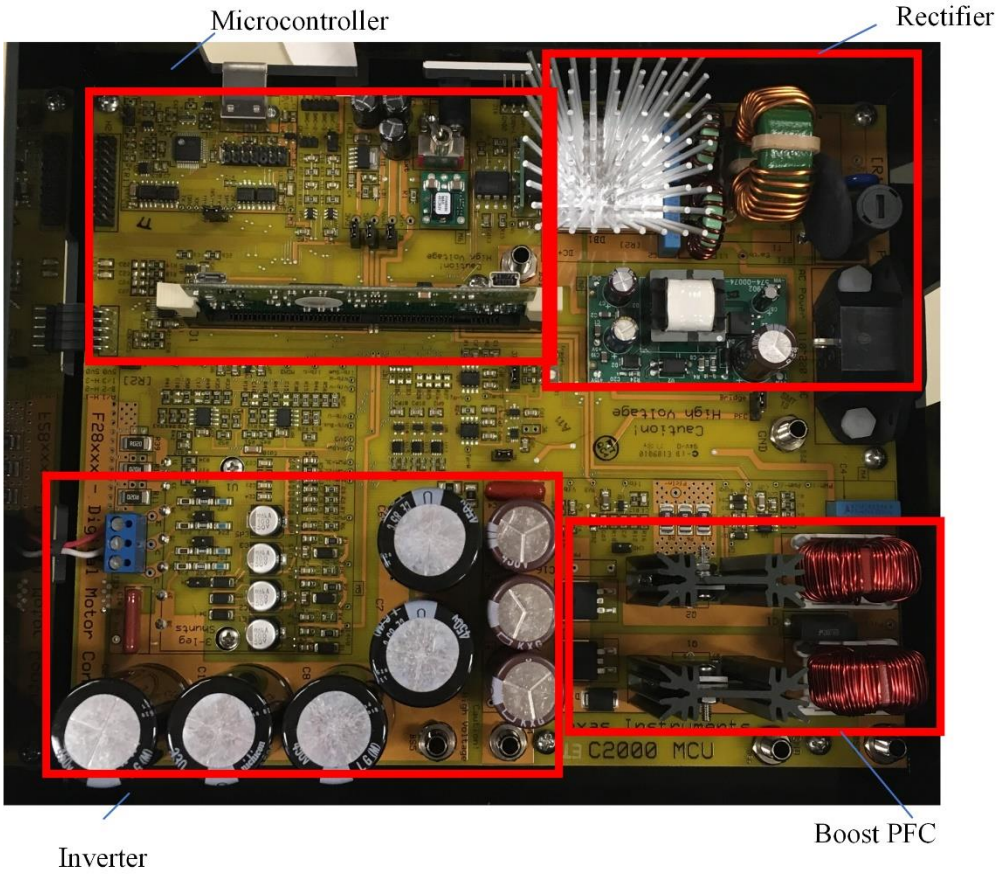

Fig.55. High Voltage Motor Drive (Texas Instrument)

5.2. Transmotor Structure

The transmotor is a mechanical machine with two mechanical ports and an electrical port. Various transmotor structures can be designed, such as squirrel cage transmotor, DC exited synchronous transmotor, permanent magnet synchronous transmotor, etc. In this experimental setup, a permanent magnet synchronous transmotor is utilized as it benefits the compact design and ease of prototyping. Furthermore, only the outer rotor requires windings, and hence, slipring and brushes unlike the DC exited synchronous transmotor. However, it needs a magnet to properly be secured on the outer rotor. Fig. 56 presents the inner rotor of the transmotor. As is shown, the ball bearing that is connecting the inner rotor to the outer rotor is located on the left side of the

picture and the ball bearing that connects the inner rotor to the mechanical ground is located on the right end. According to Fig 57, in order to have access to the inner rotor windings, the slipring is installed between the ball bearing and the windings.

Fig 58 presents the outer rotor magnet arrangement. In order to simplify the prototype and the lack of the need for field weakening in the emulation scenarios, the surface mount permanent magnet is implemented.

Fig 59 presents the inner rotor and outer rotor installed in the outer rotor housing. The shaft of the transmotor is trimmed to be installed in the outer rotor housing. A third ball bearing is utilized, outside the outer rotor housing, to connect the transmotor to the second shaft (the shaft that is connected to flywheel A).

Fig 60 presents the implementation of the sliprings and brushes in order to have access to the transmotor's electrical port. It is noteworthy to mention that in the final product the outer rotor and slipring and brushes, need to be in a housing that is connected to the ground in order to protect the rotating parts and slipring/brushes.

Fig. 61 presents the back-emf voltage induced in the inner rotor (windings) when one shaft is locked and the other is connected to the prime mover. The prime mover is rotating the unlocked shaft is rotating at 500 rpm.

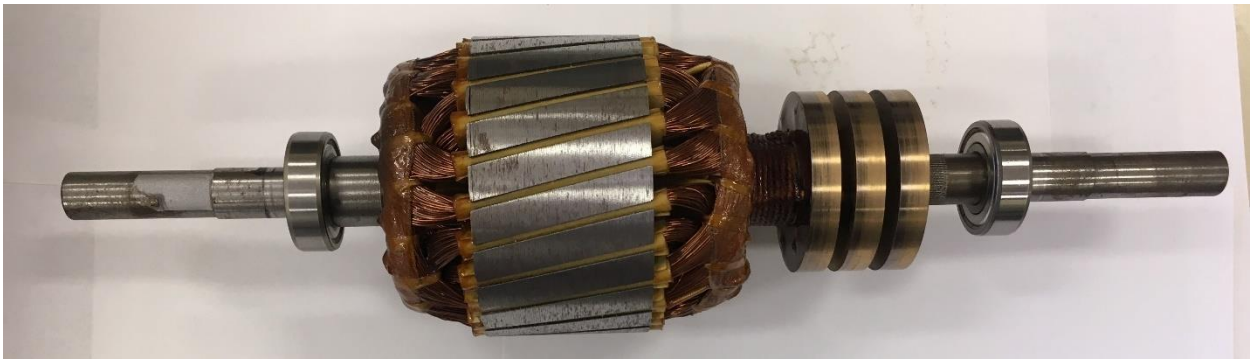

Fig. 56. Inner Rotor Wiring

Fig. 57. Sliprings Installed on the Inner Rotor

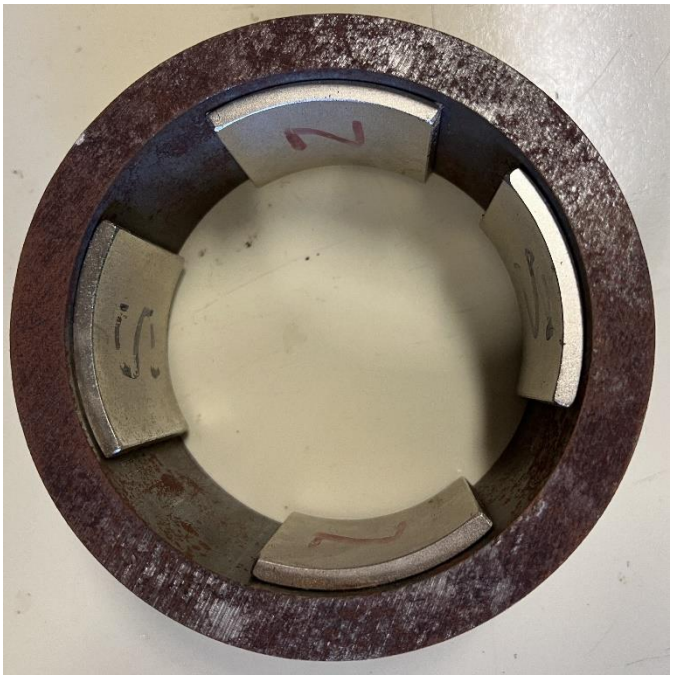

Fig. 58. Magnet Arrangement Installed on the Outer Rotor (Example)

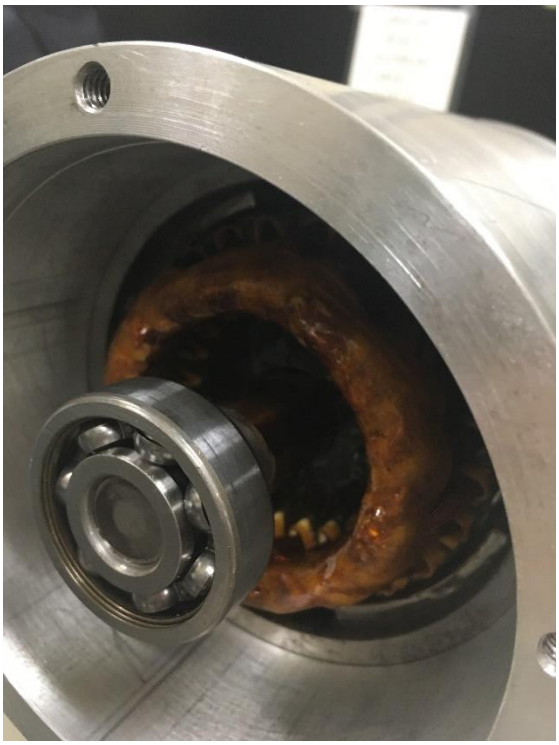

Fig. 59. Inner Rotor Inside the Outer Rotor

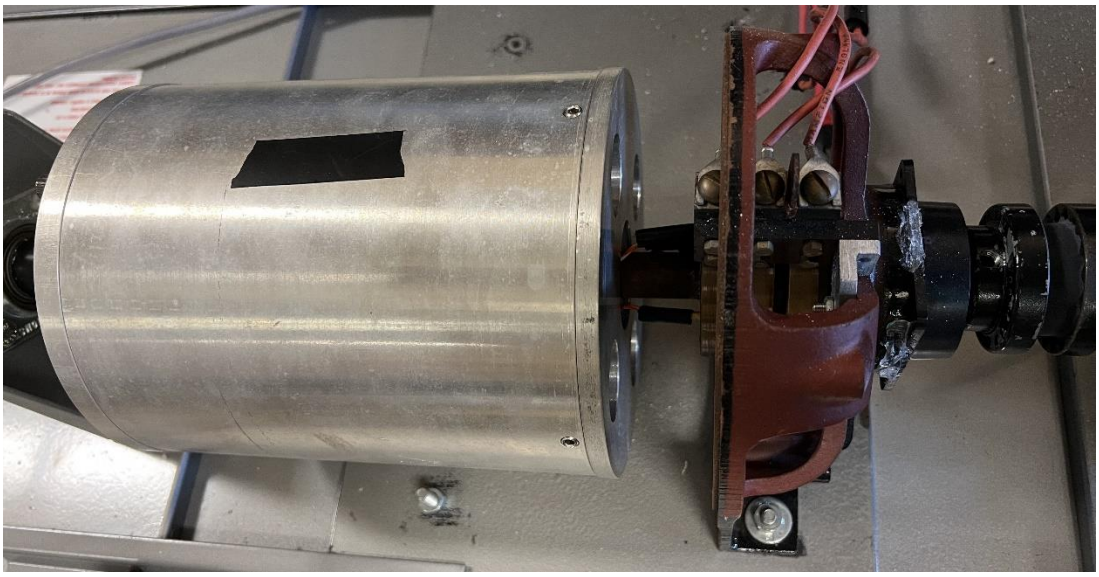

Fig. 60. Brush and Sliprings Contact and Wiring on the Designed Prototype

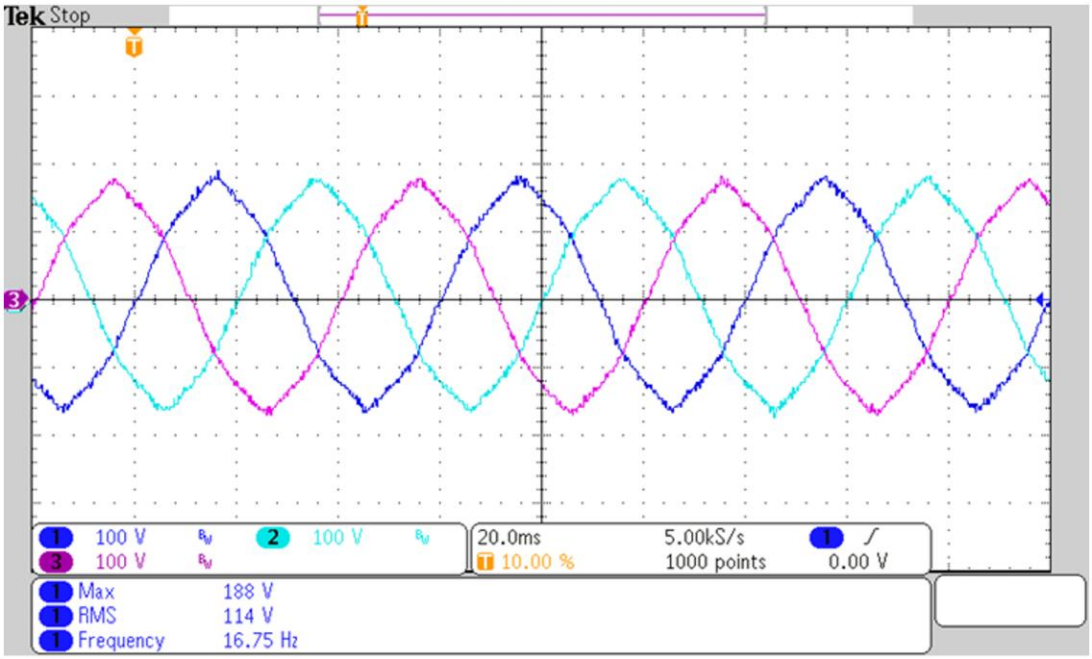

Fig. 61. The Prototype Transmotor Measured Back-Emf Voltage Waveform at 500 rpm [46]

5.3 Emulation Results and Discussion

In this section, a small-scale transmotor-flywheel, assisted by a capacitor (emulating an ultracapacitor) powertrain setup is utilized to present an approach to control the ultracapacitor voltage in the proposed powertrain. The setup consists of two flywheels each with 0.08 kgm2 inertia, one horsepower transmotor, a motor control kit (TI-InstaSpin kit), a controllable high voltage DC power supply (300 V_{DC}), some capacitor, and the required instruments. Some capacitor is added to the DC link to emulate the ultracapacitor in a full-size powertrain. The total capacitance of the DC link in this setup is increased to be around 2.75 mF from its initial value of 1.35 mF. A simplified schematic used in this emulation is shown in Fig. 54.

Fig. 62 presents a setup to study the power transfer between two flywheels (flywheels A and B, as is shown in Fig.8). Both flywheels have about the same moment of inertia as explained. The

transmotor electrical port is connected to a PPU (Power Processing Unit) with a DC link capacitance of around 2.75 mF.

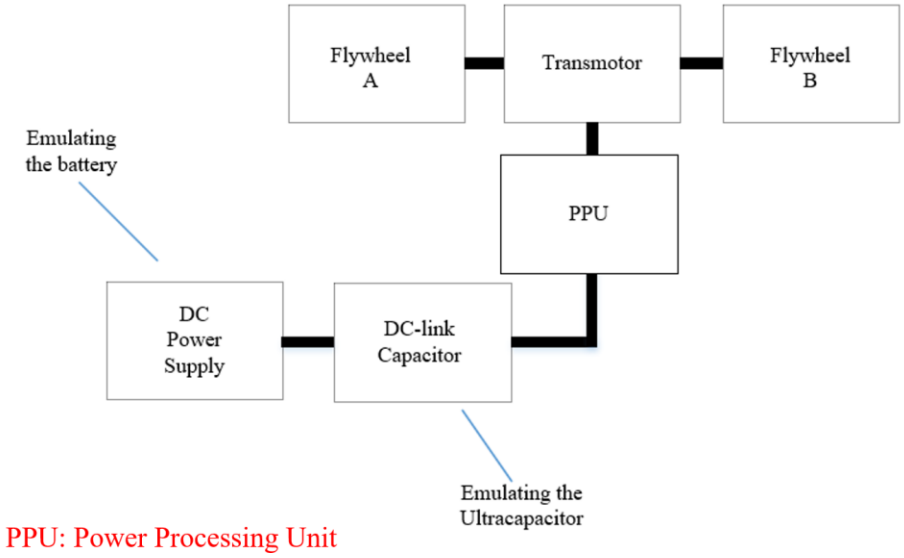

Fig. 62- The Transmotor-Flywheel Assisted by an Ultracapacitor (Capacitor) in an Emulation Setup.

The initial angular velocity of flywheels A and B is set to be 0 rpm and 500 rpm, respectively. The goal is to transfer energy from flywheel A to flywheel B in such a way that Both flywheel's angular velocity reaches 250 rpm in a second as is shown in the first half of Fig.63 (c). During this process, since flywheel A angular velocity is less than that in flywheel B, the extra power needs to be absorbed by the capacitor, as is shown in Fig.63 (d). Further, the set point of the capacitor is modified from 200 V to 272 V which could be the maximum assumed capacitor voltage if the transmotor's maximum speed is 500 rpm. The new setpoint is adjusted because the transmotor angular velocity is equal, so whether the command is to increase or decrease the flywheel A's or B's angular velocity, some power needs to be injected by the capacitor. Therefore, the capacitor voltage should be adjusted to be around its maximum voltage when the transmotor shafts have equal angular velocities, to optimize the required ultracapacitor (capacitor) in the given powertrain system.

In the second half of the experiment (between 5 and10 seconds), the goal is to increase the flywheel B angular velocity to its initial value and reduce the flywheel angular velocity to a standstill, as is shown in Fig.63 (c). Since flywheel B's angular velocity is more than that in flywheel A, the capacitor alongside the limited DC supply is required to inject power into the system, as is shown in Fig.63 (d). During this process, the capacitor set point voltage is changed to 200 V. Since there are losses associated with the emulation components of the setup, the DC power supply also injected power to restore the capacitor voltage to 200 V.

It is noteworthy to mention that in a conventional battery electric vehicle powertrain assisted with the ultracapacitor, the ultracapacitor voltage is adjusted to be close to the maximum value at the vehicle standstill. Furthermore, the ultracapacitor voltage is commonly set to be near its minimum value at higher vehicle speeds to minimize the required ultracapacitor. However, in the case of the transmotor-flywheel, assisted by the ultracapacitor (the proposed powertrain), the relative angular velocity of the two shafts is to be considered while controlling the ultracapacitor instead of the vehicle speed.

If it is assumed that all inefficiencies, electrical and mechanical losses, are compensated by the DC power supply with limited power output. The net power between the flywheels and the UC should be zero, as shown in Fig. 63 (d). For instance, at t= 3s we have:

$$t = 3s \rightarrow \omega_A = 100rpm(10.47rad/s) \,\&\, \omega_B = 420rpm(44rad/s) \,\&\, |T_A| = |T_B| = 3$$
$$P_A = T_A\omega_A \approx 32W(Receiving)$$
$$P_B = T_B\omega_B \approx 132W(Deleivering)$$
$$P_e = 132 - 32 \approx 100W(Receiving)$$

So, flywheel B injects 132W power into the system. The injected power is distributed between flywheel A and the electrical port (capacitors). As the above calculations show, the electrical port receives 100W, and flywheel A received 32 W at this specific point of time (t=3s).

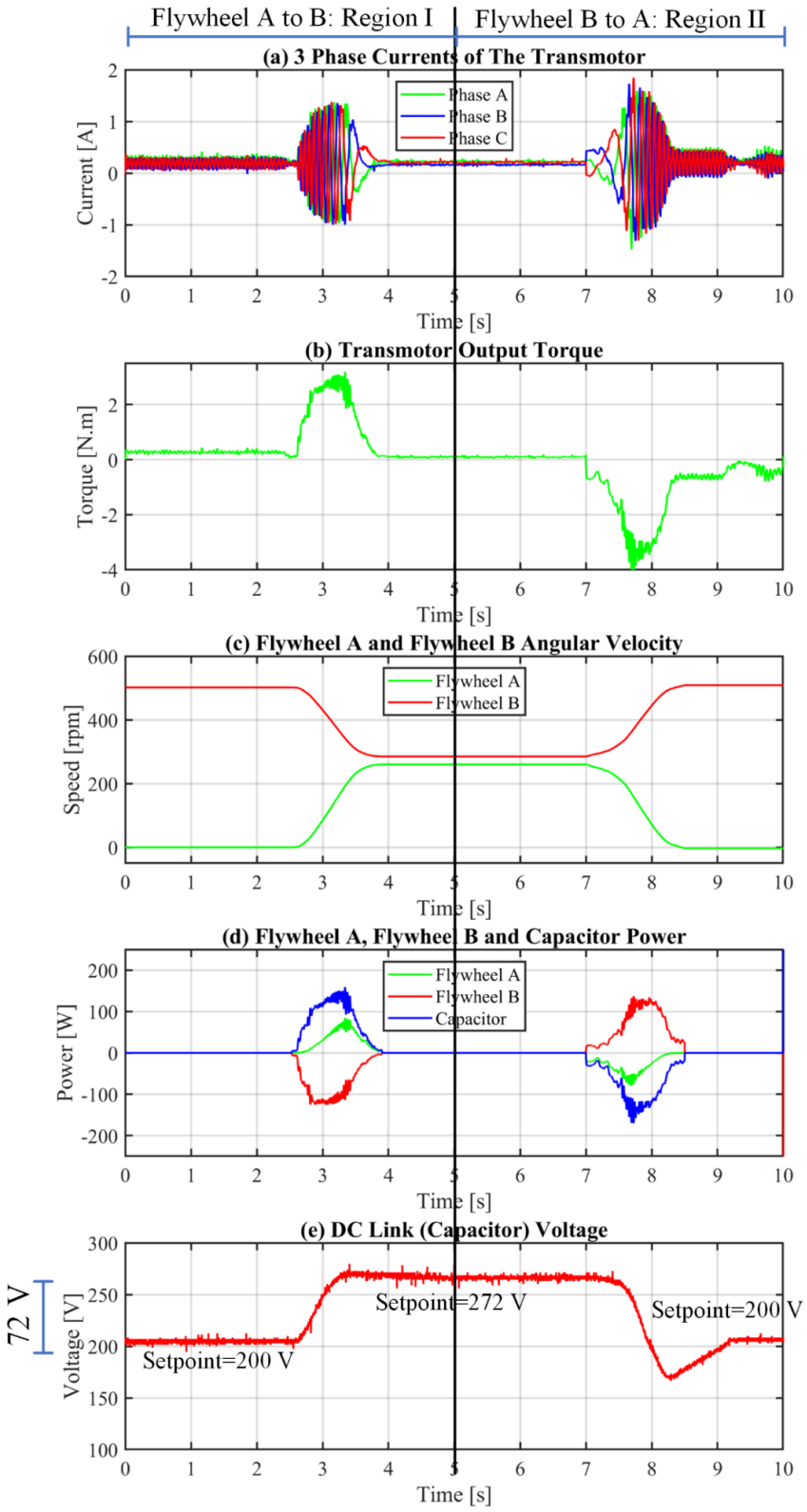

Fig. 63. Emulation Result (a) Transmotor's Three-Phase Current. (b) Transmotor Output Torque (c) Flywheel and Driveshaft Angular Velocity (d) Flywheel, Driveshaft, and Capacitor's Power (e) Capacitor's Voltage with Adjusted Setpoint

6. CONCLUSION AND FUTURE WORK

In this paper, the transmotor-flywheel powertrain assisted by ultracapacitor was introduced to improve the Battery Electric Vehicle (BEV) regenerative braking performance. Further, the battery power rating is reduced to the extent that the battery is only required for low power demands such as cruising. Alternatively, the FC technology is utilized, instead of the battery technology, in the proposed transmotor-flywheel powertrain assisted by an ultracapacitor, and the benefits and challenges are explained.

Chapter 2 reviewed various energy storage media that are suitable for vehicle applications. The battery and FC technology as the main energy storage media and flywheel and ultracapacitor as a power buffer are studied. Chapter 3 explained the transmotor characteristics and power flow in this electric machine. Then, the transmotor-flywheel powertrain with and without an ultracapacitor was discussed and compared with a conventional electric vehicle (Chevrolet Bolt). According to the braking scenario simulation results, presented in Chapter 4, the proposed powertrain is capable of recuperating up to two times more available kinetic energy than conventional electric vehicles during a harsh braking scenario. Further, the battery pack power rating required for the proposed powertrain is reduced to 30kW which is sufficient for the electric vehicle's losses and low-demand powers such as air drag and rolling resistance. This lets the BEV have a longer range by using more appropriate energy storage technologies, including various battery technology, as the primary energy storage source in the BEV powertrain. That is because it is possible to consider energy storage media technologies with lower specific power than the Li-ion technology, such as the Li-air battery technology, which is, until now, generally considered not suitable for BEV applications. Furthermore, it enables us to have similar regenerative braking as BEV in vehicles with FC technology as the prime energy storage media.

The proposed transmotor-flywheel powertrain assisted by an ultracapacitor can noticeably improve the regenerative braking capability of the vehicle. However, the vehicle range is limited by the prime energy storage media's energy capacity. Therefore, improving regenerative braking can only improve the vehicle's max range to some extent, and it would be significantly less than the conventional ICE-based vehicles. If the proposed powertrain is utilized in an HEV, it can improve the vehicle's fuel economy while maintaining the same vehicle's range as conventional ICE-based vehicles.

REFERENCE

[1] B. Frieske, M. Kloetzke and F. Mauser, "Trends in vehicle concept and key technology development for hybrid and battery electric vehicles," 2013 World Electric Vehicle Symposium and Exhibition (EVS27), Barcelona, Spain, 2013, pp. 1-12, doi: 10.1109/EVS.2013.6914783.

[2] M. Ehsani, Y. Gao, S. Longo and K. Ebrahimi, Modern electric, hybrid electric, and fuel cell vehicles. CRC press, 2018.

[3] A. Ostadi, M. Kazerani and S. Chen, "Hybrid Energy Storage System (HESS) in vehicular applications: A review on interfacing battery and ultra-capacitor units," 2013 IEEE Transportation Electrification Conference and Expo (ITEC), Detroit, MI, USA, 2013, pp. 1-7, doi: 10.1109/ITEC.2013.6573471.

[4] K. Rajashekara, "Present Status and Future Trends in Electric Vehicle Propulsion Technologies," in IEEE Journal of Emerging and Selected Topics in Power Electronics, vol. 1, no. 1, pp. 3-10, March 2013, doi: 10.1109/JESTPE.2013.2259614.

[5] Khaligh and Z. Li, "Battery, Ultracapacitor, Fuel Cell, and Hybrid Energy Storage Systems for Electric, Hybrid Electric, Fuel Cell, and Plug-In Hybrid Electric Vehicles: State of the Art," in IEEE Transactions on Vehicular Technology, vol. 59, no. 6, pp. 2806-2814, July 2010, doi: 10.1109/TVT.2010.2047877.

[6] E. Maximiliano Asensio, G. A. Magallán, C. H. De Angelo, F. M. Serra, “Energy Management on Battery/Ultracapacitor Hybrid Energy Storage System based on Adjustable Bandwidth Filter and Sliding-mode Control,” in Journal of Energy Storage, Volume 30, 2020,101569, ISSN 2352-152X, doi: 10.1016/j.est.2020.101569.

[7] M. Alamgir, "Lithium Has Transformed Vehicle Technology: How trends in Li-ion battery technology have developed for vehicle electrification," in IEEE Electrification Magazine, vol. 5, no. 1, pp. 43-52, March 2017, doi: 10.1109/MELE.2016.2644558.

[8] J. Liu, M. Anwar, P. Chiang, S. Hawkins, Y. Jeong, F. Momen, S. Poulos and S. Song "Design of the Chevrolet Bolt EV propulsion system." in SAE International Journal of Alternative Powertrains, vol. 5, no. 1, pp. 79-86, May 2016.

[9] F. Momen, K. M. Rahman, Y. Son and P. Savagian, "Electric motor design of general motors’ Chevrolet Bolt electric vehicle." in SAE International Journal of Alternative Powertrains, vol. 5, no. 2, pp. 286-293, July 2016.

[10] X. Gong, R. Xiong and C. C. Mi, "Study of the characteristics of battery packs in electric vehicles with parallel-connected lithium-ion battery cells," 2014 IEEE Applied Power Electronics Conference and Exposition - APEC 2014, Fort Worth, TX, USA, 2014, pp. 3218-3224, doi: 10.1109/APEC.2014.6803766.

[11] R. Xiong, Y. Zhang, J. Wang, H. He, S. Peng and M. Pecht, "Lithium-Ion Battery Health Prognosis Based on a Real Battery Management System Used in Electric Vehicles," in IEEE

Transactions on Vehicular Technology, vol. 68, no. 5, pp. 4110-4121, May 2019, doi: 10.1109/TVT.2018.2864688.

[12] J. Cao and A. Emadi, "A New Battery/UltraCapacitor Hybrid Energy Storage System for Electric, Hybrid, and Plug-In Hybrid Electric Vehicles," in IEEE Transactions on Power Electronics, vol. 27, no. 1, pp. 122-132, Jan. 2012, doi: 10.1109/TPEL.2011.2151206.

[13] J. Shen and A. Khaligh, "An energy management strategy for an EV with two propulsion machines and a hybrid energy storage system," 2015 IEEE Transportation Electrification Conference and Expo (ITEC), Dearborn, MI, USA, 2015, pp. 1-5, doi: 10.1109/ITEC.2015.7165791.

[14] H. A. Yavasoglu, C. Shi and K. Gokce, "Energy storage systems for EVs with two propulsion machines," 2017 IEEE Transportation Electrification Conference and Expo (ITEC), Chicago, IL, 2017, pp. 696-700, doi: 10.1109/ITEC.2017.7993354.

[15] J. Shen and A. Khaligh, "A Supervisory Energy Management Control Strategy in a Battery/Ultracapacitor Hybrid Energy Storage System," in IEEE Transactions on Transportation Electrification, vol. 1, no. 3, pp. 223-231, Oct. 2015, doi: 10.1109/TTE.2015.2464690.

[16] K. R. Bharath, G. Sivaraman, B. Harivishnu and M. P. Haridas, "Design and implementation of electric speed booster and kinetic energy recovery system for electric vehicle," 2017 International Conference on Technological Advancements in Power and Energy (TAP Energy), Kollam, India, 2017, pp. 1-6, doi: 10.1109/TAPENERGY.2017.8397326.

[17] S. Hu, Z. Liang, D. Fan and X. He, "Hybrid Ultracapacitor–Battery Energy Storage System Based on Quasi-Z-source Topology and Enhanced Frequency Dividing Coordinated Control for EV," in IEEE Transactions on Power Electronics, vol. 31, no. 11, pp. 7598-7610, Nov. 2016, doi: 10.1109/TPEL.2016.2518749.

[18] J. Shen, S. Dusmez and A. Khaligh, "Optimization of Sizing and Battery Cycle Life in Battery/Ultracapacitor Hybrid Energy Storage Systems for Electric Vehicle Applications," in IEEE Transactions on Industrial Informatics, vol. 10, no. 4, pp. 2112-2121, Nov. 2014, doi: 10.1109/TII.2014.2334233.

[19] H. A. Yavasoglu, J. Shen, C. Shi, M. Gokasan and A. Khaligh, "Power Split Control Strategy for an EV Powertrain With Two Propulsion Machines," in IEEE Transactions on Transportation Electrification, vol. 1, no. 4, pp. 382-390, Dec. 2015, doi: 10.1109/TTE.2015.2504406.

[20] N. F. Ershad, R. T. Mehrjardi and M. Ehsani, "Development of a Kinetic Energy Recovery System Using an Active Electromagnetic Slip Coupling," in IEEE Transactions on Transportation Electrification, vol. 5, no. 2, pp. 456-464, June 2019, doi: 10.1109/TTE.2019.2891045.

[21] N. Farrokhzad Ershad, R. T. Mehrjardi and M. Ehsani, "Electro-Mechanical EV Powertrain With Reduced Volt-Ampere Rating," in IEEE Transactions on Vehicular Technology, vol. 68, no. 1, pp. 224-233, Jan. 2019, doi: 10.1109/TVT.2018.2881385.

[22] N. Farrokhzad Ershad, R. Tafazzoli Mehrjardi and M. Ehsani, "Efficient Flywheel-Based All-Wheel-Drive Electric Powertrain," in IEEE Transactions on Industrial Electronics, doi: 10.1109/TIE.2020.2992942.

[23] N. Farrokhzad Ershad, R. Tafazzoli Mehrjardi and M. Ehsani, "High-Performance 4WD Electric Powertrain With Flywheel Kinetic Energy Recovery," in IEEE Transactions on Power Electronics, vol. 36, no. 1, pp. 772-784, Jan. 2021, doi: 10.1109/TPEL.2020.3004866

[24] R. Tafazzoli Mehrjardi, N. F. Ershad and M. Ehsani, "Transmotor-Based Powertrain for High-Performance Electric Vehicle," in IEEE Transactions on Transportation Electrification, vol. 6, no. 3, pp. 1199-1210, Sept. 2020, doi: 10.1109/TTE.2020.2995872.

[25] General Motors. 2021. Chevrolet Bolt: User Manual. Litho in U.S.A.

[26] Verma, Sujata, S. K. Singh, and A. G. Rao. "Overview of control Techniques for DC-DC converters." Research Journal of Engineering Sciences 2.8 (2013): 18-21.

[27] F. Momen, K. Rahman and Y. Son, "Electrical Propulsion System Design of Chevrolet Bolt Battery Electric Vehicle," IEEE Transactions on Industry Applications, vol. 55, no. 1, pp. 376-384, Jan.-Feb. 2019.

[28] S. He, “NVH Design, Analysis and Optimization of Chevrolet Bolt Battery Electric Vehicle” SAE Technical Paper, No. 2018-01-0994. Apr. 2018.

[29] A. Khaligh and Z. Li, "Battery, Ultracapacitor, Fuel Cell, and Hybrid Energy Storage Systems for Electric, Hybrid Electric, Fuel Cell, and Plug-In Hybrid Electric Vehicles: State of the Art," IEEE Transactions on Vehicular Technology, vol. 59, no. 6, pp. 2806-2814, July 2010.

[30] K. M. Rahman, S. Jurkovic, C. Stancu, J. Morgante and P. J. Savagian, "Design and Performance of Electrical Propulsion System of Extended Range Electric Vehicle (EREV) Chevrolet Volt," IEEE Transactions on Industry Applications, vol. 51, no. 3, pp. 2479-2488, May-June 2015.

[31] M. Hedlund, “Electrified Integrated Kinetic Energy Storage,” Ph.D. dissertation, Acta Universitatis Upsaliensis, 2017.

[32] M. E. Amiryar and K. R. Pullen, "A review of flywheel energy storage system technologies and their applications." Applied Sciences, vol. 7, no. 3, pp. 286, March 2017.

[33] H. Cai and L. Xu, "Modeling and Control for Cage Rotor Dual Mechanical Port Electric Machine–Part I: Model Development," IEEE Transactions on Energy Conversion, vol. 30, no. 3, pp. 957-965, Sept. 2015.

[34] H. Cai and L. Xu, "Modeling and Control for Cage Rotor Dual Mechanical Port Electric Machine—Part II: Independent Control of Two Rotors," IEEE Transactions on Energy Conversion, vol. 30, no. 3, pp. 966-973, Sept. 2015.

[35] Department of Energy. (2022) “Types of Fuel Cells”, ENERGY.GOV, https://www.energy.gov/eere/fuelcells/types-fuel-cells

[36] R. Tafazzoli Mehrjardi, N. F. Ershad and M. Ehsani, "Transmotor-Flywheel Powertrain Assisted by Ultracapacitor," in IEEE Transactions on Transportation Electrification, vol. 8, no. 3, pp. 3686-3695, Sept. 2022, doi: 10.1109/TTE.2022.3152793.

[37] M. Ehsani, et al. "Hybrid Energy Storage Systems for Vehicle Applications." Electric, Hybrid, and Fuel Cell Vehicles, edited by Amgad Elgowainy, Springer Nature, 2021, pp. 275-292.

[38] Y. S. Wong, et al. "Vehicle Energy Storage: Batteries." Electric, Hybrid, and Fuel Cell Vehicles, edited by Amgad Elgowainy, Springer Nature, 2021, pp. 292-313.

[39] E. Ubong " Fuel Cell-Powered HEV Design and Control." Electric, Hybrid, and Fuel Cell Vehicles, edited by Amgad Elgowainy, Springer Nature, 2021, pp. 191-224

[40] A. Burke "Energy Storage: Ultracapacitor." Electric, Hybrid, and Fuel Cell Vehicles, edited by Amgad Elgowainy, Springer Nature, 2021, pp. 407-442.

[41] Maxwell, “3.0V 150F ULTRACAPACITOR CELL Advanced Small Cell with Snap-In Terminals” 3003112-EN.1 datasheet, 2019.

[42] Maxwell, “3.0V 100F ULTRACAPACITOR CELL Advanced Small Cell with Snap-In Terminals” 3003111-EN.1 datasheet, 2019.

[43] Maxwell, “2.7V 325F ULTRACAPACITOR CELL High Power Energy Solution in Compact Form Factor” 3003346-EN.1 datasheet, 2021.

[44] SKELETON, “PCB-Mountable Cell” 01-DS-211222-SKELCAP-SCA0300-1C datasheet, 2022.

[45] SKELETON, “SkelCap Ultracapacitor” 02-SCA-181029-1B datasheet, 2019.

[46] N. Farrokhzadershad “Development of dual shaft electric motor with independent input-output torque-speed for vehicle kinetic energy recovery systems.” Doctoral dissertation, Texas A&M University, 2018.